Exotic phases of correlated electrons in two dimensions

Author: Yuan-Ming Lu

Boston College
The Graduate School of Arts and Sciences
Department of Physics

EXOTIC PHASES OF CORRELATED ELECTRONS IN TWO DIMENSIONS

a dissertation

by

YUAN-MING LU

submitted in partial fulfillment of the requirements

for the degree of

Doctor of Philosophy

September 2011

Thesis advisor

Ziqiang Wang

Author

Yuan-Ming Lu

Exotic phases of correlated electrons in two dimensions

Abstract

Exotic phases and associated phase transitions in low dimensions have been a fascinating frontier and a driving force in modern condensed matter physics since the 80s. Due to strong correlation effect, they are beyond the description of mean-field theory based on a single-particle picture and Landau's symmetry-breaking theory of phase transitions. These new phases of matter require new physical quantities to characterize them and new languages to describe them. This thesis is devoted to the study on exotic phases of correlated electrons in two spatial dimensions. We present the following efforts in understanding two-dimensional exotic phases:

(I) Using Z_n vertex algebra, we give a complete classification and characterization of different one-component fractional quantum Hall (FQH) states[130], including their ground state properties and quasiparticles.

(II) In terms of a non-unitary transformation, we obtain the exact form of statistical interactions between composite fermions in the lowest Landau level (LLL) with $\nu = \frac{1}{2m},\ m = 1, 2, \cdots$[131]. By studying the pairing instability of composite fermions we theoretically explains recently observed FQHE in LLL with $\nu = 1/2,\ 1/4$[132, 190, 189].

(III) We classify different Z_2 spin liquids (SLs) on kagome lattice in Schwinger-fermion representation using projective symmetry group (PSG). We propose one most

promising candidate[129] for the numerically discovered SL state in nearest-neighbor Heisenberg model on kagome lattice[240].

(IV) By analyzing different Z_2 spin liquids on honeycomb lattice within PSG classification, we find out the nature of the gapped SL phase in honeycomb lattice Hubbard model[136], labeled sublattice pairing state (SPS) in Schwinger-fermion representation. We also identify the neighboring magnetic phase of SPS as a chiral-antiferromagnetic (CAF) phase and analyze the continuous phase transition between SPS and CAF phase. For the first time we identify a SL (0-flux state in Ref. [210]) in Schwinger-boson representation with one (SPS) in Schwinger-fermion representation by a duality transformation[128].

(V) We show that when certain non-collinear magnetic order coexists in a singlet nodal superconductor, there will be Majorana bound states in vortex cores/on the edges of the superconductor. This proposal opens a window for discovering Majorana fermions in strongly correlated electrons.

(VI) Motivated by recent numerical discovery of fractionalized phases in topological flat bands, we construct wavefunctions for spin-polarized fractional Chern insulators (FCI) and time reversal symmetric fractional topological insulators (FTI) by parton approach. We show that lattice symmetries give rise to different FCI/FTI states even with the same filling fraction. For the first time we construct FTI wavefunctions in the absence of spin conservation which preserve all lattice symmetries[127]. The constructed wavefunctions also set up the framework for future variational Monte Carlo simulations.

Contents

Citations to Previously Published Work

Chapter 2 has appeared in the following paper:

> "Non-Abelian Quantum Hall States and their Quasiparticles: from the Pattern of Zeros to Vertex Algebra", Yuan-Ming Lu, Xiao-Gang Wen, Zhenghan Wang and Ziqiang Wang, *Phys. Rev. B* **81** 115124 (2010), e-print arXiv:cond-mat/0910.3988 (2009).

Chapter 3 has appeared in

> "Correlation-hole induced paired quantum Hall states in lowest Landau level", Yuan-Ming Lu, Yue Yu and Ziqiang Wang, *Phys. Rev. Lett.* **105** 216801 (2010), e-print arXiv:cond-mat/0911.1775 (2009).

Chapter 4 has appeared in

> "Z_2 spin liquids in the $S = 1/2$ Heisenberg model on the kagome lattice: A projective symmetry-group study of Schwinger fermion mean-field states", Yuan-Ming Lu, Ying Ran and Patrick A. Lee, *Phys. Rev. B* **83**, 224413 (2011), e-print arXiv:cond-mat/1104.1432 (2011).

Chapter 5 has appeared in

> "Z_2 spin liquid and chiral antiferromagnetic phase in the Hubbard model on a honeycomb lattice", Yuan-Ming Lu and Ying Ran, *Phys. Rev. B* **84**, 024420 (2011), e-print arXiv:cond-mat/1005.4229 and e-print arXiv:cond-mat/1007.3266 (2010).

Chapter 6 is to appeared as

> "Majorana fermions in nodal singlet superconductors with coexisting non-collinear magnetic orders", Yuan-Ming Lu and Ziqiang Wang.

Chapter 7 has appeared in

> "Symmetry protected fractional Chern insulators and fractional topological insulators", Yuan-Ming Lu and Ying Ran, e-print arXiv:cond-mat/1109.0226 (2011).

Electronic preprints (shown in `typewriter font`) are available on the Internet at the following URL:

> `http://arXiv.org`

Acknowledgments

Time passed so fast that I can still feel the excitement that I felt on my arrival to Boston. Thanks to many people, four years of graduate study has become a fascinating and unfadable memory in my life. I've benefited so much from their adorable characters and I owe them my deepest gratitude.

First of all, I'm deeply indebted to my advisor, prof. Ziqiang Wang, without whom this thesis would not be possible. When I was in China struggling to apply for a PhD candidate position, it was him who offered me an opportunity in Boston College. I not only learnt lots of physics from him but owe him so much for all the guidance and support on my career as well. Among all his amazing features his enthusiasm for research inspired me the most, which sets up the prototype of a scientist for me to follow. I'm also grateful to him for giving me the freedom to collaborate with other faculties, even when I went too far away from my main research with him sometimes.

I'm also deeply thankful to prof. Xiao-Gang Wen at MIT for giving me an opportunity to work with him. It was very fortunate for me to have many illuminating discussions with him and I was always amazed by his knowledge and as well as his wisdom. He taught me to do research in an open-minded way and always to keep the physical picture in front. Although I'm not his student, he supported me in every way he could and for that I owe him more than words can describe.

I'd like to express my utmost appreciation to prof. Ying Ran for his support and help during the past two years. In spite of being a faculty member, Ying is more like an older brother to me with his warmth and passion. I thank him for numerous discussions we had (sometimes till midnight), the frustration, and the excitement of discovery. I also owe him deep gratitude for the physics he taught me as well as for

his precious advice on my career, especially on my postdoc application.

I thank prof. Vidya Medhavan and prof. David Broido for being my committee members. I thank prof. Zhenghan Wang at station Q and prof. Yue Yu at ITP@CAS for enjoyable collaborations and for inviting me to visit. Also I'd like to thank prof. Patrick A. Lee at MIT for collaborations and encouragements. And I feel blessed to have all faculty and staff members who made BC physics department such a wonderland.

Besides, I've got to thank my undergraduate thesis advisor, prof. Zheng-Yu Weng at Tsinghua University. When I was frustrated by PhD application it was him who introduced me to Ziqiang and supported me wholeheartedly. I'll always remember how nice an advisor should be to a rookie student, a lesson I started to learn from him. Also I'm grateful to Zheng-Cheng Gu for all his help especially during my early days in Boston, in particular for introducing me to Xiao-Gang. It was my great pleasure to be the best man in his wedding. I thank Liang Ren, Sen Zhou, Feng Cai, Yiming Xu, Andrej Mesaros and especially Yi Zhang, Chunhua Li and Kai-Yu Yang for great company at BC and countless discussions on physics, life and whatever. I thank all my PhD classmates, especially my former officemate/tennis partner Marco Almeida for the time we spent together. I'm also grateful to all my friends because of whom I feel not alone during the four years in Boston.

Finally, I owe everything to the most important people of all: my parents. In my life they've always been my ultimate source of encouragement, guidance and love. Therefore I devote this thesis to them.

Dedicated to my father Jing-Li Lu,
my mother Wan-Xiang Shi
and my grandmother Qi-Lin Yang.

List of Figures

List of Tables

Chapter 1

Introduction

1.1 An introduction to condensed matter physics

Condensed matter physics studies the physical properties of a huge number (of order 10^{23}) of atoms/molecules which interact with each other and are highly concentrated in a system. The most familiar examples of condensed matters are solids and liquids. The length scale ranges from the size of individual atoms to the macroscopic scale. Different from chemistry, atomic/moleculer and nuclear physics which handle a relatively small number of particles, condensed matter physics deals with a practically infinite number of degrees of freedom and so does particle physics. Even when the behavior of a single particle or a few particles is well understood, as a large number of particles gather together and interact with each other, completely new collective phenomena may emerge which reaches far beyond the scope of few-body physics.

The concept of *emergence* is incisively summarized in a famous quote of P. W. Anderson[7]: *more is different*. Take helium-3 as an example[209]. As the isotope of

inert noble gas element helium, one helium-3 nucleus consists of two protons and one neutron and therefore a single helium-3 atom is a fermion. A macroscopic sample of pure helium-3 however possesses a very rich phase diagram as shown in the left panel of FIG. 1.1, including two superfluid phases (A phase and B phase) with different symmetries in contrast to a usual solid-liquid-gas phase diagram. Helium-4 is another isotope whose nucleus has two protons and two neutrons and hence is a boson. Its phase diagram is different from that of helium-3, including a low-temperature superfluid phase due to Bose-Einstein condensation of helium-4 atoms. On the other hand, fermions don't condense at low temperature and the superfluid ^{3}He are very different from superfluid ^{4}He: *e.g.* stable gapless surface states appear in superfluid ^{3}He-B phase but not in superfluid ^{4}He. As we increase the complexity and go from elements to binary, tertiary and quaternary compounds, the number of possible materials exponentiates by at least a factor of 100 at each stage[32]. Since materials composed of different isotopes of one element can be so different and exhibit so many different phases, potential discovery of fundamentally new phases of matter could be made in the vast phase space of complex compounds. The phase diagrams of binary compound UGe_2 and tertiary compound $CeRhIn_5$ are also shown in FIG. 1.1, featuring coexistence of magnetism (ferromagnetism, FM or antiferromagnetism, AF) and superconductivity in low temperature under certain pressure. The main challenge for condensed matter physicists is to *explore and understand new phases of matter and the phase transitions between them.*

The constituents of a condensed matter system are a myriad of interacting particles (*e.g.* ions and electrons). People believe that such a many-body system is governed

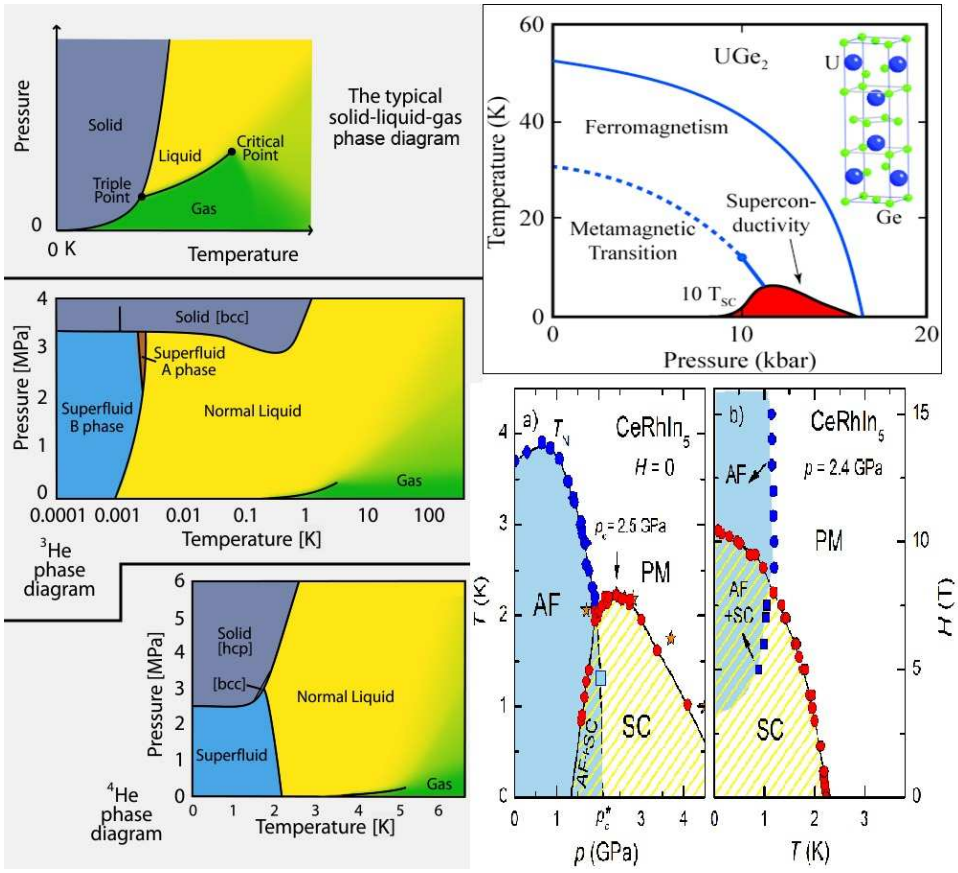

Figure 1.1: Phase diagrams of several different condensed matters: helium-3 and helium-4 consisting of a single element, binary compound UGe_2 and tertiary compound $CeRhIn_5$. All these materials exhibit a very rich phase diagram when temperature, pressure and external magnetic field are varied.

by quantum mechanics: once we solve the many-body Schrödinger equation involving all the particles, we know all physical properties and time evolution of the system. However for particles of order 10^{23} it's practically impossible to either solve this many-body Hamiltonian or to store the eigenstate vectors, simply because the dimension of the Hilbert space grows exponentially with the particle number (*e.g.* the Hilbert space of a system of N spin-1/2 quantum magnets is 2^N-dimensional). In fact a classical computer made by all atoms in our universe can only solve the Schrödinger equation for about 100 particles. How can we understand the many-body physics in condensed matters, without literally solving the many-body Schrödinger equation?

The building block of traditional many-body physics is mean field theory. Although the many-body problem cannot be solved exactly, we can always diagonalize a single-body Hamiltonian (at least numerically). The basic idea of mean field theory is to reduce the many-body problem to a solvable single-body problem with an external field. The interaction between one particle and all others is replaced by an effective external field (*mean field*) for this particle. It turns out this single-body problem is a good approximation to the actual many-body problem when the interaction between particles is not too strong compared with kinetic energy. The ground states obtained by filling single-particle levels (and the perturbation theory around this ground state) give simple explanations to many ordered/disordered phases and transitions between them. For example, it explains the origin of metal, insulator and semiconductor. In solids the ions form a crystal and a single electron moving in the lattice of ions feels an effective periodic (static) potential, which accounts for the interaction between this electron and other electrons/ions. Solutions to such a single-body problem give rise

to energy bands and electrons fill these bands one by one from the bottom. Metals contain a partially-filled band while in insulators/semiconductors all bands are either fully occupied or completely empty. Ordered phases such as magnetism and superconductivity can also be understood in terms of mean field theory and the associated effective external field is called an order parameter. The order parameter corresponds to a local physical quantity such as spin density. These mean-field ground states are rather "classical" coherent states and the corresponding many-electron wavefunctions are nothing but Slater determinants.

The physical concept behind mean field theory is long-range order, symmetry breaking and order parameter. In this framework introduced by Landau[110] different phases are characterized by their different symmetries. Associated with each ordered phase there is an order parameter which breaks certain global symmetry of the original microscopic Hamiltonian. *e.g.* in a magnetic phase the order parameter breaks spin rotational symmetry while in a superfluid phase the order parameter breaks global $U(1)$ gauge symmetry. These phenomena only happen in the thermodynamical limit (with infinite degrees of freedom) and are called *spontaneous symmetry breaking of continuous symmetries*. In Landau and Ginzburg's theory of phase transitions[112], a continuous phase transition are always accompanied by symmetry breaking. To be precise the symmetry group of the low temperature phase must be a subgroup of that of the high temperature phase. The low energy excitations in an ordered phase which breaks continuous symmetry is the long-wavelength fluctuations of the order parameter, called Nambu-Goldstone bosons[145, 60]. Simplest examples are spin waves in a magnetic phase (which breaks spin rotational symmetry) and phonon

modes in a solid (which breaks translation symmetry in free space).

To summarize, the "conventional" ordered phases share the following characters:

- A phase is completely characterized by its symmetry and associated long-range orders.
- Phase transitions from a high temperature phase to low temperature one are characterized by symmetry breaking.
- Gapless Goldstone bosons are the elementary excitations corresponding to the broken continuous symmetries.
- The low-energy effective theory are described by long-wavelength fluctuations of local order parameters, *i.e.* Landau theory.

1.2 Exotic phases in two dimensions: an overview

For a long time people believed that all condensed matter phases and phase transitions can be described by mean field theory and symmetry breaking concept. However a series of experimental discoveries made since the 80s, such as fractional quantum Hall effects[207] and high temperature superconductivity[20] reveals that lots of exotic phases and phase transitions could happen at low temperature. In fact traditional many-body physics (including mean field theory and Landau theory) provides a proper description for finite temperature phases and phase transitions where thermal fluctuations dominate. When temperature is low enough (compared with other energy scales) quantum fluctuations become important and fundamentally new

states of matter emerge. These exotic phases and associated zero-temperature phase transitions cannot be described by mean-field theory and symmetry breaking picture: *e.g.* different phases can have exactly the same symmetry, and zero-temperature quantum phase transitions (induced by tuning physical parameters such as pressure and magnetic field) are not always symmetry-breaking type.

A common feature shared by these phases is that interaction (correlation) energy scale in the system is comparable with (or larger than) the kinetic energy scale (or band width). This strong correlation (or interaction) effect is believed to be the reason why mean field theory and perturbation theory around the mean field ground states fail. Correlation effects beyond mean field theory becomes more and more important when the (spatial) dimension of the many-body system becomes lower. Intuitively in a higher dimension one particle has more neighbors (or a larger coordination number) and this makes it more accurate to approximate the interaction between particles by a mean field. In general there is a critical dimension d_c beyond which mean field theory fails[86], *e.g.* for Landau's free energy theory (Gaussian model) the critical dimension is $d_c = 4$. One important manifestation of correlation effects is quantum fluctuations around the mean-field ground state. Sometimes these fluctuations are strong enough to destroy the order in the mean-field ground states: *e.g.* in two spatial dimensions the quantum fluctuation is so strong that there are no spontaneous symmetry breaking (or associated true long range order) at any finite temperature[137, 85].

Aside from strong correlation effects, another special feature of two spatial dimensions is nontrivial quantum statistics of free (hard-core) identical particles[121, 232]. Quantum statistics is the symmetry of many-body wavefunctions under exchange of

any two identical particles. In three (spatial) dimensions, adiabatically wrapping one particle around another (*i.e.* interchange the two particles twice) is topologically equivalent to a process in which none of the particles move at all. Since the many-body wavefunction should be invariant under such an operation, the only two possibilities are to change by a ± 1 sign for the wavefunction under a single interchange, hence the bosons and fermions in 3+1-D. In two spatial dimensions things are qualitatively different: a particle loop encircling another particle in two dimensions cannot be continuously deformed to a point. The many-body wavefunction doesn't necessarily go back to the same state under such a braiding operation. As a result free hard-core particles in two dimensions can be either bosons or fermions, and these exotic particles with nontrivial braiding statistics are called *anyons*[231]. When an adiabatic (counter-clockwise) interchange of two particles brings only a phase factor $e^{\mathrm{i}\theta}$ for the many-body wavefunction, the particles are called abelian anyons since the phase factor forms a one-dimensional abelian representation of braid group. θ is called the statistical angle of the particles. Notice that for bosons $\theta = 2\pi$ and for fermions $\theta = \pi$. In other cases the adiabatic interchange of two particles will evolve the many-body system into a new state, corresponding to a non-abelian representation of braid statistics. These identical particles are called non-abelian anyons. It has been shown that anyons can be used to build fault-tolerant quantum computers[101]. As will be discussed later, abelian and non-abelian anyons emerge as elementary excitations of many exotic phases in two dimensions. In a system of correlated electrons these elementary excitations (or quasiparticles) sometimes carry a fraction of the electron quantum number (charge/spin) and this emergent phenomenon is called *fractional-*

ization.

Exploring exotic phases in low dimensions is a frontier of condensed matter physics and so far we only have partial understanding of these exotic phases. Compared with the "conventional" phases described earlier, these exotic phases confront us with the following new questions:

- Symmetry alone cannot characterize an exotic phase. What are the quantum numbers fully characterizing an exotic phase?
- Quantum phase transitions at zero-temperature are not necessarily symmetry-breaking type. What are the new mechanisms for these phase transitions?
- Examples of elementary excitations of exotic phases are fractionalized quasiparticles in the bulk, and stable gapless states on the edge/surface.
- Landau theory cannot describe the low-energy physics. What are the low-energy effective theory describing these quantum phase transitions?

In the following sections I'll show several examples of exotic phases in two-dimensional systems of correlated electrons. This thesis will focus on these exotic phases.

1.3 Fractional quantum Hall liquids

For a system of electrons gas confined in a two-dimensional plane, when a strong external magnetic field perpendicular to the plane is applied, solutions to the single-body (non-interacting) problem gives rise to *Landau levels* each of which has a large

degeneracy. Electrons fill these Landau levels one by one from the lowest level. Considering the effect of disorder, the perfect degeneracy of each Landau level is lifted and one Landau level now becomes a "Landau band" in the presence of disorder. Extended states which contribute to the conductance (if they are filled by electrons) are located in the center of each Landau band, while non-conducting localized states are on the edge of each band. The degeneracy of each Landau level (or Landau band) is proportional to the amplitude of magnetic field B. As the magnetic field is tuned one changes the filling fraction of Landau bands or effectively shift the Fermi level. As the Fermi level lies in the extended states around the center of a Landau band, the electron state is a metallic one with non-vanishing conductance $\sigma_{xx} \neq 0$. However when Fermi level lies in the localized states on the edge of a band, the corresponding electron state is an insulator with $\sigma_{xx} = 0$. Besides, each filled Landau bands contribute a quantized Hall conductance of $\sigma_{xy} = e^2/h$, which is a topological invariant from linear response theory calculations[205]. The quantization of the Hall conductance is extremely precise as in experiments because it's based on gauge invariance[113, 71]. An intuitive way to understand this fact is the edge state picture: although the bulk state is an insulator with energy gap $\hbar\omega_c$ (ω_c is the cyclotron frequency), the cyclotron motion of electrons under the magnetic field gives rise to gapless current-carrying states localized on the edge. It can be shown that the quantized Hall conductance has a one-to-one correspondence with these edge states[78]. The above facts correspond to the integer quantum Hall effect[105] (IQHE), which is featured by quantized plateaus with Hall conductance $\sigma_{xy} = \rho_{xy}^{-1} = ne^2/h,\ n = 1, 2, \cdots$ as shown in FIG. 1.2. Integer quantum Hall effects can be explained in this simple picture in terms of

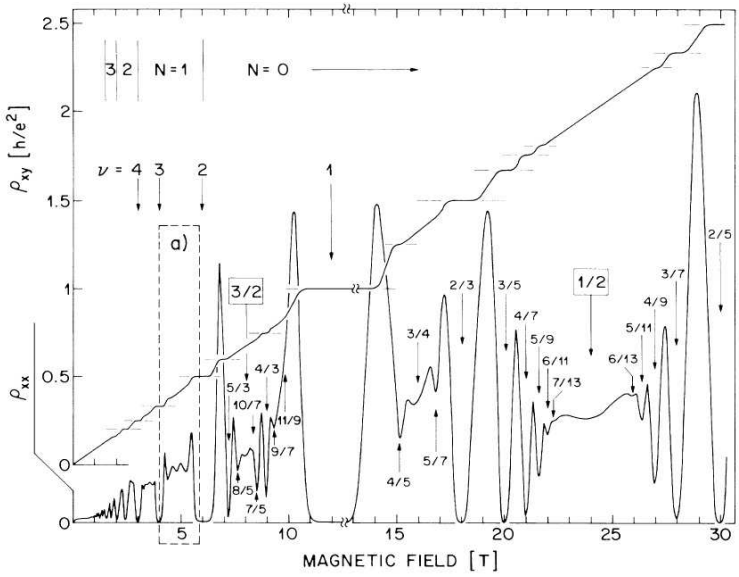

Figure 1.2: Resistance measurements of integer and fractional quantum Hall effects. Notice the relations between resistance and conductance are $\sigma_{xy} = \rho_{xy}/(\rho_{xy}^2 + \rho_{xx}^2)$ and $\sigma_{xx} = \rho_{xx}/(\rho_{xy}^2 + \rho_{xx}^2)$. Figure from Ref. [234].

non-interacting electrons moving in a magnetic field in the presence of disorder. The electron wavefunctions of IQH states are Slater determinants since they correspond to band insulators obtained by filling single-particle states.

This is not the whole story. Later on in resistance measurements of cleaner samples, at lower temperature people found new "fractionally" quantized plateaus with $\sigma_{xy} = \frac{p}{q}e^2/h,\ p, q$ being integers[207]. The associated filling fraction (of Landau levels/bands) is also p/q. These phenomena are called fractional (or anomalous) quantum Hall effects in comparison to integer quantum Hall effects. In integer quantum Hall effects, a plateau with $\sigma_{xy} = ne^2/h$ corresponds to a insulating state with n filled Landau bands. Such a band insulator has an energy gap of order $\hbar\omega_c$. It also has stable edge states which contribute to the Hall conductance. In the case of fractional quantum Hall effects (FQHEs), however, the topmost Landau band is only partially

filled (with filling fraction $[\frac{p}{q}]$) and naively the state should be a metallic one with nonzero conductance $\sigma_{xx} \neq 0$. However this plateau corresponds to an insulating state ($\sigma_{xx} = 0$) with a finite energy gap. The only possibility is that electrons form an incompressible (meaning a finite gap) state at this filling fraction due to correlation/interaction effect. Formation of this correlation-induced insulator in FQHE requires the following conditions:

- Interaction energy is comparable with (or larger than) the band width which is determined by disorder strength: hence cleaner samples are required.

- Since energy gap is determined by Coulomb interaction between electrons, the gap $\sim e^2/l_B$ (l_B is the magnetic length) in FQHE is smaller than that in IQHE ($\sim \hbar\omega_c$): hence lower temperature is required.

How to understand these correlated insulating states? FQH states with different Hall conductance have exactly the same symmetry (as the original two-dimensional electron gas). Symmetry alone cannot describe these different incomprehensible (meaning a finite energy gap for excitations above the ground state) liquids of electrons in two dimensions. The first theoretical breakthrough was made by Laughlin[114]: he simply guessed a correct many-body wavefunction for FQH states at filling fraction $\nu = 1/m,\ m$ being an *odd* integer. Laughlin's state is written as

$$\Phi\Big(\{z_i = x_i + \mathrm{i}y_i\}\Big) = \prod_{i<j}(z_i - z_j)^m \cdot e^{-\sum_{k=1}^{N}|z_k|^2/(4l_B^2)} \tag{1.1}$$

under symmetric gauge $\vec{A} = B(-y, x)/2$ in a disc geometry. This wavefunction is a holomorphic function of electron coordinates $\{z_i = x_i + \mathrm{i}y_i\}$ (except for Gaussian factor due to disc geometry) and it involves only single-particle states in the

lowest Landau level (LLL). This many-body wavefunction is an exotic correlated state which cannot be written as a Slater determinant unless $m = 1$ (corresponding to a fully filled LLL). Elementary excitations of such a state are quasiholes and quasielectrons[114] each of which carries a fractional charge $e_0 = \pm e/m$ (e denotes the electron charge) and fractional statistical angle $\theta = \pi/m$[12, 73]. Although there is a finite energy gap for quasihole/quasielectron excitations in the bulk, there are gapless edge excitations[217] on the boundary of these correlated FQH liquids. Another important feature of these gapped FQH states is robust (against any local perturbations) ground state degeneracy depending on the topology of the manifolds: *e.g.* Langhlin state at filling fraction $\nu = 1/m$ have m^g-fold degenerate ground states on a genus-g Riemann surface. As a consequence these non-symmetry-breaking "orders" in FQH liquids are termed "topological orders"[218], since the physical properties such as quasiparticle charge/statistics and ground state degeneracy are topological invariants and stable against perturbations. Later Laughlin's idea was generalized to other filling fractions[67, 73, 94, 172] and associated ground state wavefunctions are constructed. These states all have quasiparticles obeying (anyonic) abelian statistics and they are called abelian FQH states. It has be shown that the topological orders in any abelian FQH state are fully characterized by a matrix whose elements are all integers, called K-matrix[219]. This K-matrix allows allows us to obtain all topological properties of an abelian FQH state, such as quasiparticle charge/statistics, ground state degeneracy and structure of edge states.

Possibility of quasiparticles obeying non-abelian statistics in FQH states is first revealed by Moore and Read[140]. Their idea was to construct trial wavefunctions of

FQH states as correlation functions of certain conformal field theories[36]. They found that the FQH wavefunction constructed from Ising conformal field theory (CFT) has quasihole excitations described by the disorder operator of Ising CFT, and these quasiholes actually obey non-abelian statistics[147]. This so-called Moore-Read pfaffian state is likely to be the true ground state of $\nu = 5/2$ FQHE[234]. Other trial wavefunctions of non-abelian FQH states have also been proposed for other filling fraction[216, 176]. Unlike abelian FQH states, these non-abelian FQH states cannot be characterized by their K-matrices. So a natural question is: how to systematically characterize the topological orders in these non-abelian FQH states? Or more precisely, how to extract a set of data as the "ID" of a non-abelian FQH state from its trial wavefunction? In Chapter 2 we will give a (partial) answer to this problem.

Recently non-abelian FQH states attracted lots of attention due to their potential use in topological quantum computation[146]. To be precise, when there are multiple quasiparticles which obey non-abelian statistics in the system, the degenerate ground states can serve as qubits in a fault-tolerant quantum computer and operations on the qubits can be realized by braiding these non-abelian anyons[34]. Among these non-abelian states, Moore-Read pfaffian state is a most promising candidate that might be realized in practical materials, *i.e.* $\nu = 2 + 1/2 = 5/2$ FQHE[234] of two-dimensional electron gas in GaAs/AlGaAs heterostructures. There is a simple explanation of this non-abelian FQH state based on the composite fermion picture of FQHE. The basic idea of composite fermion picture[94] is to attach an even number of flux quanta to each electrons to form a "composite fermion" and these composite fermions effectively see a different magnetic field than the external field.

Although it's difficult to figure out ground state of electrons, the composite fermions may still form a rather "normal" state. This simple picture interprets a large class of FQH states in a unified framework[96], *e.g.* the Laughlin state at filling fraction $\nu = 1/(2m+1),\ m = 0, 1, 2\cdots$ can be understood as one filled LLL of composite fermions each of which combines one electron and $2m$ flux quanta. In this picture Moore-Read pfaffian state corresponds to a chiral $p+\mathrm{i}p$ triplet superconductor of spin-polarized composite fermions. By combining two flux quanta with one electron to form a composite fermion, for filling fraction $\nu = 1/2$ the composite fermions don't see any magnetic field on average and a "composite fermi liquid" has been proposed[74] to be the ground state of a half-filled LLL. However due to the Aharonov-Bohm effect, the composite fermions not only interact with each other through Coulomb force (inherited from electrons) but there are so-called statistical interactions between them as well. Formally this statistical interaction is described by a Chern-Simons gauge field[59, 243, 171] coupled to composite fermions. Fluctuations of this gauge field around its saddle-point is important for a half-filled LLL since it might lead to instabilities of the composite fermi liquid. Previous perturbative calculations of the gauge field fluctuations are not controllable treatments and even lead to opposite conclusions[62, 25]. Are there any non-perturbative way in which we can take care of the gauge fluctuations and find a reliable ground state for composite fermions? Recently FQHEs at $\nu = 1/2$ and $1/4$ have been observed in wide GaAs quantum wells[132, 190, 189], whose electron density are higher than previous experiments that reported no signs of FQHE. How to explain this experimental observation? These two questions will be answered in Chapter 3.

1.4 Quantum spin liquids

The simplest and most well-known model to study strongly correlated electrons (*e.g.* in *d*-electron system) is the one-band tight-binding Hubbard model[14]:

$$H_{hubbard} = -t \sum_{<ij>} \sum_{\sigma=\uparrow,\downarrow} c^{\dagger}_{i,\sigma} c_{j,\sigma} + U \sum_{i} c^{\dagger}_{i,\uparrow} c_{i,\uparrow} c^{\dagger}_{i,\downarrow} c_{i,\downarrow} \tag{1.2}$$

where $< i, j >$ represents i, j being nearest neighbors (NNs) on the lattice. Hopping parameter t controls the bandwidth while on-site Coulomb repulsion energy U controls electron correlation in the system. At half-filling with one electron per site, the charge fluctuations will be suppressed when U/t is large enough since Hubbard U provides an energy barrier for any charge transfer. Such an interaction-driven insulator at half-filling is intrinsically different from a usual band insulator (with an even number of electrons per unit cell) and is called a *Mott insulator*[1]. In the weak coupling limit when U/t is small, the ground state should be metallic with a half-filled band. Therefore there is a metal-insulator transition (MIT)[87] called Mott transition[2], occurring at an intermediate value of U/t. Starting from half-filling, a Mott insulator can be destroyed either by changing U/t (called bandwidth-controlled MIT of BC-MIT) or by changing the carrier density (the average electron number per site) n through doping (called filling-controlled MIT or FC-MIT) as shown in FIG. 1.3.

At half-filling the electron spin on each site is the only low-energy degree of freedom

[1]Strictly speaking a Mott insulator has an odd number of electrons per unit cell. However in some cases even when there are even electrons per unit cell such as a half-filled band on honeycomb lattice, in large U/t limit the insulating phase is driven by Hubbard interaction and cannot be continuously tuned into a band insulator without a phase transition. In this sense we still term it a Mott insulator.

[2]There is an exception in one dimension: it has been proved[125] that there is no Mott transition for one-band Hubbard model in 1-D.

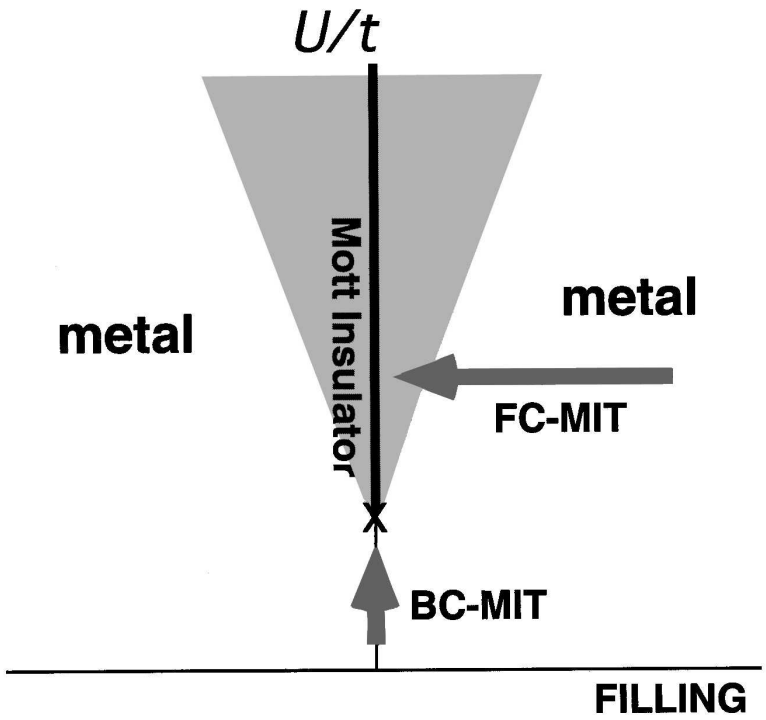

Figure 1.3: Metal-insulator phase diagram based on one-band Hubbard model in the plane of U/t and filling n. Shaded area stands for the Mott insulator phase. Two routes for the MIT (metal-insulator transition) are shown: the FC-MIT (filling-control MIT) and the BC-MIT (bandwidth-control MIT). Figure from Ref. [87].

in large U/t limit, and the low-energy effective Hamiltonian for the electron spins $\{\vec{S}_i\}$ can be obtained by perturbation theory from (1.2):

$$H_{eff} = \frac{4t^2}{U} \sum_{<i,j>} \vec{S}_i \cdot \vec{S}_j + O(\frac{t^3}{U^2}) \tag{1.3}$$

The leading-order term can be calculated from 2nd-order perturbation theory[63] and is called the (isotropic) spin-1/2 Heisenberg model. In many cases around half-filling certain magnetic (depending on the lattice geometry) order will develop in the Mott insulator due to the Heisenberg interaction. For example on square lattice an antiferromagnetic *Néel* order as shown in FIG. 1.4 is formed to minimize the interaction energy. This magnetic order generally exists in many bipartite[3] lattices in the strong-coupling limit of Hubbard model at half-filling. Notice that for the classical spin configuration of *Néel* order can simultaneously minimize *every single term* $\vec{S}_i \cdot \vec{S}_j, \quad < i, j >$ of the NN Heisenberg model. On the other hand, one can see from FIG. 1.4 on a triangular lattice (not bipartite) in each plaquette the three NN terms cannot be simultaneously minimized by any classical spin configuration. This classical effect against ordering is called *geometric frustration*[15]. For a system of spin-1/2 quantum magnets the quantum fluctuations around the classical ordering pattern (or the saddle point) is also large. Both geometric frustration and quantum fluctuation would jeopardize the ordering tendency at low temperature and therefore frustrated quantum magnets have been considered as an promising candidate to look for a king of exotic phases featured by disordered spins at zero temperature called *quantum spin liquids*. The definition of spin liquids is given as follows[161]:

[3] A bipartite lattice can be divided into two sublattices, so that all nearest neighbors of sublattice A belong to sublattice B.

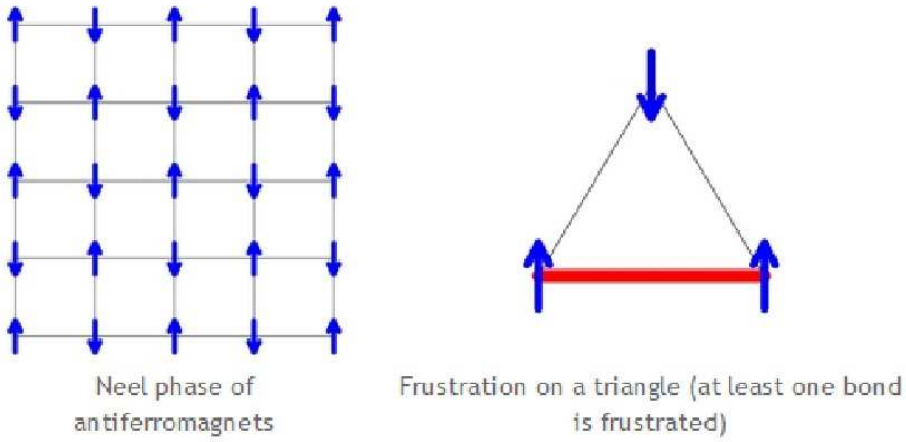

Figure 1.4: The effect of geometric frustration for nearest-neighbor antiferromagnetic Heisenberg model: a pictorial illustration.

A spin liquid has a ground state in which there is no long-range magnetic order and no breaking of spatial symmetries (rotation or translation) and which is not adiabatically connected to the band (Bloch) insulator.

Theoretically spin liquid states have been shown to exist as the ground state of certain artificial models which can be exactly solved[179, 138, 226, 101, 102]. They are divided into four subclasses[225]: rigid (or gapped) spin liquids, fermi spin liquids, bose spin liquids and algebraic spin liquids. Usually these spin liquid states have fractionalized quaisparticles, such as *spinons* which carry only spin but no charge. For example rigid spin liquid is described by spinons coupled with a gauge fields, where the spectra of both spinon and vison (gauge flux excitations) have an energy gap separating the ground states and excited states. Experimental signatures of quantum spin liquids are also observed[115, 15]. However whether these exotic phases can be the ground states of simple and physically realistic models (such as Hubbard model and Heisenberg model) remains enigmatic for a long time.

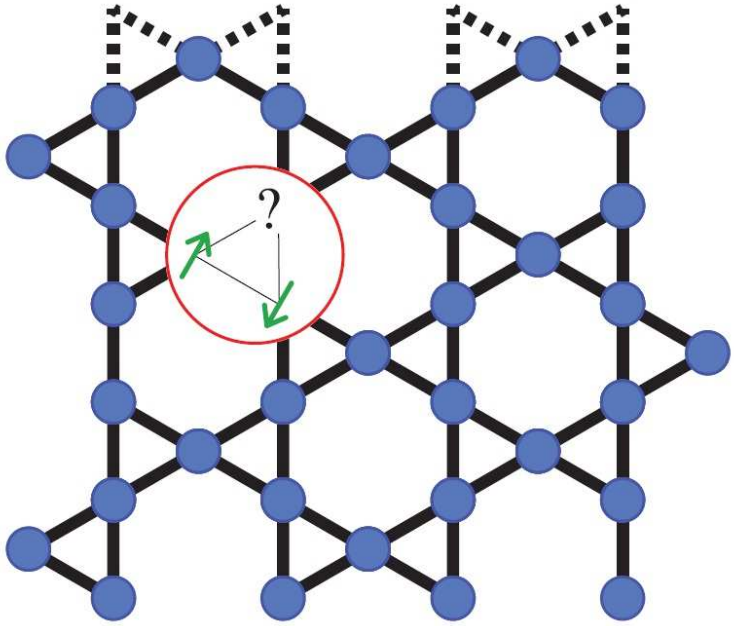

Figure 1.5: The two-dimensional kagome lattice. Figure from Ref. [240].

Recently there are evidences of spin liquid ground state in numerical studies of NN spin-1/2 Heisenberg model on kagome lattice[240], which is a highly-frustrated two dimensional lattice as shown by FIG. 4.1. A fully gapped ground state is found which preserves all lattice symmetry as well as spin rotational symmetry. They even observed signatures of Z_2 gauge fields in this spin liquid state. What is the nature of this spin liquid state? Can one construct a variational wavefunction for this exotic state which allows further understanding of this quantum spin liquid? These questions will be answered in Chapter 4.

Even on a bipartite lattice free from geometric frustration, quantum fluctuations could be very strong close to the Mott transition and they can drive the system into a disordered spin liquid state. Another remarkable numerical discovery made recently on the honeycomb lattice Hubbard model (1.2) at half-filling[136]: by tuning U/t a

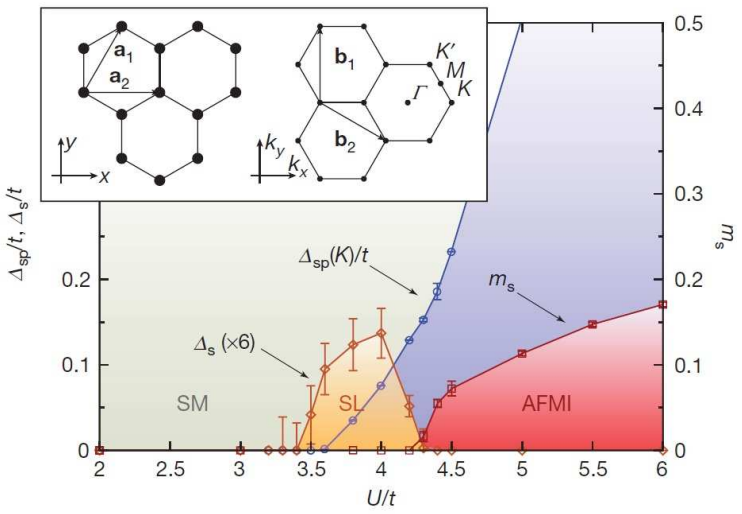

Figure 1.6: The U/t phase diagram of half-filled Hubbard model on honeycomb lattice. SM is short for semimetal, SL for spin liquid and AFMI for antiferromagnetic Mott insulator. Figure from Ref. [136].

spin liquid phase emerges between antiferromagnetic (AF) Mott insulating phase and the semimetal phase as shown in FIG. 1.6. This spin liquid is also a fully gapped phase for both charge and spin excitations and it is connected to both the semimetal phase and the AF ordered insulating phase by continuous phase transitions as suggested by numerical results[136]. What is the nature of this spin liquid phase? How to understand the continuous phase transitions between this spin liquid phase and the other two phases? In Chapter 5 we'll answer these questions and give a systematic way to identify the neighboring phases of a spin liquid state.

1.5 Topological superconductors and Majorana bound states

It has long been believed that a superconductor is fully characterized by the symmetry of its pairing order parameter[9, 193]. Given a symmetry group related to the structure of a specific material, the possible superconducting phases are believed to be classified by the symmetry breaking pattern of the pairing order parameter. In other words, the pairing order parameter (corresponding to the minimum of the associated Ginzburg-Landau free energy) breaks the original symmetry group[4] into one of its subgroup and this subgroup characterizes the superconducting state. However this is not true: even with fixed symmetry of pairing order parameter, phase transitions driven by *e.g.* doping or pressure can happen in a superconductor. Symmetry is not enough to characterize such a superconductor, and we need new quantum numbers to label the superducting phases. In a large class of superconductors these new quantum numbers are topological invariants robust against perturbations[5] and these superconducting phases are called *topological superconductors*.

Consider a two-dimensional superconductor which can be well described by the following mean-field Hamiltonian of spinless fermions in momentum space

$$H_{MF} = \sum_{\mathbf{k}} (\epsilon_{\mathbf{k}} - \mu) c^\dagger_{\mathbf{k}} c_{\mathbf{k}} + \Delta_{\mathbf{k}} c^\dagger_{\mathbf{k}} c^\dagger_{-\mathbf{k}} + \text{ h.c.} \tag{1.4}$$

where $\epsilon_{\mathbf{k}}$ is the kinetic energy (or band structure) and $\Delta_{\mathbf{k}}$ is the pairing order param-

[4]The total symmetry group is generated by all lattice symmetries, time reversal symmetry, spin rotational symmetry, and $U(1)$ gauge symmetry associated with electromagnetic field.

[5]Some topological superconductors are protected by certain symmetries, such as time reversal symmetry. They are robust against any perturbations that preserve these symmetries. The classification of topological superconductors are studied in Ref. [186, 103, 49, 50].

eter. μ is the chemical potential which can be tuned by changing the carrier density. For a chiral $p-\mathrm{i}p$ superconductor in the longwavelength limit we have $\xi_{\mathbf{k}} = \hbar^2 k^2/2m$ and $\Delta_{\mathbf{k}} = v_\Delta(k_x - \mathrm{i}k_y)$. With a fixed order parameter, as chemical potential μ changes sign the system would go through a phase transition[176]. $\mu < 0$ corresponds to a trivial superconductor with no stable edge states or any bound states in the vortex core, called the *strong pairing phase*. When $\mu > 0$ the superconductor enters a topologically nontrivial phase featured by stable gapless neutral modes on the edge and majorana bound states in its vortex core[176], called the *weak pairing phase*. To be precise, by solving the Bogoliubov-de-Gennes equation for a half-flux-quantum vortex configuration, one find that there is a zero-energy bound state localized in the vortex core. These half-flux-quantum vortices obey non-abelian statistics[91, 200] and are analogs of fractional quasiparticles in the Moore-Read pfaffian state in $\nu = 5/2$ FQHE[6]. The new quantum number which differentiate these two phases is the winding number Q of the following "pseudospin vector"[5, 6]

$$\vec{n}_{\mathbf{k}} \equiv \frac{\mathrm{Re}\Delta_{\mathbf{k}}, -\mathrm{Im}\Delta_{\mathbf{k}}, \xi_{\mathbf{k}} - \mu}{E_{\mathbf{k}}}, \quad E_{\mathbf{k}} = \sqrt{(\epsilon_{\mathbf{k}} - \mu)^2 + |\Delta_{\mathbf{k}}|^2}. \tag{1.5}$$

in the whole momentum space[7]. Winding number is always an integer: $Q = 0$ in the strong pairing state and $Q = 1$ in the weak pairing phase. In fact the winding number is well defined for any fully gapped (singlet or triplet) superconductor and for spin-unpolarized superconductors Q is proportional to the quantized Hall spin conductance[176]. However if the superconductor is gapless (such as the critical point

[6] As mentioned earlier the Moore-Read pfaffian state is in fact a chiral p-wave superconductor of composite fermions.

[7] Mathematically this winding number Q is the degree of the following mapping: $\mathbf{k} \to \vec{n}_{\mathbf{k}}$. It corresponds to the homotopy class of $\pi_2(S^2)$.

between strong and weak pairing phase) the winding number Q will not be well-defined anymore.

In many strongly-correlated electronic systems such as high-Tc cuprates[118] and heavy fermion compounds[126], unconventional (*i.e.* not conventional s-wave) singlet superconducting orders appear in proximity or even coexists with magnetic orders in low temperature. The phase diagram of $CeRhIn_5$ in FIG. 1.1 is an example where the superconducting order is likely to be d-wave singlet superconductor with nodal excitations[238]. Can a topologically non-trivial phase arises in coexistence of nodal singlet superconductivity and magnetic orders, which hosts majorana bound states in its vortex core? In Chapter 6 we'll give a positive answer to this question and propose a new route to realize majorana fermion bound states in two-dimensional strongly correlated electrons. These non-abelian quasiparticles, once realized, could become the building block of a fault-tolerant topological quantum computer[146].

1.6 Novel correlated phases in partially-filled topological flat bands

The standard QHE was first discovered in semiconductor heterostructures[105, 207], where the electrons gas essentially lives in two-dimensional free space. The mere effect of the surrounding lattice is to change the effective mass of electrons. On the other hand, a uniform magnetic field does two things: it breaks time reversal symmetry and it quantizes the electrons with Landau levels. Are these two factors crucial for the QHE? The answer is no for integer QHE. In a landmark paper Haldane

constructed a tight-binding lattice model which exhibits IQHE in the absence of magnetic field[68]. In his model, time-reversal symmetry is broken by a spatially inhomogeneous magnetic field with zero average, and the Hall conductance equals the Chern number, an integer depending on the momentum topology of the band. Such a band with nontrivial momentum topology is called a Chern band. The next question is: can FQHE, driven by interaction/correlation effects in a fractionally filled Landau level, also be separated from the weak lattice and uniform magnetic field limit? More precisely, if it is true in weak correlation limit that a filled Chern band is equivalent to a filled Landau level, is it also true in the strong correlation limit?

The answer is yes, when the bandwidth of the Chern band is small compared with interaction energy scale. Recently FQHE has been theoretically proposed[204, 202, 149] and numerically discovered[149, 191] in flat Chern bands. These phases are lattice versions of FQH states and are called *fractional Chern insulators*. Numerical results also suggest that these fractional Chern insulators (FCIs) preserve all lattice symmetries. Since the symmetry group of any lattice is only a subgroup of the free space symmetry group, with lower symmetry requirements could there be more than one FCI states corresponding to a certain filling fraction?

Besides, in associated lattice models that preserve time reversal symmetry, each flat Chern band is almost degenerate with its time reversal counterpart. What happens when such a pair of so-called Z_2 flat bands are partially filled? Numerical studies[148] suggest that a class of time-reversal-symmetric fractionalized phases, called *fractional topological insulators* may appear. What are the nature of these

phases realized in a lattice model? Can we write down some variational wavefunctions which could help analytical understanding of these phases? All the above questions will be answered in Chapter 7.

Chapter 2

Vertex algebra characterization of non-abelian quantum Hall states

2.1 Introduction

Materials can have many different forms, which is partially due to the very rich ways in which atoms and electrons can organize. The different organizations correspond to different phases of matter (or states of matter). It is very important for physicists to understand these different states of matter and the phase transitions between them. At zero-temperature, the phases are described by the ground state wave functions, which are complex wave functions $\Phi(\mathbf{r}_1, \mathbf{r}_2, \cdots, \mathbf{r}_N)$ with $N \to \infty$ variables. So mathematically, to describe zero-temperature phases, we need to characterize and classify the ground state wave functions with ∞ variables, which is a very challenging mathematical problem.

For a long time we believe that all states of matter and all phase transitions

between them are characterized by their broken symmetries and the associated order parameters[110]. A general theory for phases and phase transitions is developed based on this symmetry breaking picture. So within the paradigm of symmetry breaking, a many-body wave function is characterized by its symmetry properties. Landau's symmetry breaking theory is a very successful theory and has dominated the theory of phases and phase transitions until the discovery of fractional quantum Hall (FQH) effect[207, 114].

FQH states cannot be described by symmetry breaking since different FQH states have exactly the same symmetry. So different FQH states must contain a new kind of order. The new order is called topological order[218, 223, 225] and the associated phase called topological phase, because their characteristic universal properties (such as the ground states degeneracy on a torus[218]) are invariant under *any* small perturbations of the system. Unlike symmetry-breaking phases described by local order parameters, a topological phase is characterized by a pattern of long-range quantum entanglement[104, 123, 124]. In Ref. [215], the non-Abelian Berry phases for the degenerate ground states are introduced to systematically characterize and classify topological orders in FQH states (as well as other topologically ordered states). In this chapter, we further develop another systematic characterization of the topological orders in FQH states based on the pattern of zeros approach.[229, 228]

In the strong magnetic field limit, a FQH wave function with filling factor $\nu < 1$ is an anti-symmetric holomorphic polynomial of complex coordinates $\{z_i = x_i + \mathrm{i}y_i\}$ (except for a common factor that depends on geometry: say, a Gaussian factor $\exp\left(\sum_i \frac{|z_i|^2}{4}\right)$ for a planar geometry). After factoring out an anti-symmetric factor

of $\prod_{i<j}(z_i - z_j)$, we can describe a quantum Hall state by a symmetric polynomial $\Phi(z_1, \cdots, z_N)$ in the $N \to \infty$ limit.[**?**] So the characterization and classification of long-range quantum entanglements in FQH states become a problem of characterizing and classifying symmetric polynomials with infinite variables.

In a recent series of work,[229, 228, 16] the pattern of zeros is introduced to characterize and classify symmetric polynomials of infinite variables. The pattern of zeros is described by a sequence of integers $\{S_a | a = 1, 2, ...\}$, where S_a is the lowest order of zeros of the symmetric polynomial when we fuse a different variables together. The data $\{S_a | a = 1, 2, ...\}$ can be further compactified into a finite set $\{n; m; S_a | a = 1, 2, ..., n; n, m \in \mathbb{N}\}$ for n-cluster quantum Hall states. Here $\mathbb{N} = \{0, 1, 2, ...\}$ is the set of non-negative integers. It has been shown[229, 228] that all known one-component Abelian and non-Abelian quantum Hall states can be (partially) characterized by pattern of zeros. It is also shown[229, 228] that, for any given pattern of zeros $\{S_a\}$, we can construct an ideal local Hamiltonian[67, 162, 62, 178, 175] $H_{\{S_a\}}$ such that the FQH state with the pattern of zeros is a zero energy ground state of the Hamiltonian.

We would like to point out that, strictly speaking, a FQH state must be a state with a finite energy gap. But in this chapter, we will use the term more loosely. We will call one state a FQH state if it can be an zero energy state of an ideal Hamiltonian. So our FQH states may not be gapped.

Due to the length of this chapter, in the following, we are going to summarize the issues that we are going to discuss in this chapter. We will also summarize the main results that we obtain on those issues.

2.1.1 Sufficient conditions on pattern of zeros

Within the pattern-of-zero approach, two questions naturally arise: (1) Does any pattern of zeros, *i.e.* an arbitrary integer sequence $\{n; m; S_a\}$ corresponds to a symmetric polynomial $\Phi(z_1, \cdots, z_N)$? Are there any "illegal" patterns of zeros that do not correspond to any symmetric polynomial? (2) Given a "legal" pattern of zeros, can we construct a corresponding FQH many-body wave function? Is the FQH many-body wave function uniquely determined by the pattern of zeros?

For question (1), it turns out that the pattern of zeros must satisfy some consistent conditions[229, 228] in order to describe an existing symmetric polynomial. In other words, some sequences $\{n; m; S_a\}$ don't correspond to any symmetric polynomials. However, Ref. [229, 228] only obtain some necessary conditions on the pattern of zeros $\{n; m; S_a\}$. We still do not have a set of sufficient conditions on pattern of zeros that guarantee a pattern of zeros to correspond to an existing symmetric polynomial.

For the question (2), right now, we do not have an efficient way to obtain corresponding FQH many-body wave function from a "legal" pattern of zeros. Further more, while some patterns of zeros can uniquely determine the FQH wave function, it is known that some other patterns of zeros cannot uniquely determine the FQH wave function: *i.e.* in those cases, two different FQH wave functions can have the same pattern of zeros.[229, 195] This means that, some patterns of zeros do not provide complete information to fully characterize FQH states. In this case it is important to expand the data of pattern of zeros to obtain a more complete characterization of FQH states.

We see that the above two questions are actually closely related. In this chapter,

we will try to address those questions. Motivated by the conformal field theory (CFT) construction of FQH wave functions,[140, 221, 230, 54, 11] we will try to use the patterns of zeros to define and construct vertex algebras (which are CFTs). Since the correlation function of the electron operator in the constructed vertex algebra gives us the FQH wave function, once the vertex algebra is obtained from a pattern of zeros, we effectively find the corresponding FQH wave function for the pattern of zeros. In this way, we establish the connection between the pattern of zeros and the FQH wave function through the vertex algebra.

In order for the correlation of electron operators in the vertex algebra to produce a single-valued electron wave function with respect to electron variables $\{z_1, \cdots, z_N\}$, electron operators need to satisfy a so-called "simple-current" property (see eqn. (2.23) and eqn. (2.40)). Also the vertex algebra need to satisfy the generalized Jacobi identity (GJI) which guarantees the associativity of the corresponding vertex algebra.[151] We find that only a certain set of patterns of zeros can give rise to simple-current vertex algebras that satisfy the GJI. So the GJIs in simple-current vertex algebras give us a set of sufficient conditions on a pattern of zeros so that this pattern of zeros does correspond to an existing symmetric polynomial.

In this chapter, we first try to use the pattern of zeros $\{n; m; S_a\}$ to define a Z_n vertex algebra. From some of the GJI of the Z_n vertex algebra, we obtain more necessary conditions on the pattern of zeros $\{n; m; S_a\}$ than those obtained in Ref. [229, 228] (see section 2.3). It is not clear if those conditions are actually sufficient or not.

Then, we try to use the pattern of zeros $\{n; m; S_a\}$ to define a Z_n simple-current vertex algebra. From the complete GJI of the Z_n simple-current vertex algebra, we

obtain sufficient conditions on the pattern of zeros $\{n; m; S_a\}$ (see section 2.4).

2.1.2 How to expand the pattern-of-zeros data to completely characterize the topological order

If a pattern of zeros $\{n; m; S_a\}$ can uniquely describe the topological order in a quantum Hall ground state, then from such a quantitative description, we should be able to calculate the topological properties from the data $\{n; m; S_a\}$. Indeed, this can be done. First different types of quasiparticles can also be quantitatively described and labeled by a set of sequences $\{S_{\gamma;a}\}$ that can be determined from the pattern-of-zeros data $\{n; m; S_a\}$[228]. Those quantitative characterizations of the quantum Hall ground state and quasiparticles allow us to calculate the number of different quasiparticle types, quasiparticle charges, fusion algebra between the quasiparticles, and topological ground state degeneracy on a Riemann surface of any genus.[228, 16]

However, from the pattern-of-zeros data, $\{n; m; S_a\}$ and $\{S_{\gamma;a}\}$, we still do not know how to calculate the quasiparticle statistics and scaling dimensions, as well as the central charge c of the edge states. This difficulty is related to the fact that some patterns of zeros do not uniquely characterize a FQH state. Thus one cannot expect to calculate the topological properties of FQH state from the pattern-of-zeros data alone in those cases.

In this chapter, we will try to solve this problem. We first introduce a more complete characterization for FQH states in terms of a expanded data set: $\{n; m; S_a; c\}$. Then, we use the data set $\{n; m; S_a; c\}$ to define a so called Z_n simple-current vertex algebra. The Z_n simple-current vertex algebra contain a subalgebra, Virasoro

algebra, generated by the energy-momentum tensor T and c is the central charge of the Virasoro algebra. It contains only n primary fields ψ_a, $a = 0, 1, ..., n-1$ of the Virasoro algebra, with a Z_n fusion rule $\psi_a\psi_b \sim \psi_{(a+b) \bmod n}$, $\psi_n = \psi_0$. Those ψ_a are called simple currents. The extra data c is the one of the structure constants of the Z_n simple-current vertex algebra. One may want to include all the structure constants $\{C_{ab}\}$ in the data set to have a complete characterization. But for the examples discussed in this chapter, we find that data set $\{n; m; S_a; c\}$ already provides a complete characterization. So in this chapter, we will use $\{n; m; S_a; c\}$ to characterize FQH states. If later we find that $\{n; m; S_a; c\}$ is not sufficient, we can always add additional data, such as C_{ab}. Every Z_n simple-current vertex algebra uniquely define a FQH state, and the data $\{n; m; S_a; c\}$ that defines a Z_n simple-current vertex algebra also completely characterizes a FQH state.

We would like to remark that although the data $\{n; m; S_a; c\}$ and the corresponding Z_n simple-current vertex algebras describe a large class of FQH states, they do not describe all FQH states. For example let $\Phi_{\mathcal{A}_i}$ be the FQH wave function described by a Z_{n_i} simple-current vertex algebra $\mathcal{A}_i$, $i = 1, 2$. Then, in general, the FQH state described by the product wave function $\Phi = \Phi_{\mathcal{A}_1}\Phi_{\mathcal{A}_2}$ cannot be described by a simple-current vertex algebra. Such a product state is described by the product vertex algebra $\mathcal{A}_1 \otimes \mathcal{A}_2$, which is in general no longer a simple-current vertex algebra. So a more general FQH state should have a form

$$\Phi = \prod_i \Phi_{\mathcal{A}_i}. \tag{2.1}$$

The study in Ref. [229, 228, 16] reveal that many FQH states described by pattern

of zeros have the following form

$$\Psi(\{z_i\}) = \prod_a \Phi_{Z_{n_a}^{(k_a)}}(\{z_i\}) \tag{2.2}$$

where $\Phi_{Z_{n_a}^{(k_a)}}(\{z_i\})$ is the wave function described by $Z_{n_a}^{(k_a)}$ parafermion vertex algebra.[16] The Z_n simple-current vertex algebra mentioned above is a natural generalization of the $Z_{n_a}^{(k_a)}$ parafermion vertex algebra, and eqn. (2.1) naturally generalizes eqn. (2.2). (Note that there are many Z_n simple-current vertex algebras even for a fixed n, so there are many different Z_n simple-current states.)

For the subclass of FQH states described by Z_n simple-current vertex algebra (which includes Virasoro algebra as an essential part), the quasiparticle statistics and scaling dimensions, as well as the central charge c of the edge states can be calculated from the data $\{n; m; S_a; c\}$. Certainly, we can also calculate the number of different quasiparticle types, quasiparticle charges, fusion algebra between the quasiparticles, and topological ground state degeneracy on a Riemann surface of any genus.

Obviously, not every collection $\{n; m; S_a; c\}$ corresponds to a Z_n simple-current vertex algebra and a FQH state. GJIs of the Z_n simple-current vertex algebra generate the consistent conditions on the data set $\{n; m; S_a; c\}$. Only those data sets $\{n; m; S_a; c\}$ that satisfy the GJIs can describe a Z_n simple-current vertex algebra and FQH states.

For some patterns of zeros $\{n; m; S_a\}$, we find that they uniquely define the vertex algebras by completely determining the structure constants c and C_{ab}. So those patterns of zeros completely specify the corresponding FQH wave functions. While for other patterns of zeros, we find that they cannot uniquely define the vertex algebras. For those patterns of zeros, many different sets of structure constants can satisfy

the GJIs for the same set of pattern of zeros. This corresponds to the situation where there are many different FQH wave functions that share the same pattern of zeros. In this case, the pattern of zeros does not completely characterize FQH wave functions. We need additional data to completely characterize quantum Hall wave functions. Here we choose to add the structure constant c of the Virasoro algebra (which is the central charge) and use $\{n; m; S_a; c|a = 1, ..., n; n, m, S_a \in \mathbb{N}; c \in \mathbb{R}\}$ to characterize FQH states. For all the examples that we considered in this chapter, the data $\{n; m; S_a; c\}$ completely determine the simple-current vertex algebra.

Due to the limited length of this chapter, we refer Ref. [130] to interested readers where *i.e.* lots of different FQH wavefunctions are discussed as examples of our Z_n vertex algebra description. The characterization of quasiparticles in these non-Abelian FQH states are also discussed in Ref. [130].

2.2 Pattern-of-zeros approach to generic FQH states

In this section, we will review how to use the pattern of zeros to characterize and classify different FQH states that have one component.[229, 228, 16] A discussion on two-component FQH states can be find in Ref. [17].

2.2.1 FQH wave functions and symmetric polynomials

Generally speaking, to classify generic complex wave functions $\Phi(\mathbf{r}_1, \cdots, \mathbf{r}_N)$ is not even a well-defined problem. Fortunately, under a strong magnetic field, electrons are spin-polarized in the lowest Landau level (LLL) when the electron filling fraction ν_e is less than 1. The wave function of a single electron in LLL (we set magnetic length

$l_B = \sqrt{\hbar/eB}$ to be unity hereafter) is $\Psi_m(z) = z^m \mathrm{e}^{-|z|^2/4}$ in a planar geometry. m is the angular momentum of this single particle state. Thus the many-body wave function of *spin-polarized* electrons in the LLL should be

$$\Psi_e(z_1, \cdots, z_N) = \tilde{\Phi}_e(z_1, \cdots, z_N) \mathrm{e}^{-\sum_{i=1}^{N} \frac{|z_i|^2}{4}} \tag{2.3}$$

where $\tilde{\Phi}_e(\{z_i\})$ is an anti-symmetric holomorphic polynomial of electron coordinates $\{z_i = x_i + \mathrm{i}y_i\}$. The electron filling fraction ν_e is defined as:

$$\nu_e = \lim_{N\to\infty} \frac{N}{N_\phi} = \lim_{N\to\infty} \frac{N^2}{2N_p} \tag{2.4}$$

where N_ϕ is the total number of flux quanta piercing through the sample, and N_p is the total degree of polynomial $\tilde{\Phi}_e(\{z_i\})$. For FQH states $\nu_e < 1$, we can extract a Jastraw factor $\prod_{i<j}(z_i - z_j)$ and the remaining part

$$\Phi(z_1, \cdots, z_N) = \frac{\tilde{\Phi}_e(z_1, \cdots, z_N)}{\prod_{i<j}(z_i - z_j)} \tag{2.5}$$

would be a symmetric polynomial of $\{z_i\}$. We will concentrate on this symmetric polynomial to characterize and classify FQH states.

For the symmetric polynomial $\Phi(\{z_i\})$ we can also define a filling fraction ν in the same way as in eqn. (2.4), only N_p replaced by the total degree of bosonic polynomial $\Phi(\{z_i\})$. The electron filling fraction ν_e has the following relation with this *bosonic filling fraction* ν:

$$\nu_e = \frac{1}{1 + \nu^{-1}} < 1 \tag{2.6}$$

2.2.2 Fusion of a variables: the Pattern of Zeros

The pattern of zeros[229, 228] is introduced to describe symmetric polynomials $\Phi(\{z_i\})$ through certain local properties, i.e. fusion of a different variables $z_1, \cdots, z_a$.

More specifically, we bring these a variables together, viewing $z_{a+1}, \cdots, z_N$ as fixed coordinates. By writing the a variables in the following manner $z_i = \lambda\xi_i + z^{(a)}$, $i = 1, \cdots, a$, where $z^{(a)} = \frac{z_1+\cdots+z_a}{a}$ and $\sum_{i=1}^{a} \xi_a = 0$, we can bring these a variables together by letting λ tend to zero. Then we can expand the polynomial $\Phi(\{z_i\})$ in powers of λ:

$$\begin{aligned} &\lim_{\lambda\to 0^+} \Phi(\lambda\xi_1 + z^{(a)}, \cdots, \lambda\xi_a + z^{(a)}; z_{a+1}, \cdots, z_N) \\ &= \lambda^{S_a} P_{S_a}[z^{(a)}, (\xi_1, \cdots, \xi_a); z_{a+1}, \cdots, z_N] + O(\lambda^{S_a+1}) \end{aligned} \tag{2.7}$$

In other words, $\{S_a\}$ is the lowest order of zeros when we fuse a variables together. The pattern of zeros, by definition, is this sequence of integers $\{S_a\}$. In this chapter, we will only consider the polynomials that satisfy a unique fusion condition: the fusion of a variables is unique, i.e. P_{S_a} in eqn. (2.7) has the same form except for an overall factor no matter how $\{\xi_i\}$ are chosen.

There are other equivalent descriptions of the pattern of zeros. One of them is the orbital description:

$$l_a = S_a - S_{a-1} \quad a = 1, 2, \cdots \tag{2.8}$$

where $\{l_a\}$ labels the orbital angular momentum of the single-particle state occupied by the a-th particle. Another is the occupation description in terms of a sequence of integers $\{n_l\}$[188, 22, 24, 23], denoting the number of particles occupying the orbital with angular momentum l.

2.2.3 Consistent conditions for the Pattern of Zeros

To summarize, the pattern of zeros for an n-cluster polynomial is described by a set of positive integers $\{n; m; S_2, ..., S_n\}$. Introducing $S_1 = 0$ and

$$S_{a+kn} = S_a + kS_n + mn\frac{k(k-1)}{2} + kma \tag{2.9}$$

which define S_{n+1}, S_{n+2}, ..., we find that the data $\{n; m; S_2, ..., S_n\}$ must satisfy

$$\begin{aligned} D_{a,b} &= S_{a+b} - S_a - S_b \geq 0 \\ D_{a,a} &= \text{even} \end{aligned} \tag{2.10}$$

$$\begin{aligned} &\Delta_3(a,b,c) \\ &= S_{a+b+c} + S_a + S_b + S_c - S_{a+b} - S_{a+c} - S_{b+c} \geq 0 \end{aligned} \tag{2.11}$$

for all $a, b, c = 1, 2, 3 \cdots$.

The conditions (2.10) and (2.11) are necessary conditions for a pattern of zeros to represent a symmetric polynomial. Although eqn. (2.10) and eqn. (2.11) are very simple, they are quite restrictive and are quite close to be sufficient conditions. In fact if we add an additional condition

$$\Delta_3(a,b,c) = \text{even} \tag{2.12}$$

the three conditions (2.10), (2.11), and (2.12) may even become sufficient conditions for a pattern of zeros to represent a symmetric polynomial.[229, 228] However, this condition is too strong to include many valid symmetric polynomials such as Gaffnian,[194] a nontrivial Z_4 state discussed in detail in section **??**. We will obtain some additional conditions in section 2.3.3, which combined with (2.10) and (2.11)

form a set of necessary and (potentially) sufficient conditions for a valid pattern of zeros.

2.2.4 Label the pattern of zeros by $h_a^{\mathbf{sc}}$

In this section, we will introduce a new labeling scheme of the pattern of zeros. We can label the pattern of zeros in terms of

$$h_a^{\rm sc} = S_a - \frac{aS_n}{n} + \frac{am}{2} - \frac{a^2 m}{2n}. \tag{2.13}$$

This labeling scheme is intimately connected to the vertex algebra approach that we will discuss later.

The n-cluster condition (2.9) of S_a implies that $h_a^{\rm sc}$ is periodic

$$h_0^{\rm sc} = 0, \qquad h_a^{\rm sc} = h_{a+n}^{\rm sc} \tag{2.14}$$

The two sets of data $\{n; m; S_2, ..., S_n\}$ and $\{n; m; h_1^{\rm sc}, ..., h_{n-1}^{\rm sc}\}$ has a one-to-one correspondence, since

$$S_a = h_a^{\rm sc} - a h_1^{\rm sc} + \frac{a(a-1)m}{2n}. \tag{2.15}$$

We can translate the conditions on $\{m; S_a\}$ to the equivalent conditions on $\{m; h_a^{\rm sc}\}$. First, we have

$$\begin{aligned} &2nS_a = 2nh_a^{\rm sc} - 2nah_1^{\rm sc} + a(a-1)m = 0 \bmod 2n \\ &nS_{2a} = nh_{2a}^{\rm sc} - 2nah_1^{\rm sc} + a(2a-1)m = 0 \bmod 2n \\ &m > 0, \quad mn = \text{even} \end{aligned} \tag{2.16}$$

$nS_{2n} = 0 \bmod 2n$ in eqn. (2.16) leads to $2nh_1^{\rm sc} + m = 0 \bmod 2$, from which we see that $2nh_1^{\rm sc}$ is an integer. From $2nh_a^{\rm sc} - a(2nh_1^{\rm sc}) + a(a-1)m =$ even integer, we see

that $2nh_a^{\rm sc}$ are always integers. Also $2nh_{2a}^{\rm sc}$ are always even integers, and $2nh_{2a+1}^{\rm sc}$ are either all even or all odd. Since $h_n^{\rm sc}=0$, thus when $n=$ odd, $2nh_a^{\rm sc}$ are all even. Only when $n=$ even, can $2nh_{2a+1}^{\rm sc}$ either be all even or all odd. When $m=$even, $2nh_{2a+1}^{\rm sc}$ are all even. When $m=$odd, $2nh_{2a+1}^{\rm sc}$ are all odd.

The two concave conditions become

$$h_{a+b}^{\rm sc}-h_a^{\rm sc}-h_b^{\rm sc}+\frac{abm}{n}=D_{ab}=\text{integer}\geq 0 \tag{2.17}$$

$$\begin{aligned}&h_{a+b+c}^{\rm sc}-h_{a+b}^{\rm sc}-h_{b+c}^{\rm sc}-h_{a+c}^{\rm sc}+h_a^{\rm sc}+h_b^{\rm sc}+h_c^{\rm sc}\\ =\;&\Delta_3(a,b,c)=\text{integer}\geq 0\end{aligned} \tag{2.18}$$

The valid data $\{n;m;h_1^{\rm sc},...,h_{n-1}^{\rm sc}\}$ can be obtained by solving eqn. (2.14), eqn. (2.16), eqn. (2.17), and eqn. (2.18).

Choosing $1\leq a,b<a+b\leq n$ in eqn. (2.18), we have

$$\begin{aligned}0&\leq\Delta_3(a,b,n-a-b)\\ &=(h_{n-a-b}^{\rm sc}-h_{a+b}^{\rm sc})-(h_{n-a}^{\rm sc}-h_a^{\rm sc})-(h_{n-b}^{\rm sc}-h_b^{\rm sc})\\ &=-\Delta_3(n-a,n-b,a+b)\leq 0\end{aligned}$$

which implies the following *reflection condition* on $\{h_a^{\rm sc}\}$:

$$h_a^{\rm sc}-h_{n-a}^{\rm sc}=a(h_1^{\rm sc}-h_{n-1}^{\rm sc})=0 \tag{2.19}$$

From (2.19) we see that partially solving conditions (2.18) reduces the number of independent variables characterizing a pattern of zeros from $n-1$ in $\{S_2,\cdots,S_n\}$ to $[\frac{n}{2}]$ in $\{h_1^{\rm sc},\cdots,h_{[\frac{n}{2}]}^{\rm sc}\}$.

2.3 Constructing FQH wave functions from Z_n vertex algebras

If we use $\{n; m; h_a^{\text{sc}}\}$ to characterize n-cluster symmetric polynomial $\Phi(\{z_i\})$, the conditions (2.16), (2.17), and (2.18) are required by the single-valueness of the symmetric polynomial. Or more precisely, eqns. (2.16), (2.17), and (2.18) come from a simple requirement that the zeros in $\Phi(\{z_i\})$ all have integer orders. However, the conditions (2.16), (2.17), and (2.18) are incomplete in the sense that some patterns of zeros $\{n; m; h_a^{\text{sc}}\}$ can satisfy those conditions but still do not correspond to any valid polynomial.

2.3.1 FQH wave function as a correlation function in Z_n vertex algebra

To find more consistent conditions, in the rest of this chapter, we will introduce a new requirement for the symmetric polynomial. We require that the symmetric polynomial can be expressed as a correlation function in a vertex algebra. More specifically, we have[140, 221, 230]

$$\Phi(\{z_i\}) = \lim_{z_\infty \to \infty} z_\infty^{2h_N} \langle V(z_\infty) \prod_{i=1}^{N} V_e(z_i) \rangle \tag{2.20}$$

where $V_e(z)$ is an electron operator and $V(\infty)$ represents a positive background to guarantee the charge neutral condition. This new requirement, or more precisely, the associativity of the vertex algebra, leads to new conditions on h_a^{sc}.

The electron operator has the following form

$$V_e(z) = \psi(z) : \mathrm{e}^{\mathrm{i}\phi(z)/\sqrt{\nu}} : \tag{2.21}$$

where $: \mathrm{e}^{\mathrm{i}\phi(z)/\sqrt{\nu}} :$ (:: stands for normal ordering, which is implicitly understood hereafter) is a vertex operator in a Gaussian model. It has a scaling dimension of $\frac{1}{2\nu}$ and the following operator product expansion (OPE)[36]

$$\mathrm{e}^{\mathrm{i}a\phi(z)}\mathrm{e}^{\mathrm{i}b\phi(w)} = (z-w)^{ab}\mathrm{e}^{\mathrm{i}(a+b)\phi(w)} + O\Big((z-w)^{ab+1}\Big) \tag{2.22}$$

The operator ψ is a primary field of Virasoro algebra obeys an quasi-Abelian fusion rule

$$\psi_a\psi_b \sim \psi_{a+b} + ..., \qquad \psi_a \equiv (\psi)^a. \tag{2.23}$$

where ... represent other primary fields of Virasoro algebra whose scaling dimensions are higher than that of ψ_{a+b} by some integer values. We believe that the integral difference of the scaling dimensions is necessary to produce a single-valued correlation function(see eqn. (2.20)).

Let $\tilde{h}_a^{\mathrm{sc}}$ be the scaling dimension of the simple current ψ_a. Therefore the a-cluster operator

$$V_a \equiv (V_e)^a = \psi_a(z)\mathrm{e}^{\mathrm{i}a\phi(z)/\sqrt{\nu}} \tag{2.24}$$

has a scaling dimension of

$$h_a = \tilde{h}_a^{\mathrm{sc}} + \frac{a^2}{2\nu} \tag{2.25}$$

The vertex algebra is defined through the following OPE of the a-cluster operators

$$V_a(z)V_b(w) = C_{a,b}^V \frac{V_{a,b}(w)}{(z-w)^{h_a+h_b-h_{a+b}}} + O\Big((z-w)^{h_{a+b}-h_a-h_b+1}\Big). \tag{2.26}$$

where $C_{a,b}^{V}$ are the structure constants. However, the above OPE is not quite enough. To fully define the vertex algebra, we also need to define the relation between $V_a(z)V_b(w)$ and $V_b(w)V_a(z)$.

The correlation functions is calculated through the expectation value of radial-ordered operator product.[58, 36, 151] The radial-ordered operator product is defined through

$$\begin{aligned}&(z-w)^{\alpha_{V_aV_b}}R[V_a(z)V_b(w)]\\ =&\begin{cases}(z-w)^{\alpha_{V_aV_b}}V_a(z)V_b(w), & |z|>|w|\\ \mu_{ab}(w-z)^{\alpha_{V_aV_b}}V_b(w)V_a(z), & |z|<|w|\end{cases}\end{aligned} \tag{2.27}$$

where

$$\alpha_{V_aV_b}=h_a+h_b-h_{a+b}. \tag{2.28}$$

Note that the extra complex factor μ_{ab} is introduced in the above definition of radial order. In the case of standard conformal algebras, where $\alpha_{V_aV_b}\in\mathbb{Z}$, we choose $\mu_{ab}=-\mathrm{e}^{\mathrm{i}\pi\alpha_{V_aV_b}}$ if both V_a and V_b are fermionic and $\mu_{ab}=\mathrm{e}^{\mathrm{i}\pi\alpha_{V_aV_b}}$ if at least one of them is bosonic. But in general, the commutation factor can be different from ±1 and can be chosen more arbitrarily.

To gain an intuitive understanding of the above definition of radial order, let us consider the Gaussian model and choose $V_a=\mathrm{e}^{\mathrm{i}a\phi}$ and $V_b=\mathrm{e}^{\mathrm{i}b\phi}$. The scaling dimension of V_a and V_b are $h_a=\frac{a^2}{2}$ and $h_b=\frac{b^2}{2}$. $\alpha_{V_aV_b}=h_a+h_b-h_{a+b}$. We see that $\alpha_{V_aV_b}\in\mathbb{Z}$ if $a,b\in\mathbb{Z}$ and such a Gaussian model is an example of standard conformal algebras. If both a and b are odd, then h_a and h_b are half integers and V_a and V_b are fermionic operators. In this case $\alpha_{V_aV_b}=-ab=$ odd. So under the standard choice

$\mu_{ab} = -\mathrm{e}^{\mathrm{i}\pi\alpha_{V_aV_b}}$, we have $\mu_{ab} = 1$. If one of a and b is even, $\alpha_{V_aV_b} = -ab =$ even and one of V_a and V_b is bosonic operators. Under the standard choice $\mu_{ab} = \mathrm{e}^{\mathrm{i}\alpha_{V_aV_b}}$, we have again $\mu_{ab} = 1$. Even when a and b are not integers, in the Gaussian model, the radial order of $V_a = \mathrm{e}^{\mathrm{i}a\phi}$ and $V_b = \mathrm{e}^{\mathrm{i}b\phi}$ is still defined with a choice $\mu_{ab} = 1$. This is a part of the definition of the Gaussian model. In this chapter, we will choose a more general definition of radial order where μ_{ab} are assumed to be generic complex phases $|\mu_{ab}| = 1$.

The vertex algebra generated by ψ have a form

$$\psi_a(z)\psi_b(w) = C_{a,b}\frac{\psi_{a+b}(w)}{(z-w)^{\tilde{h}^{\mathrm{sc}}_a+\tilde{h}^{\mathrm{sc}}_b-\tilde{h}^{\mathrm{sc}}_{a+b}}} + O\Big((z-w)^{\tilde{h}^{\mathrm{sc}}_{a+b}-\tilde{h}^{\mathrm{sc}}_a-\tilde{h}^{\mathrm{sc}}_b+1}\Big). \tag{2.29}$$

where

$$C_{a,b} \neq 0. \tag{2.30}$$

When combined with the $U(1)$ Gaussian model, the above vertex algebra can produce the wave function for a FQH state (see eqn. (2.20)).

We will also limit ourselves to the vertex algebra that satisfies the n-cluster condition:

$$\psi_n = 1 \tag{2.31}$$

where 1 stands for the identity operator. Those vertex algebras are in some sense "finite" and correspond to rational conformal field theory. We will call such vertex algebra Z_n vertex algebra. We see that in general, a FQH state can be described by

the direct product of a $U(1)$ Gaussian model and a Z_n vertex algebra. Some examples of Z_n vertex algebra are studied in Ref. [38, 37].

Note that the Z_n vertex algebras are different from the Z_n simple-current vertex algebras that will be defined in section 2.4. The Z_n simple-current vertex algebras are special cases of the Z_n vertex algebras. In this and the next sections, we will consider Z_n vertex algebras. We will further limit ourselves to Z_n simple-current vertex algebras in section 2.4 and later.

As a result

$$\begin{aligned}
&\tilde{h}^{\rm sc}_a = \tilde{h}^{\rm sc}_{a+n}, \qquad \tilde{h}^{\rm sc}_n = 0 \\
&\mu_{ab} = \mu_{a+n,b} = \mu_{a,b+n}, \qquad \mu_{n,a} = \mu_{a,n} = 1 \\
&C_{a,b} = C_{a+n,b} = C_{a,b+n}, \qquad C_{n,a} = C_{a,n} = 1 \\
&C_{a,b} = \mu_{a,b} C_{b,a}
\end{aligned} \tag{2.32}$$

By choosing proper normalizations for the operators ψ_a, we can have

$$\begin{aligned}
C_{a,-a} &= \begin{cases} 1, & a \bmod n \le n/2 \\ \mu_{a,-a}, & a \bmod n > n/2 \end{cases} \\
C_{a,b} &= 1, \quad \text{if } a \text{ or } b = 0 \bmod n
\end{aligned} \tag{2.33}$$

To summarize, we see that the Z_n vertex algebras (whose correlation functions give rise to electron wave functions) are characterized by the following set of data $\{n; m; \tilde{h}^{\rm sc}_a; C_{a,b}, ...|a, b = 1, ..., n\}$, where $m = n/\nu$. Here the ... represent other structure constants in the subleading terms. The commutation factors μ_{ab} are not included in the above data because they can be expressed in terms of $\tilde{h}^{\rm sc}_a$ and are not independent. Since the Z_n vertex algebra encodes the many-body wave function of electrons,

we can say that the data $\{n; m; \tilde{h}_a^{\rm sc}; C_{a,b}, ...|a, b = 1, ..., n\}$ also characterize the electron wave function. We can study all the properties of electron wave functions by studying the data $\{n; m; \tilde{h}_a^{\rm sc}; C_{a,b}, ...|a, b = 1, ..., n\}$. In the pattern-of-zero approach, we use data $\{n; m; h_a^{\rm sc}\}$ to characterize the wave functions. We will see that the $\{n; m; \tilde{h}_a^{\rm sc}; C_{a,b}, ...|a, b = 1, ..., n\}$ characterization is more complete, which allows us to obtain some new results.

2.3.2 Relation between $\tilde{h}_a^{\rm sc}$ and $h_a^{\rm sc}$

What is the relation between the two characterizations: $\{n; m; h_a^{\rm sc}|a = 1, ..., n\}$ and $\{n; m; \tilde{h}_a^{\rm sc}; C_{ab}|a, b = 1, ..., n\}$? The single-valueness of the correlation function $\Phi(\{z_i\})$ requires that the zeros in $\Phi(\{z_i\})$ all have integer orders. In this section, we derive conditions on the scaling dimension $\tilde{h}_a^{\rm sc}$, just from this integral-zero condition. This allows us to find a simple relation between $\{n; m; h_a^{\rm sc}|a = 1, ..., n\}$ and $\{n; m; \tilde{h}_a^{\rm sc}; C_{ab}|a, b = 1, ..., n\}$.

From the definition of D_{ab} and the OPE (2.26), we see that

$$\begin{aligned} D_{a,b} &\equiv S_{a+b} - S_a - S_b = h_{a+b} - h_a - h_b \\ &= \tilde{h}_{a+b}^{\rm sc} - \tilde{h}_a^{\rm sc} - \tilde{h}_b^{\rm sc} + \frac{ab}{\nu} = D_{b,a} \end{aligned} \tag{2.34}$$

We see that $D_{1,n} = \frac{n}{\nu}$. So $\frac{n}{\nu}$ is an positive integer which is called m.

From eqn. (2.34), we can show that[229, 228]

$$S_a = \sum_{i=1}^{a-1} D_{i,1} = h_a - a h_1 = \tilde{h}_a^{\rm sc} - a\tilde{h}_1^{\rm sc} + \frac{a(a-1)}{2\nu} \tag{2.35}$$

and

$$\tilde{h}_a^{\rm sc} = S_a - \frac{aS_n}{n} + \frac{am}{2} - \frac{a^2 m}{2n}. \tag{2.36}$$

Therefore, the $h_a^{\rm sc}$ introduced before is nothing but the scaling dimensions $\tilde{h}_a^{\rm sc}$ of the simple currents ψ_a (see eqn. (2.13)). In the following, we will use $h_a^{\rm sc}$ to describe the scaling dimensions of ψ_a. Thus the data $\{n; m; \tilde{h}_a^{\rm sc}; C_{a,b} | a, b = 1, ..., n\}$ can be rewritten as $\{n; m; h_a^{\rm sc}; C_{a,b} | a, b = 1, ..., n\}$. Those $h_a^{\rm sc}$ satisfy eqns. (2.16), (2.17), and (2.18).

As emphasized in Ref. [229, 228], the conditions (2.16), (2.17), and (2.18), although necessary, are not sufficient. In the following, we will try to find more conditions from the vertex algebra.

2.3.3 Conditions on $h_a^{\rm sc}$ and $C_{a,b}$ from the associativity of vertex algebra

The multi-point correlation of a Z_n vertex algebra can be obtained by fusing operators together, thus reducing the original problem to calculating a correlation of fewer points.[242] It is the associativity of this vertex algebra that guarantees any different ways of fusing operators would yield the same correlation in the end,[151] so that the electron wave function would be single-valued. The associativity of a Z_n vertex algebra requires $h_a^{\rm sc}$ and $C_{a,b}$ to satisfy many consistent conditions. Those are the extra consistent conditions we are looking for. The consistent conditions come from two sources. The first source is the consistent conditions on the commutation factors $\mu_{a,b}$. When applied to our vertex algebra (2.29), we find that some consistent conditions on $\mu_{a,b}$ allow us to express $\mu_{a,b}$ in terms of $h_a^{\rm sc}$. Then other consistent conditions on $\mu_{a,b}$ will become consistent conditions on $h_a^{\rm sc}$. The second source is GJI for the vertex algebra (2.29). We like to stress that the discussions so far are

very general. The consistent conditions that we have obtained for generic Z_n vertex algebra are necessary conditions for any FQH states.

A detailed derivation of those conditions on $h_a^{\rm sc}$ and $C_{a,b}$ is given in Ref. [130]. Here we just summarize the new and old conditions in a compact form. The consistent conditions can be divided in two classes. The first type of consistent conditions act only on the pattern of zeros $\{n; m; h_a^{\rm sc}\}$:

$$\begin{aligned}
&nh_{2a}^{\rm sc} - 2nah_1^{\rm sc} + a(2a-1)m = 0 \bmod 2n,\\
&m > 0, \quad mn = \text{even},\\
&h_{a+b}^{\rm sc} - h_a^{\rm sc} - h_b^{\rm sc} + \frac{abm}{n} \in \mathbb{N},\\
&h_{a+b+c}^{\rm sc} - h_{a+b}^{\rm sc} - h_{b+c}^{\rm sc} - h_{a+c}^{\rm sc} + h_a^{\rm sc} + h_b^{\rm sc} + h_c^{\rm sc} \in \mathbb{N},\\
&n\alpha_{1,1} = \text{even},\\
&a^2\alpha_{1,1} - \alpha_{a,a} = \text{even} \quad \forall a = 1, 2, \cdots n-1,\\
&\Delta_3(\frac{n}{2}, \frac{n}{2}, \frac{n}{2}) = 4h_{\frac{n}{2}}^{\rm sc} \neq 1, \quad \text{if } n = \text{ even},
\end{aligned} \tag{2.37}$$

where $h_a^{\rm sc} = h_{a+n}^{\rm sc}$ and $\alpha_{a,b} = h_a^{\rm sc} + h_b^{\rm sc} - h_{a+b}^{\rm sc}$.

The second type of consistent conditions act on the structure constants: For any a, b, c

$$\begin{aligned}
C_{a,b}C_{a+b,c} &= C_{b,c}C_{a,b+c} = \mu_{a,b}C_{a,c}C_{b,a+c}\\
&\text{if } \Delta_3(a,b,c) = 0,\\
C_{a,b}C_{a+b,c} &= C_{b,c}C_{a,b+c} + \mu_{a,b}C_{a,c}C_{b,a+c}\\
&\text{if } \Delta_3(a,b,c) = 1,
\end{aligned} \tag{2.38}$$

where $\mu_{a,b}$ is a function of the pattern of zeros $\{h_a^{\rm sc}\}$:

$$\mu_{ij} = (-1)^{ij\alpha_{1,1}-\alpha_{i,j}} = \pm 1.$$

For any $a \neq n/2$

$$\begin{aligned} C_{a,-a} &= C_{a,a}C_{2a,-a} = 1 && \text{if } \Delta_3(a,a,-a) = 0, \\ 2C_{a,-a} &= C_{a,a}C_{2a,-a} && \text{if } \Delta_3(a,a,-a) = 1. \end{aligned} \tag{2.39}$$

Here $C_{a,b}$ satisfies the normalization condition (2.33). There may be additional conditions when $\Delta_3(a,b,c) \neq 0, 1$. But we do not know how to derive those conditions systematically at this time.

2.3.4 Summary

In Ref. [229, 228], we have seen that the conditions (2.16), (2.17), and (2.18) are not enough since they allow the following pattern of zeros $\{n; m; h_a^{\rm sc}\} = \{2; 1; \frac{1}{4}\}$. Such a pattern of zeros does not correspond to any valid polynomial. The conditions (2.37) obtained in this chapter rule out the above invalid solution. So the conditions (2.37) is more complete than the conditions (2.16), (2.17), and (2.18). However, the conditions (2.37) is still incomplete, since they allow the invalid patterns of zeros such as $\{n; m; h_a^{\rm sc}\} = \{4; 2; \frac{1}{4}\ 0\ \frac{1}{4}\}$ and $\{4; 4; 1\ 1\ 1\}$. Both of them can be ruled out by the conditions (2.38) and (2.39).

The conditions (2.37), (2.38), and (2.39) are the consistent conditions that we can find from some of GJI, based on the most general form of OPE (2.29). So those conditions are necessary, but may not be sufficient.

The correspondence between the patterns of zeros $\{n; m; h_a^{\text{sc}}\}$ and FQH states is not one-to-one. There can be many polynomials that have the same pattern of zeros. This is not surprising since the pattern of zeros only fixes the highest-order zeros in electron wave functions (symmetric polynomials), while different patterns of lower-order zeros could lead to different polynomials in principle. In other words, the leading-order OPE (2.29) alone might not suffice to uniquely determine the correlation function of the vertex algebra. The examples studied in this section support such a belief. Explicit calculations for some examples suggest that the pattern of zeros *together with* the central charge c and simple current condition would uniquely determine the FQH state. This is a reason why we introduce Z_n simple-current vertex algebra in the next section.

2.4 Z_n simple-current vertex algebra

In the last section, we discuss "legal" patterns of zeros that satisfy the consistent conditions (2.37), (2.38), and (2.39) and describe existing FQH states. If we believe that a "legal" pattern of zeros $\{n; m; h_a^{\text{sc}}\}$, or more precisely the data $\{n; m; h_a^{\text{sc}}; c\}$, can completely describe a FQH state, then we should be able to calculate all the topological properties of the FQH states. But so far, from the pattern of zeros $\{n; m; h_a^{\text{sc}}\}$, we can only calculate the number of different quasiparticle types, quasiparticle charges, and the fusion algebra between the quasiparticles.[228, 16] Even with the more complete data $\{n; m; h_a^{\text{sc}}; c\}$, we still do not know, at this time, how to calculate the quasiparticle statistics and scaling dimensions.

One idea to calculate more topological properties from the data $\{n; m; h_a^{\text{sc}}; c\}$ is to

use the data to define and construct the corresponding Z_n vertex algebra, and then use the Z_n vertex algebra to calculate the quasiparticle scaling dimensions and the central charge c. However, so far we do not know how to use the data $\{n; m; h_a^{\text{sc}}; c\}$ to completely construct a Z_n vertex algebra in a systematic manner.

Starting from this section, we will concentrate on a subset of "legal" patterns of zeros that correspond to a subset of Z_n vertex algebra. Such a subset is called Z_n simple-current vertex algebras. The FQH states described by those Z_n simple-current vertex algebras are called Z_n simple-current states. We will show that in many cases the quasiparticle scaling dimensions and the central charge c can be calculated from the data $\{n; m; h_a^{\text{sc}}; c\}$ for those Z_n simple-current states.

2.4.1 OPE's of Z_n simple-current vertex algebra

The Z_n simple-current vertex algebra is defined through an Abelian fusion rule with cyclic Z_n symmetry for primary fields $\{\psi_a\}$ of Virasoro algebra[242, 57]

$$\psi_a\psi_b \sim \psi_{a+b}, \qquad \psi_a \equiv (\psi)^a. \tag{2.40}$$

Compared to eqn. (2.23), here we require that ψ_a and ψ_b fuse into a single primary field of Virasoro algebra ψ_{a+b}. Such operators are called simple currents. The Z_n simple-current vertex algebra is defined by the following OPE of ψ_a[242, 57]:

$$\psi_a(z)\psi_b(w) = C_{a,b}\frac{\psi_{a+b}(w)}{(z-w)^{\alpha_{a,b}}} + O\Big((z-w)^{1-\alpha_{a,b}}\Big) \tag{2.41}$$

$$\psi_a(z)\psi_{-a}(w) = \frac{1+\frac{2h_a^{\text{sc}}}{c}(z-w)^2T(w)}{(z-w)^{2h_a^{\text{sc}}}} + O\Big((z-w)^{3-2h_a^{\text{sc}}}\Big) \tag{2.42}$$

where we define

$$\alpha_{a,b} \equiv h_a^{\rm sc} + h_b^{\rm sc} - h_{a+b}^{\rm sc} \tag{2.43}$$

$\psi_{-a} \equiv \psi_{n-a}$ and $\psi_a = \psi_{n+a}$ is understood due to the Z_n symmetry. In the context the subscript a of Z_n simple currents is always defined as a mod n.

We like to point out here that the form of the OPE (2.42) is a special property of the Z_n simple-current vertex algebra. For a more general Z_n vertex algebra that describes a generic FQH state, the correspond OPE has a more general form

$$\begin{aligned}\psi_a(z)\psi_{-a}(w) = &\frac{1+\frac{2h_a^{\rm sc}}{c}(z-w)^2T(w)}{(z-w)^{2h_a^{\rm sc}}} \\ &+ \frac{T'_a}{(z-w)^{2h_a^{\rm sc}-2}} + O\Big((z-w)^{3-2h_a^{\rm sc}}\Big)\end{aligned} \tag{2.44}$$

where T'_a are dimension-2 primary fields of Virasoro algebra ($\{T'_a,\ a=1,\cdots,[\frac{n}{2}]\}$ may not be linearly independent though). Also, for the Z_n simple-current vertex algebra, the subleading terms in (2.41) are also determined.

$\{C_{a,b}\}$ are the structure constants of this vertex algebra. We also have conformal symmetry

$$T(z)\psi_a(w) = \frac{h_a^{\rm sc}}{(z-w)^2}\psi_a(w) + \frac{1}{z-w}\partial\psi_a(w) + O(1) \tag{2.45}$$

and Virasoro algebra

$$T(z)T(w) = \frac{c/2}{(z-w)^4} + \frac{2T(w)}{(z-w)^2} + \frac{\partial T(w)}{z-w} + O(1) \tag{2.46}$$

where $T(z)$ represents the energy-momentum tensor, which has a scaling dimension of 2. c stands for the central charge as usual, which is also a structure constant.

Using the notation of generalized vertex algebra[151], we have

$$[\psi_i\psi_j]_{\alpha_{i,j}} = C_{i,j}\psi_{i+j}, \quad i+j \neq 0 \text{ mod } n \tag{2.47}$$

$$[\psi_i\psi_{-i}]_{\alpha_{i,-i}} = 1, \quad [\psi_i\psi_{-i}]_{\alpha_{i,-i}-1} = 0,$$
$$[\psi_i\psi_{-i}]_{\alpha_{i,-i}-2} = \frac{2h_i^{\rm sc}}{c}T \tag{2.48}$$

$$[T\psi_i]_2 = h_i^{\rm sc}\psi_i = [\psi_i T]_2, \quad [T\psi_i]_1 = \partial\psi_i \tag{2.49}$$
$$[\psi_i T]_1 = (h_i^{\rm sc} - 1)\partial\psi_i$$

$$[TT]_4 = \frac{c}{2}, \quad [TT]_3 = 0, \quad [TT]_2 = 2T, \quad [TT]_1 = \partial T \tag{2.50}$$

with $\alpha_{T,\psi_i} = 2,\ \alpha_{T,T} = 4$. We call it a *special Z_n simple-current vertex algebra* if it satisfies OPE's (2.47)-(2.50). For example, the Z_n parafermion states[178] correspond to a series of special Z_n simple-current vertex algebras. Two other OPE conditions for quasiparticles ($\sigma_{\gamma+a}$ with scaling dimension $h_{\gamma+a}^{\rm sc}$) are shown in Ref. [130]

$$[\psi_a\sigma_{\gamma+b}]_{\alpha_{a,\gamma+b}} = C_{a,\gamma+b}\sigma_{\gamma+a+b} \tag{2.51}$$
$$[\sigma_{\gamma+b}\psi_a]_{\alpha_{a,\gamma+b}} = \mu_{\gamma+b,a}C_{a,\gamma+b}\sigma_{\gamma+a+b}$$

$$[T\sigma_{\gamma+a}]_2 = h_{\gamma+a}^{\rm sc}\sigma_{\gamma+a} = [\sigma_{\gamma+a}T]_2, \tag{2.52}$$
$$[T\sigma_{\gamma+a}]_1 = \partial\sigma_{\gamma+a}, \quad [\sigma_{\gamma+a}T]_1 = (h_{\gamma+a}^{\rm sc} - 1)\partial\sigma_{\gamma+a}$$

with $\alpha_{T,\sigma_{\gamma+a}} = 2$.

The commutation factor μ_{AB} equals unity if either A or B is the energy-momentum tensor T: $\mu_{T,\psi_i} = \mu_{\psi_i,T} = \mu_{T,T} = 1$. Similarly we have $\mu_{A,1} = \mu_{1,A} = 1$ for the identity operator 1 and any operator A. However, $\mu_{i,j} \equiv \mu_{\psi_i,\psi_j}$ can be ± 1 in general. In deriving OPE (2.48) we have assumed that $\mu_{i,-i} = 1,\ \forall i$, which is not necessary. For example, the Z_4 Gaffnian does not satisfy $\mu_{i,-i} = 1,\ \forall i$. So, we will adopt the more

general OPE in Ref. [130] instead of eqn. (2.48) to include examples like Gaffnian which do give a FQH wave function. OPE (2.48) is for a special Z_n simple-current vertex algebra that satisfies $\mu_{i,-i} = 1, \quad \forall i$. For a more general Z_n simple-current vertex algebra, they become

$$\begin{aligned}
&[\psi_i\psi_{-i}]_{\alpha_{i,-i}} = C_{i,-i}, \quad [\psi_i\psi_{-i}]_{\alpha_{i,-i}-1} = 0,\\
&[\psi_i\psi_{-i}]_{\alpha_{i,-i}-2} = \frac{2C_{i,-i}h_i^{\rm sc}}{c}T \qquad (2.53)\\
&C_{i,-i} = \begin{cases} 1, & i \le n/2 \bmod n \\ \mu_{i,-i}, & i > n/2 \bmod n \end{cases}
\end{aligned}$$

so that we always have $C_{a,b} = \mu_{a,b}C_{b,a}$ for any subscripts a and b in such an associative vertex algebra.

The OPE's (2.47), (2.53), (2.49), (2.50), (2.51) and (2.52) define the *generalized Z_n simple-current vertex algebra*, or simply Z_n simple-current vertex algebra. The Gaffnian state corresponds to a generalized Z_4 simple-current vertex algebra with $\mu_{a,-a} \neq 1$. When $\mu_{a,-a} = 1$, we have a special Z_n simple-current vertex algebra.

What kind of pattern of zeros $\{n; m; h_a^{\rm sc}\}$, or more precisely what kind of data $\{n; m; h_a^{\rm sc}; c, C_{ab}\}$, can produce a Z_n simple-current vertex algebra? Since the Z_n simple-current vertex algebras are special cases of Z_n vertex algebras, the data $\{n; m; h_a^{\rm sc}; c, C_{ab}\}$ must satisfy the conditions (2.37), (2.38), and (2.39). However, the data $\{n; m; h_a^{\rm sc}; c, C_{ab}\}$ for Z_n simple-current vertex algebras should satisfy more conditions. Those conditions can be obtained from the GJI of Z_n simple-current vertex algebras. In Ref. [130], we derived all those extra consistent conditions for a generic Z_n vertex algebra, from the useful GJI's based on OPE (2.29). Now based on OPE's summarized in this section, we can similarly derive a set of extra consistent conditions for a Z_n simple-current

vertex algebra. These conditions are summarized in section **??**. For those valid data that satisfy all the consistent conditions, the full properties of simple-current vertex algebra can be obtained. This in turn allows us to calculate the physical topological properties of the FQH states associated with those valid patterns of zeros.

We like to point out that many examples of Z_n simple-current vertex algebra have been studied in detail. They include the simplest Z_n simple-current vertex algebra – the Z_n parafermion algebra.[242, 241, 57] More general exmaples that have been studied are the higher generations of Z_n parafermion algebra[40, 41, 43, 42, 44] and graded parafermion algebra.[152, 92, 93] In those exapmles, the Z_n simple-current algebras are studied by embedding the algebras into some known CFT, such as coset models of Kac-Moody current algebras and/or Coulomb gas models. However, in this chapter, we will not assume such kind of embeding. We will try to calculate the properties of Z_n simple-current vertex algebra directly from the data $\{n; m; h_a^{\text{sc}}, c, ...\}$ without assuming any embedding.

The consistent conditions derived from useful GJI's for a Z_n simple current algebra are listed in Ref. [130].

2.5 Summary

The pattern-of-zeros is a powerful way to characterize FQH states.[229, 228, 16] However, the pattern-of-zeros approach is not quite complete. It is known that some patterns of zeros do not uniquely describe the FQH states. As a result, we cannot obtain all the topological properties of FQH states from the data of pattern of zeros $\{n; m; S_a\}$.

In this chapter, we combine the pattern-of-zero approach with the vertex algebra approach. We find that we can generalize the data of pattern of zeros $\{n; m; S_a\}$ to $\{n; m; S_a; c\}$ to completely describe a FQH state, at least for the many examples discussed in this Ref. [130]. Many consistent conditions on the new set of data $\{n; m; S_a; c\}$ are obtained from the GJI of the simple-current vertex algebra. Those consistent conditions are sufficient: *i.e.* if the data $\{n; m; S_a; c\}$ satisfy those conditions, then the data will define a Z_n simple-current vertex algebra and a FQH wave function. Using the new characterization scheme and the Z_n simple-current vertex algebra, we can calculate quasiparticle scaling dimensions, fractional statistics, the central charge of the edge states, as well as many other properties, from the data $\{n; m; S_a; c\}$.

The study in this chapter is based on the Z_n simple-current vertex algebra. But the Z_n simple-current vertex algebra makes some unnecessary assumptions. It is much more natural to study FQH state based on the more general Z_n vertex algebra. This will be a direction of future exploration.

Chapter 3

Correlation-hole induced paired quantum Hall states in lowest Landau level

3.1 Introduction

The fractional quantum Hall effect (FQHE) observed at Landau level filling fraction $\nu = 5/2$ [234] signifies a new state of correlated electrons. This state is believed to be described by the Moore-Read pfaffian (MRP) [140] and supports fractionalized quasiparticle excitations [39, 166] that obey non-abelian statistics relevant for topological quantum computing [101]. An outstanding question has been whether such non-abelian topological phases exist in the lowest Landau level (LLL). Several recent experiments [132, 190, 189] indeed observed FQHE at $\nu = 1/2$ and $1/4$, suggesting that these, too, may be in the MRP phase. Although the abelian two-component

Halperin (331) and (553) states [72] can be strong contenders for these FQHE [154], fresh experiments and numerical studies found strong evidence for the one-component FQHE at $\nu = 1/2$ and $1/4$ in asymmetric wide quantum wells [189, 155]. Whether the observed FQHE can be understood as pfaffians in the LLL is the focus of this work.

The MRP is a chiral p-wave paired quantum Hall state [176]. In principle, it can emerge as a p-wave pairing instability of the composite Fermi liquid (CFL), a gapless state of electrons attached to flux tubes[74]. The leading-order statistical interaction mediated by the Chern-Simons (CS) gauge field fluctuations can produce a p-wave pairing potential for the composite fermion [62] (CF). However, since the coupling between the CF and the CS gauge field is not small, diagrammatic perturbation theory is not controllable. Within the random-phase approximation, the gauge fluctuations are in fact singular and pair-breaking[25]. Therefore, the ground states at filling fractions $1/2$ and $1/4$ remained enigmatic [157, 156].

The key to solve this problem is to properly account for the effects of the correlation hole, i.e. the local charge depletion caused by attaching flux to an electron. A CF feels the correlation hole of the other CFs, which is captured by the Jastrow factor in the Laughlin wavefunction. In the unitary CF theory [94, 74], only an infinitely thin flux tube associated with a U(1) phase is attached to each electron without accounting for the Jastrow factor, i.e. the correlation hole. Read improved the concept of CF by attaching finite size vortices to electrons [171, 173, 174, 181] such that the Jastrow factor naturally appears in the ground state wavefunction. Binding zeros of the wavefunction to electrons keeps them apart and lowers the Coulomb energy. The

vortex attachment can be achieved through a non-unitary but nevertheless canonical transformation on the electron operators [167]. The saddle point solutions of such a non-unitary CF (NUCF) field theory recover the Laughlin state for the odd denominator FQHE [167] and the Rezayi-Read CFL at $\nu = 1/2$ [235]. The effective interaction induced by the vortex attachment has also been studied at $\nu = 1/2$ [142].

In this chapter, we show that paired quantum Hall states emerge in the LLL using the NUCF field theory where a vortex with vorticity-$\tilde{\phi}$ ($\tilde{\phi}$ = even integer) is attached to an electron at filling fraction $\nu = 1/\tilde{\phi}$. An important feature of attaching vortices to electrons is that the diamagnetic coupling, quadratic in the gauge field, to the CF density is canceled by its dual contribution from the correlation hole associated with the vortex. As a result, we show that the gauge fluctuations can be integrated out exactly, leading to an *instantaneous* statistical interaction between the NUCFs which is attractive for chiral $p_x - \mathrm{i}p_y$ pairing [142] and scales linearly with the vorticity $\tilde{\phi}$. We construct the variational ground state wavefunction for such a *correlation-hole induced paired quantum Hall state*, introducing two canonically dual gap functions related by the radial distribution function of the corresponding bosonic Laughlin wavefunction. Variational calculations are carried out in the presence of the pair-breaking Coulomb interaction $V_c(r) = e^2/4\pi\epsilon_r\epsilon_0 r = \lambda\frac{2\sqrt{2\nu}\ell_B}{r}\hbar\omega_c$, where ℓ_B is the magnetic length and λ is a dimensionless coupling constant. We find that for weak Coulomb interaction $\lambda < \lambda_{c1}$, the ground state is a MRP in the long wavelength limit. However, the pairing function deviates significantly from that of the MRP at shorter distances, consistent with recent numeric studies in the projected LLL [139]. Remarkably, we find that for intermediate Coulomb interactions, $\lambda_{c1} < \lambda < \lambda_{c2}$, the paired state is different

from the MRP even in the asymptotic long wavelength limit. The pairing function in this new phase is oscillatory with its amplitude decaying as the inverse square root of the distance. For sufficiently strong Coulomb interactions $\lambda > \lambda_{c2}$, the paired state becomes unstable and the ground state undergoes a transition to the Rezayi-Read CFL[181] phase. The topological properties and the effect of a short-ranged interaction are also studied.

3.2 Formulation and results

We consider 2D spin-polarized interacting electrons described by the field operator ψ_e in a uniform perpendicular magnetic field B. The electron density is n_e and the density operator $\rho = \psi_e^\dagger \psi_e$. The vortex attachment is through the following non-unitary transformation [167]:

$$\Phi(\mathbf{r}) = e^{-J_{\tilde{\phi}}(\mathbf{r})}\psi_e(\mathbf{r}), \quad \Pi(\mathbf{r}) = \psi_e^\dagger(\mathbf{r})e^{J_{\tilde{\phi}}(\mathbf{r})}, \tag{3.1}$$

where $J_{\tilde{\phi}}(\mathbf{r}) = I_{\tilde{\phi}}(\mathbf{r}) - \frac{|z|^2}{4l_{\tilde{\phi}}^2}$, $\ell_{\tilde{\phi}} = \sqrt{\frac{\hbar c}{\nu\tilde{\phi}eB}}$, and

$$I_{\tilde{\phi}}(\mathbf{r}) = \tilde{\phi}\int d^2\mathbf{r}'\rho(\mathbf{r}')\log(z-z'), \quad z = x+iy.$$

We set $\hbar = |e|/c = 1$ hereafter. The imaginary part of $I_{\tilde{\phi}}$ coincides with the unitary CS transformation, while its real part describes the finite vortex core (correlation hole) accompanying the flux attachment. Note that the fields Φ and Π are not hermitian conjugate, $\Pi = \Phi^\dagger e^{J_{\tilde{\phi}}+J_{\tilde{\phi}}^\dagger}$. However, they form a pair of canonical fields obeying fermion anti-commutation relations; the operator Π creates a NUCF while

Φ annihilates one and $\rho = \Pi\Phi$. The transformed Hamiltonian reads

$$H^{\rm CF} = \frac{1}{2m_b}\int d^2\mathbf{r}\Pi(\mathbf{r})[-\mathrm{i}\nabla - (\mathbf{A} - \mathbf{v}_{\tilde{\phi}})]^2\Phi(\mathbf{r}) + \frac{1}{2}\int d^2\mathbf{r}d^2\mathbf{r}'\delta\rho(\mathbf{r})V_c(\mathbf{r}-\mathbf{r}')\delta\rho(\mathbf{r}') \tag{3.2}$$

where $\mathbf{v}_{\tilde{\phi}}(\mathbf{r}) = -\mathrm{i}\nabla J_{\tilde{\phi}} = \mathbf{a}(\vec{x}) + \mathrm{i}\hat{n}\times\mathbf{a}(\mathbf{r}) - \mathrm{i}\frac{B}{2}\mathbf{r}$ with $\hat{n}$ normal to the 2D plane and the CS gauge field is

$$\mathbf{a}(\mathbf{r}) = \tilde{\phi}\nabla\int d^2\mathbf{r}'\rho(\mathbf{r}')\mathrm{Im}\log(z-z'). \tag{3.3}$$

The statistical magnetic field $b = \nabla\times\mathbf{a} = 2\pi\tilde{\phi}\rho$.

One of the physical justifications to introduce such a NUCF field theory lies in the fact that the resulting mean-field states give rise to numerically well-tested wavefunctions [167, 235]. At the mean field level, one takes gauge field $\mathbf{a}$ to be a classical one determined by (3.3) with a uniform density $\bar{\rho}(\mathbf{r}) = n_e$, and $\bar{\mathbf{a}}(\mathbf{r}) = -\frac{\nu\tilde{\phi}B}{2}\hat{n}\times\mathbf{r}$. Thus, the mean-field theory describes free NUCFs in an effective magnetic field $\Delta B = B - \nu\tilde{\phi}B = \nabla\times\Delta\mathbf{A}$ with $\Delta\mathbf{A} = \mathbf{A} - \bar{\mathbf{a}}$. At even-denominator filling fractions $\nu = 1/\tilde{\phi}$, $\ell_{\tilde{\phi}} = \ell_B$ and the effective $\Delta B = 0$, the mean-field ground state is the Rezayi-Read CFL [181].

An important, non-perturbative feature of this NUCF theory is that the usual diamagnetic fermion density-gauge field coupling of the form $\rho\delta\mathbf{a}^2$, where $\delta\mathbf{a} = \mathbf{a} - \bar{\mathbf{a}}$, is canceled in Eq. (3.2) by the contribution from the correlation holes since $(\delta\mathbf{a} \pm \mathrm{i}\hat{n}\times\delta\mathbf{a})^2 = 0$. As a result, the gauge fluctuations in the CS action can be exactly

integrated out to obtain a closed-form effective Hamiltonian:

$$\begin{aligned} H_{\text{eff}}^{\text{CF}} &= \sum_{\mathbf{k}} (\xi_{\mathbf{k}} + \frac{\omega_c}{2}) \Pi_{\mathbf{k}} \Phi_{\mathbf{k}} \\ &+ \frac{\pi \tilde{\phi}}{m_b} \sum_{\mathbf{q}\neq 0,\mathbf{k},\mathbf{p}} \frac{k+p}{q} \Pi_{\mathbf{k}-\mathbf{q}} \Pi_{\mathbf{q}-\mathbf{p}} \Phi_{-\mathbf{p}} \Phi_{\mathbf{k}} \\ &+ \sum_{\mathbf{q}\neq 0,\mathbf{k},\mathbf{p}} \frac{v_{\mathbf{q}}}{2} \Pi_{\mathbf{k}-\mathbf{q}} \Phi_{\mathbf{k}} \Pi_{\mathbf{q}-\mathbf{p}} \Phi_{-\mathbf{p}} \Phi_{-\mathbf{p}} \Phi_{\mathbf{k}}. \end{aligned} \tag{3.4}$$

Here $\xi_{\mathbf{k}} = \frac{\hbar^2 |\mathbf{k}|^2}{2m_b} - \mu$ and $\omega_c = |B|/m_b$ is the cyclotron frequency. The second term is the induced *instantaneous* statistical interaction written in terms of the complex momenta $k = k_x + \mathrm{i}k_y$ (similarly for p, q). For $\mathbf{k} = \mathbf{p}$, it reduces to a singular pairing interaction that scatters a pair of NUCFs with zero center-of-mass momentum from $(\mathbf{k}, -\mathbf{k})$ to $(\mathbf{k}', -\mathbf{k}')$ with momentum transfer $\mathbf{q} = \mathbf{k} - \mathbf{k}'$. Expanding in the angular-momentum channels (l):

$$\frac{1}{2} \frac{k+p}{k-k'}\Big|_{p=k} = 1 + \sum_{l\neq 0} \text{sign}(l) \left|\frac{k'}{k}\right|^l e^{\mathrm{i}l\theta_{kk'}} \theta(1 - \left|\frac{k'}{k}\right|^l)$$

where $\theta_{kk'} = \arg(k') - \arg(k)$, we see that the pairing potential is attractive for $l < 0$ with dominant $p_x - \mathrm{i}p_y$ scattering. The Coulomb interaction in Eq. (3.4), where $v_{\mathbf{q}} = e^2/2\varepsilon_r\varepsilon_0|\mathbf{q}|$, is purely repulsive in all channels. In the absence of Coulomb interaction, it can be shown that the MRP, being an antiholomorphic function, is an exact ground state of the NUCF Hamiltonian.

To study the variational ground state of Hamiltonian (3.4), we generalize the BCS theory to the non-unitary case. Introduce the Dirac ket and bra

$$|G^{(l)}\rangle \equiv e^{\frac{1}{2}\sum_{\mathbf{k}} g_{\mathbf{k}}^{(l)} \Pi_{\mathbf{k}} \Pi_{-\mathbf{k}}} |0\rangle, \quad \langle G^{(l)}| = \langle 0| e^{\frac{1}{2}\sum_{\mathbf{k}} \tilde{g}_{\mathbf{k}}^{(l)} \Phi_{-\mathbf{k}} \Phi_{\mathbf{k}}}.$$

The corresponding electron wavefunction is $\Psi_e(\{\mathbf{r}_i\}) = \text{Pf}[g^{(l)}(\mathbf{r}_i - \mathbf{r}_j)] \prod_{i<j} (z_i - z_j)^{\tilde{\phi}} e^{-\sum_i |z_i|^2/4}$. Here the the pairing function $g_{\mathbf{k}}^{(l)}$ is an eigenfunction of the angular

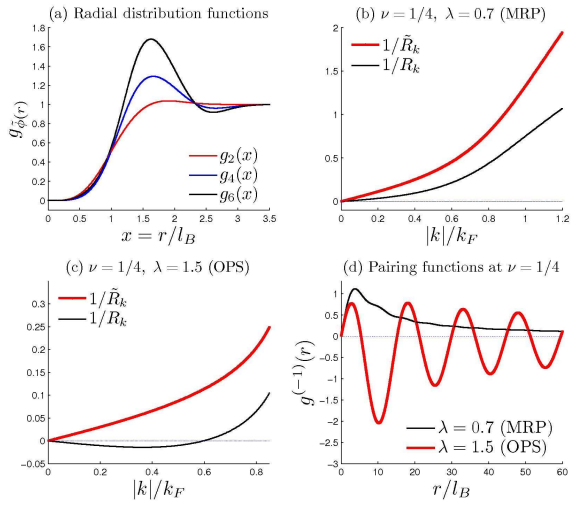

Figure 3.1: (a): Radial distribution function $g_{\tilde{\phi}}$ with even $\tilde{\phi} = 1/\nu$ from Monte-Carlo [31]. (b) and (c): Inverse pairing functions $1/R_k$ and $1/\tilde{R}_k$ at $\nu = 1/4$ for two different Coulomb strengths λ in the MRP phase (b) and the OPS phase (c). (d) Real-space chiral p-wave pairing function $g^{(-1)}(r)$ in the two phases (b) and (c). At $\nu = 1/4$, $\lambda_{c1} \approx 1.0$.

momentum $L_z = \mathrm{i}\hbar(k_y\partial_{k_x} - k_x\partial_{k_y}) = -\mathrm{i}\hbar\partial_{\theta_{\mathbf{k}}}$, i.e. $g^{(l)}_{\mathbf{k}} = e^{\mathrm{i}l\theta_{\mathbf{k}}}R_k$ with $R_k = R(|\mathbf{k}|)$ a *real* function of $|\mathbf{k}|$. The parity of the pairing function must be *odd* for spin-polarized fermions, i.e. $g^{(l)}_{-\mathbf{k}} = -g^{(l)}_{\mathbf{k}}$; thus l must be an odd integer. The expectation value of an operator $\hat{O}$ is given by $\langle\hat{O}\rangle = \langle G^{(l)}|\hat{O}|G^{(l)}\rangle/\langle G^{(l)}|G^{(l)}\rangle$.

It is important to note that $\tilde{g}^{(l)}_{\mathbf{k}}$ is not independent of $g^{(l)}_{\mathbf{k}}$ in the physical Hilbert space. The hermiticity of electron pairing,

$$\langle\psi^\dagger_e(\mathbf{r}+\mathbf{x})\psi^\dagger_e(\mathbf{x})\rangle = \langle\psi_e(\mathbf{x})\psi_e(\mathbf{r}+\mathbf{x})\rangle^*$$

implies, through relations (3.1), the following constraint between the two pairing order parameters:

$$\langle\Pi(\mathbf{r}+\mathbf{x})\Pi(\mathbf{x})\rangle \approx (g_{\tilde{\phi}}(r)\langle\Phi(\mathbf{x})\Phi(\mathbf{r}+\mathbf{x})\rangle)^* \tag{3.5}$$

where $g_{\tilde{\phi}}(r)$ is, remarkably, the *radial distribution function* of the bosonic Laughlin wavefunction $\Psi^L_{\tilde{\phi}}(\{\mathbf{r}_i\}) \equiv \prod_{i<j}(z_i - z_j)^{\tilde{\phi}}e^{-\sum_i|z_i|^2/4}$ which is shown in Fig. 3.1(a) for $\tilde{\phi} = 2, 4, 6$. This constraint describes mathematically how one NUCF feels the vortices (correlation holes) around the others. Consequently, the two gap functions $\Delta_k = -\sum_{\mathbf{k}'}V^{(l)}(\mathbf{k},\mathbf{k}')\langle\Pi_{-\mathbf{k}'}\Pi_{\mathbf{k}'}\rangle$ and $\tilde{\Delta}_k = -\sum_{\mathbf{k}'}\tilde{V}^{(l)}(\mathbf{k},\mathbf{k}')\langle\Phi_{-\mathbf{k}'}\Phi_{\mathbf{k}'}\rangle$ are related through the correlation holes. We find,

$$\tilde{\Delta}_k = \Delta_k + E_k\int_0^\infty \frac{\Delta_{k'}}{E_{k'}}\mathcal{H}_l(k,k')k'\mathrm{d}k' \tag{3.6}$$

where $\mathcal{H}_l(k,k') = \frac{1}{(2\pi)^2}\int_0^{2\pi}d\theta_{kk'}\ e^{2\mathrm{i}l\theta_{kk'}}h_{\tilde{\phi}}(|\mathbf{k}-\mathbf{k}'|)$ and $h_{\tilde{\phi}}(|\mathbf{q}|)$ is the Fourier transform of the *pair correlation function* defined as $h_{\tilde{\phi}}(r) \equiv g_{\tilde{\phi}}(r) - 1$.

Minimizing the ground state energy $E^{(l)} = \langle\hat{H}^{\mathrm{CF}}_{\mathrm{eff}}\rangle$ with respect to R_k and $\tilde{R}_k$, we obtain the self-consistent Bogoliubov-de Gennes (B-dG) equations,

$$R_k = \frac{E_k-\xi'_k}{\tilde{\Delta}_k} = \frac{\Delta_k}{E_k+\xi'_k},\quad \tilde{R}_k = \frac{E_k-\xi'_k}{\Delta_k} = \frac{\tilde{\Delta}_k}{E_k+\xi'_k} \tag{3.7}$$

where $E_k = \sqrt{(\xi'_k)^2 + \Delta_k \tilde{\Delta}_k}$ is the quasiparticle dispersion and $\xi'_k = \xi_k + \xi_k^{PH}$ is the renormalized dispersion due to the Coulomb interaction in the particle-hole channel where $\xi_k^{PH} = -\frac{2k_F\lambda}{m_b}\int_0^\infty n_{k'}|k'|\mathrm{d}|k'|M^{(0)}_{|k|,|k'|}$ and $M^{(0)}_{|k|,|k'|}$ is given by $|k-k'|^{-1} = \sum_l M^{(l)}_{|k|,|k'|}e^{\mathrm{i}l\theta}$. The dimensionless interacting strength λ measures the ratio of the Coulomb interaction strength to the Fermi energy: $\lambda = V_c(k_F^{-1})/4\epsilon_F = \frac{e^2 m_b}{8\pi\epsilon_0\epsilon_r k_F}$ with $k_F = \sqrt{4\pi n_e} = \sqrt{2\nu}/\ell_B$ the Fermi wavevector. The momentum distribution is $n_k = (E_k - \xi'_k)/2E_k$.

It is important to stress that the relation (3.6) between the two canonical conjugate gap functions projects the non-unitary theory onto the physical Hilbert space. Assuming $\bar{\Delta}_k = \Delta_k^*$ [142] would violate this constraint and fail to capture the correlation-hole effects. One can show that, if $\bar{\Delta}_k = \Delta_k^*$ is assumed, the solution of the BdG equation (3.7) is $\bar{\Delta}_k = \Delta_k^* = 0$ for all k.

We solved the BdG equations (3.7) under the constraint (3.6) for possible values of l and found that the leading pairing instability has indeed $l = -1$, i.e. $p_x - \mathrm{i}p_y$ wave symmetry, which will be our focus. For weak Coulomb interactions $\lambda < \lambda_{c1}$, the two conjugate gap functions are in-phase, i.e. $\Delta_k\tilde{\Delta}_k > 0$ and $R_k\tilde{R}_k > 0$ for all k, as shown in Fig. 3.1(b). In this case, the asymptotic solutions can be obtained analytically in the long wavelength limit: $\Delta_k, \tilde{\Delta}_k \propto |k|$ as $|k| \to 0$. Thus, the pairing function $g_k^{(-1)} \propto 1/k$ and the paired state is asymptotically a MRP. To study the paired state quantitatively for all k, we numerically solve for the gap functions using an ultraviolet cutoff in momentum space, *e.g.*, $|k| \leq \Lambda = 1.4k_F$. It is clear from Fig. 3.1(b) that $1/R_k$ deviates significantly from the linear behavior such that the wavefunction of the paired state $\mathrm{Pf}[g^{(-1)}(\mathbf{r}_i - \mathbf{r}_j)]\Psi_{\tilde{\phi}}^L(\{\mathbf{r}_i\})$ is different from a MRP

at shorter distances $|\mathbf{r}_i - \mathbf{r}_j| \leq \ell_B$.

Remarkably, a completely new paired state emerges for intermediate Coulomb interactions. When $\lambda > \lambda_{c1}$, the gap function $\tilde{\Delta}_k$ changes sign at k_0 where R_k is singular as shown in Fig. 3.1(c) and Fig. 3.2(a,b). This singularity causes the pairing function $g^{(-1)}(\mathbf{r})$ to oscillate in real space as shown in Fig. 3.1(d). We find that in the long-wavelength limit its amplitude decays as $1/\sqrt{r}$ according to $g^{(-1)}(\mathbf{r}) \sim (\sqrt{|z|}/z)\cos(k_0|z| - \frac{3}{4}\pi)$. Despite the sign change in the gap function $\tilde{\Delta}_k$, this oscillatory pfaffian state (OPS) remains fully gapped and topologically stable with quasiparticle dispersions shown in Figs. 3.2(a,b). The topological winding number associated with the mapping, via the pairing function g_k, from a compactified complex plane $k \equiv k_x + \mathrm{i}k_y$ to the two-sphere $\hat{n}_k \equiv (2\,\mathrm{Re}g_k, 2\,\mathrm{Im}g_k, 1-|g_k|^2)/(1+|g_k|^2)$ is *one*, generic of a chiral p-wave paired state. This state can be detected by spectroscopy measurements since the singularity at k_0 produces a kink in the quasiparticle density of states that moves toward the Fermi level as k_0 approaches k_F with increasing λ. For $\lambda > \lambda_{c2}$, the paired state is destroyed and the Rezayi-Read CFL becomes the variational ground state. This quantum phase transition is signaled by the closing of the quasiparticle excitation gap $\Delta_{\mathrm{eff}} \equiv \min_k\{E_k\}$ shown in Fig. 3.2(a,b) near the transition. We find that both λ_{c1} and λ_{c2} increase monotonically with $\tilde{\phi} = \nu^{-1}$, as shown in Fig. 3.2(d).

Since the interaction at short distances is reduced efficiently by the correlation-hole, the stability of the CFL against pairing must rely on the long-range part of the Coulomb interaction. As a result, the effects of screening become important. To illustrate this, we consider the 3D screened Coulomb interaction of the Yukawa

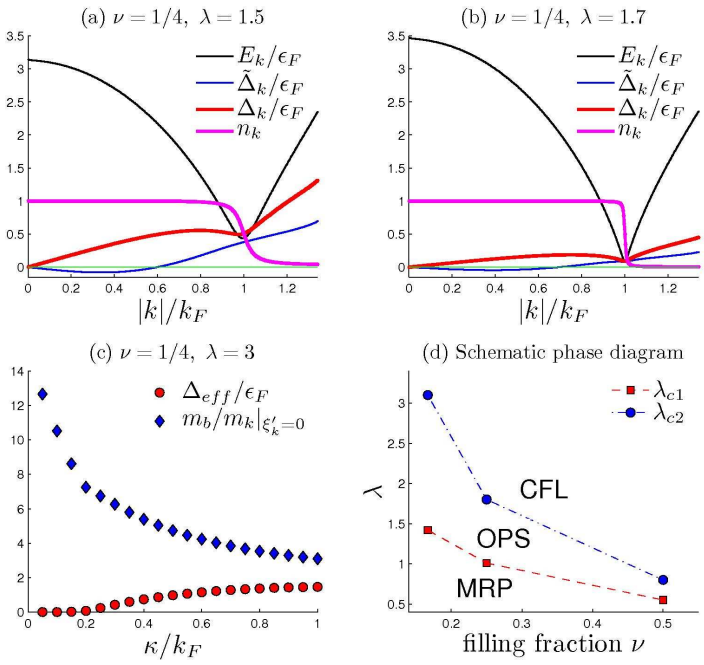

Figure 3.2: (a) and (b): The evolution of the quasiparticle dispersion E_k, the gap functions $(\Delta_k, \tilde{\Delta}_k)$, and the momentum distribution n_k at $\nu = 1/4$ with increasing λ. The excitation gap closes at $\lambda_{c2} \approx 1.8$. (c): The effects of screening at fixed $\lambda = 3$. The excitation gap Δ_{eff} and the effective mass m_k at the Fermi level ($\xi'_k = 0$) are plotted as a function of the inverse screening length κ. (d): The phase diagram of the even-denominator FQHE at $\nu = 1/2,\ 1/4,\ 1/6$.

form: $V_{\rm sc}(r) = V_c(r)e^{-\kappa r}$, where κ is the inverse screening length. Fig. 3.2(c) shows that a CFL stabilized by a large enough $\lambda > \lambda_{c2}$ can be driven through a continuous transition into a paired state by increasing screening, i.e. reducing the screening length. Concomitantly, the logarithmic divergence of the effective mass in the CFL at $\kappa = 0$ [174] is removed. We note that the MRP has been shown to be more stable when finite layer thickness is considered in the Coulomb interaction at $\nu = 5/2$ [157, 156].

3.3 Summary

To summarize, we have shown that the correlation hole, i.e. the binding of electrons to quantized finite-size vortices, is crucial for forming the paired quantum Hall states. The effective interaction is gauge-field free, instantaneous, and favors chiral p-wave pairing. The pairing potential is a direct consequence of the lowering of the Coulomb energy due to the correlation hole. We find that, with increasing Coulomb interaction strength, the ground state evolves from a $p - ip$ state asymptotically equivalent to the MRP, to a new oscillatory pfaffian state and finally to a CFL via a continuous phase transition as illustrated in Fig. 3.2(d).

Recently, FQHEs at $\nu = 1/2$ and $1/4$ have been observed in wide GaAs quantum wells[132, 190, 189] with higher electron density than in previous experiments that reported no signs of FQHE. Indeed, there are direct evidences [132, 190] that the signatures of FQHE become stronger with increasing electron density. This is consistent with our theory since λ is proportional to $k_F^{-1} \sim n_e^{-1/2}$; a smaller density would tend to destabilize the paired state. Hence, the paired quantum Hall states proposed in

this work can be prospective candidates for the observed even-denominator FQHE in the LLL.

Chapter 4

Z_2 spin liquids in the S=1/2 Heisenberg model on the kagome lattice

4.1 Introduction

At zero temperature all degrees of freedom tend to freeze and a variety of orders can develop in different materials, such as superconductivity and magnetism. However, it is natural to expect that a large zero-point energy can keep a quantum system stay in a liquid-like ground state even at $T = 0$. In a system consisting of localized quantum magnets, we call such a quantum-fluctuation-driven disordered ground state a quantum spin liquid (SL)[116]. It is an exotic phase with novel "fractionalized" excitations carrying only a fraction of the electron quantum number, *e.g.* spinons which carry spin but no charge. The internal structures of these SLs are so rich that they are

beyond the description of Landau's symmetry breaking theory[110] of conventional ordered phases. They are described by long-range quantum entanglement[123, 104] encoded in the ground state, which is coined "topological order"[214, 225] in contrast to the conventional symmetry-breaking order.

Geometric frustration in quantum magnets would lead to a huge degeneracy of classical ground state configurations. As a result the quantum tunneling among these classical ground states provides an ideal platform to realize quantum SLs. The quest for quantum SLs in frustrated magnets (for a recent review see Ref. [15]) has been pursued for decades. Among them the Heisenberg $S = 1/2$ kagome lattice model (HKLM)

$$H_{HKLM} = J \sum_{<i,j>} \boldsymbol{S}_i \cdot \boldsymbol{S}_j \tag{4.1}$$

has long been thought to be a promising candidate. Here $< i, j >$ denotes i, j being nearest neighbors. Experimental evidence of SL[135, 80, 88, 79] has been observed in $ZnCu_3(OH)_6Cl_2$ (called herbertsmithite), a spin-half antiferromagnet on the kagome lattice. Theoretically, in lack of an exact solution of the two-dimensional (2D) quantum Hamiltonian (4.1) in the thermodynamic limit, in previous studies either a honeycomb valence bond crystal[134, 150, 198, 199, 47] (HVBC) with an enlarged 6×6-site unit cell, or a gapless SL[97] were proposed as the ground state of HKLM. However, recently an extensive density-matrix-renormalization-group (DMRG) study[240] on HKLM reveals the ground state of HKLM as a gapped SL, which substantially lowers the energy compared with that of HVBC. Besides, they also observe numerical signatures of Z_2 topological order in the SL state.

Motivated by this important numerical discovery, we try to find out the na-

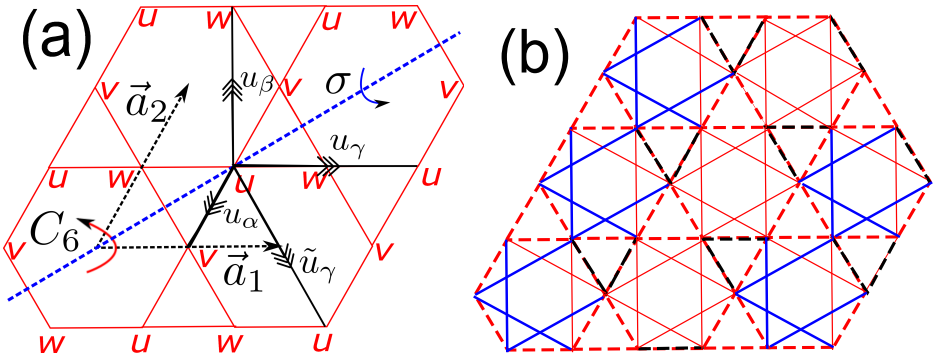

Figure 4.1: (color online) (a) kagome lattice and the elements of its symmetry group. $\vec{a}_{1,2}$ are the translation unit vectors, C_6 denotes $\pi/3$ rotation around honeycomb center and $\boldsymbol{\sigma}$ represents mirror reflection along the dashed blue line. Here u_α and u_β denote 1st and 2nd nearest neighbor (n.n.) mean-field bonds while u_γ and $\tilde{u}_\gamma$ represent two kinds of independent 3rd n.n. mean-field bonds. (b) Mean-field ansatz of $Z_2[0,\pi]\beta$ state up to 2nd nearest neighbor. Colors in general denote the sign structure of mean-field bonds. Dashed lines denote 1st n.n. real hopping terms $\chi_1 \sum_{<i,j>\alpha}(\nu_{ij} f^\dagger_{i\alpha} f_{j\alpha} + \ h.c.)$: red ones have $\nu_{ij} = 1$ and black ones have $\nu_{ij} = -1$. Solid lines stand for 2nd n.n. hopping $\chi_2 \sum_{<<ij>>\alpha} \nu_{ij}(f^\dagger_{i\alpha} f_{j\alpha} + \ h.c.)$ and singlet pairing $\sum_{<<ij>>\alpha\beta} \epsilon_{\alpha\beta}\nu_{ij}(\Delta_2 f^\dagger_{i\alpha} f^\dagger_{j\beta} + \ h.c.)$: again red ones have $\nu_{ij} = 1$ and blue ones have $\nu_{ij} = -1$. Here $\chi_{1,2}$ and Δ_2 are real parameters after choosing a proper gauge.

ture of this gapped Z_2 SL. Different Z_2 SLs on the kagome lattice have been previously studied using Schwinger-boson representation[182, 211]. We propose the candidate states of symmetric Z_2 SLs on kagome lattice by Schwinger-fermion mean field approach[19, 2, 18, 108, 144, 227, 119]. Following is the summary of our results. First we use projective symmetry group[225] (PSG) to classify all 20 possible Schwinger-fermion mean-field ansatz of Z_2 SLs which preserve all the symmetry of HKLM, as shown in TABLE 4.1. We analyze these 20 states and rule out some obviously unfavorable states: *e.g.* gapless states, and those states whose 1st nearest neighbor (n.n.) mean-field amplitudes are required to vanish by symmetry. Then we focus on the four Z_2 SLs in the neighborhood of the $U(1)$-Dirac SL[169]. In Ref. [169] it is shown that $U(1)$-Dirac SL has a significantly lower energy compared with other candidate $U(1)$ SL states, such as the uniform resonating-valence-bond (RVB) state(or the $U(1)$ SL-$[0,0]$ state in notation of Ref. [169]). We find out that there is only one gapped Z_2 SL, which we label as $Z_2[0,\pi]\beta$, in the neighborhood of $U(1)$-Dirac SL. Therefore we propose this $Z_2[0,\pi]\beta$ state as a promising candidate state for the ground state of HKLM. The mean-field ansatz of $Z_2[0,\pi]\beta$ state is shown in FIG. 4.1(b). Our work also provides guideline for choosing variational states in future numeric studies of SL ground state on kagome lattice.

4.2 Schwinger-fermion construction of spin liquids and projective symmetry group (PSG)

4.2.1 Schwinger-fermion construction of symmetric spin liquids

In the Schwinger-fermion construction[19, 2, 18, 108, 144, 227], we represent a spin-1/2 operator at site i by fermionic spinons $\{f_{i\alpha},\ \alpha =\uparrow,\downarrow\}$:

$$\vec{S}_i = \frac{1}{2} f^\dagger_{i\alpha} \vec{\sigma}_{\alpha\beta} f_{i\beta}. \tag{4.2}$$

Heisenberg hamiltonian $H = \sum_{<ij>} J_{ij} \vec{S}_i \cdot \vec{S}_j$ is represented as $H = \sum_{<ij>} -\frac{1}{2} J_{ij} \big(f^\dagger_{i\alpha} f_{j\alpha} f^\dagger_{j\beta} f_{j\beta} + \frac{1}{2} f^\dagger_{i\alpha} f_{i\alpha} f^\dagger_{j\beta} f_{j\beta} \big)$. Just like any other projective construction, this formulation enlarges the Hilbert space of the original spin system. To obtain the physical spin state from a mean-field state of f-spinons, we need to enforce the following one-f-spinon-per-site constraint:

$$f^\dagger_{i\alpha} f_{i\alpha} = 1, \qquad\qquad f_{i\alpha} f_{i\beta} \epsilon_{\alpha\beta} = 0. \tag{4.3}$$

Mean-field parameters of symmetric SLs are $\Delta_{ij}\epsilon_{\alpha\beta} = -2\langle f_{i\alpha} f_{j\beta}\rangle$, $\chi_{ij}\delta_{\alpha\beta} = 2\langle f^\dagger_{i\alpha} f_{j\beta}\rangle$, where $\epsilon_{\alpha\beta}$ is fully antisymmetric tensor. Both terms are invariant under global $SU(2)$ spin rotations. After Hubbard-Stratonovich transformation, the lagrangian of the spin system can be written as

$$\begin{aligned} L = & \sum_i \psi^\dagger_i \partial_\tau \psi_i + \sum_{<ij>} \frac{3}{8} J_{ij} \big[\frac{1}{2} \mathrm{Tr}(U^\dagger_{ij} U_{ij}) \\ & - (\psi^\dagger_i U_{ij} \psi_j + h.c.) \big] + \sum_i a^l_0(i) \psi^\dagger_i \tau^l \psi_i \end{aligned} \tag{4.4}$$

where two-component fermion notation $\psi_i = (f_{i\uparrow}, f_{i\downarrow}^\dagger)$ is introduced for reasons that will be explained shortly. We use τ^0 to denote the 2×2 identity matrix and $\tau^{1,2,3}$ are the three Pauli matrices. U_{ij} is a matrix of mean-field amplitudes:

$$U_{ij} = \begin{pmatrix} \chi_{ij}^\dagger & \Delta_{ij} \\ \Delta_{ij}^\dagger & -\chi_{ij} \end{pmatrix}. \tag{4.5}$$

$a_0^l(i)$ are the local lagrangian multipliers that enforces the constraints Eq.(5.4).

In terms of ψ, Schwinger-fermion representation has an explicit $SU(2)$ gauge redundancy: a transformation $\psi_i \to W_i\psi_i$, $U_{ij} \to W_iU_{ij}W_j^\dagger$, $W_i \in SU(2)$ leaves the action invariant. This redundancy is originated from representation Eq.(5.3): this local $SU(2)$ transformation leaves the spin operators invariant and thus does not change physical Hilbert space. One can try to solve Eq.(5.5) by mean-field (or saddle-point) approximation. At mean-field level, U_{ij} and a_0^l are treated as complex numbers, and a_0^l must be chosen such that constraints (5.4) are satisfied at the mean field level: $\langle\psi_i^\dagger\tau^l\psi_i\rangle = 0$. The mean-field ansatz can be written as:

$$H_{MF} = -\sum_{<ij>} \psi_i^\dagger\langle i|j\rangle\psi_j + \sum_i \psi_i^\dagger a_0^l\tau^l\psi_i. \tag{4.6}$$

where we defined $\langle i|j\rangle \equiv \frac{3}{8}J_{ij}U_{ij}$. Under a local $SU(2)$ gauge transformation $\langle i|j\rangle \to W_i\langle i|j\rangle W_j^\dagger$, but the physical spin state described by the mean-field ansatz $\{\langle i|j\rangle\}$ remains the same. By construction the mean-field ansatz does not break spin rotation symmetry, and the mean field solutions describe SL states if lattice symmetry is preserved. Different $\{\langle i|j\rangle\}$ ansatz may be in different SL phases. The mathematical language to classify different SL phases is projective symmetry group (PSG)[225].

4.2.2 Projective symmetry group (PSG) classification of topological orders in spin liquids

PSG characterizes the topological order in Schwinger-fermion representation: SLs described by different PSGs are different phases. It is defined as the collection of all combinations of symmetry group and $SU(2)$ gauge transformations that leave mean-field ansatz $\{\langle i|j\rangle\}$ invariant (as a_0^l are determined self-consistently by $\{\langle i|j\rangle\}$, these transformations also leave a_0^l invariant). The invariance of a mean-field ansatz $\{\langle i|j\rangle\}$ under an element of PSG $G_U U$ can be written as

$$\begin{aligned} G_U U(\{\langle i|j\rangle\}) &= \{\langle i|j\rangle\}, \\ U(\{\langle i|j\rangle\}) &\equiv \{\langle i\tilde{|}j\rangle = \langle U^{-1}(i)|U^{-1}(j)\rangle\}, \\ G_U(\{\langle i|j\rangle\}) &\equiv \{\langle i\tilde{|}j\rangle = G_U(i)\langle i|j\rangle G_U(j)^\dagger\}, \\ G_U(i) &\in SU(2). \end{aligned} \tag{4.7}$$

Here $U \in SG$ is an element of symmetry group (SG) of the corresponding SL. In our case of symmetric SLs on the kagome lattice, we use (x, y, s) to label a site with sublattice index $s = u, v, w$ and $x, y \in \mathbb{Z}$. Bravais unit vector are chosen as $\vec{a}_1 = a\hat{x}$ and $\vec{a}_2 = \frac{a}{2}(\hat{x} + \sqrt{3}\hat{y})$ as shown in FIG. 4.1(a). The symmetry group is generated by time reversal operation $\boldsymbol{T}$, lattice translations $T_{1,2}$ along $\vec{a}_{1,2}$ directions, $\pi/3$ rotation C_6 around honeycomb plaquette center and the mirror reflection $\boldsymbol{\sigma}$ (for details see Ref. [129]). For example, if $U = T_1$ is the translation along $\vec{a}_1$-direction in Fig.4.1(a), $T_1(\{x, y, s\}) = \{x + 1, y, s\}$. G_U is the gauge transformation associated with U such that $G_U U$ leave $\{\langle i|j\rangle\}$ invariant. Notice this condition (4.7) allows us to generate all

symmetry-related mean-field bonds from one by the following relation:

$$\langle i|j\rangle = G_U(i)\langle U^{-1}(i)|U^{-1}(j)\rangle G_U^\dagger(j) \tag{4.8}$$

There is an important subgroup of PSG, the invariant gauge group (IGG), which is composed of all the pure gauge transformations in PSG: $IGG \equiv \{\{W_i\}|W_i\langle i|j\rangle W_j^\dagger = \langle i|j\rangle, W_i \in SU(2)\}$. In other words, $W_i = G_{\boldsymbol{e}}(i)$ is the pure gauge transformation associated with identity element $\boldsymbol{e} \in SG$ of the symmetry group. One can always choose a gauge in which the elements in IGG is site-independent. In this gauge, IGG can be the global Z_2 transformations: $\{G_{\boldsymbol{e}}(i) \equiv G_{\boldsymbol{e}} = \pm\tau^0\}$, the global $U(1)$ transformations: $\{G_{\boldsymbol{e}}(i) \equiv e^{\mathrm{i}\theta\tau^3}, \theta \in [0, 2\pi]\}$, or the global $SU(2)$ transformations: $\{G_{\boldsymbol{e}}(i) \equiv e^{\mathrm{i}\theta\hat{n}\cdot\vec{\tau}}, \theta \in (0, 2\pi], \hat{n} \in S^2\}$, and we term them as Z_2, $U(1)$ and $SU(2)$ state respectively.

The importance of IGG is that it controls the low energy gauge fluctuations of the corresponding SL states. Beyond mean-field level, fluctuations of U_{ij} and a_0^l need to be considered and the mean-field state may or may not be stable. The low energy effective theory is described by fermionic spinon band structure coupled with a dynamical gauge field of IGG. For example, Z_2 state with gapped spinon dispersion can be a stable phase because the low energy Z_2 dynamical gauge field can be in the deconfined phase[213, 106].

Notice that the condition $\{G_{\boldsymbol{e}}(i) \equiv G_{\boldsymbol{e}} = \pm\tau^0\}$ for a Z_2 SL leads to a series of consistent conditions for the gauge transformations $\{G_U(i)|U \in SG\}$, as shown in Ref. [129]. Gauge inequivalent solutions of these conditions (**??**)-(**??**) lead to different Z_2 SLs. Soon we will show that there are 20 Z_2 SLs on the kagome lattice that can be realized by a mean-field ansatz $\{\langle i|j\rangle\}$.

4.3 Z_2 spin liquids on the kagome lattice and $Z_2[0,\pi]\beta$ state

Following previous discussions, we use PSG to classify all possible 20 Z_2 SL states on kagome lattice in this section. As will be shown later, among them there is one gapped Z_2 SL labeled as $Z_2[0,\pi]\beta$ state, which is the most promising candidate for the SL ground state of HKLM.

4.3.1 PSG classification of Z_2 spin liquids on kagome lattice

Applying the condition $G_{\boldsymbol{e}}(i) \equiv G_{\boldsymbol{e}} = \pm\tau^0$ to kagome lattice with symmetry group described in Ref. [129], we obtain a series of consistent conditions for the gauge transformation $G_U(i)$. Solving these conditions we reach all the 20 different Schwinger-fermion mean-field states of Z_2 SLs on kagome lattice, as summarized in TABLE 4.1. These 20 mean-field states correspond to different Z_2 SL phases, which cannot continuously tuned into each other without a phase transition.

As discussed in Ref. [129], from PSG elements $G_U(i)$ one can obtain all other symmetry-related mean-field bonds from one using symmetry condition (4.8). Therefore we use $u_\alpha \equiv \langle 0,0,v|0,0,u\rangle$ to represent 1st nearest neighbor (n.n.) mean-field bonds. $u_\beta \equiv \langle 0,1,w|0,0,u\rangle$ is representative of 2nd n.n. mean-field bonds. There are two kinds of symmetry-unrelated 3rd n.n. mean-field bonds, represented by $u_\gamma = \langle 1,0,u|0,0,u\rangle$ and $\tilde{u}_\gamma = \langle 1,-1,u|0,0,u\rangle$. The consistent conditions for these mean-field bonds due to symmetry are listed in Ref. [129]. Besides, the on-site

chemical potential terms $\Lambda(i)$ (which guarantee the physical constraint (5.4) on the mean-field level) also satisfy symmetry conditions. We can show that $\Lambda(x, y, s) \equiv \Lambda_s$ for these 20 Z_2 SL states. The symmetry-allowed mean-field amplitudes/bonds are also summarized in TABLE 4.1.

From TABLE 4.1 we can see there are 6 states, *i.e.* $\#7 - \#12$ that don't allow 1st n.n. mean-field amplitudes by symmetry. Moreover, they cannot realize a Z_2 SL with up to 3rd n.n. mean-field amplitudes. Therefore they are unlikely to be the HKLM ground state. Ruling out these six Z_2 SLs, we can see the other 14 Z_2 SL states fall into 4 classes. To be specific, they are continuously connected to different $U(1)$ gapless SL states on kagome lattice. These $U(1)$ SL states in general have the following mean-field ansatz

$$H_{U(1)SL} = \chi_1 \sum_{<ij>} \nu_{ij} (f^\dagger_{i\alpha} f_{j\alpha} + \ h.c.) \tag{4.9}$$

where $\nu_{ij} = \pm 1$ characterizes the sign structure of hopping terms with $\chi_1 \in \mathbb{R}$. Different such $U(1)$ SL states are featured by the flux of f-spinon hopping phases around basic plaquette: honeycombs and triangles on the kagome lattice.

The simplest example is the so-called uniform RVB state with $\nu_{ij} \equiv 1$ for all 1st n.n. mean-field bonds. The hopping phase around any plaquette is $1 = \exp[\mathrm{i}0]$, and thus the corresponding flux is $[0, 0]$ for [triangle,honeycomb] motifs. The 4 possible Z_2 spin liquids in the neighborhood[130] of uniform RVB states (*i.e.* $U(1)$ SL-$[0, 0]$ state in Ref. [169]) are classified in Ref. [129]. They are $\#1, \#5, \#15, \#13$ in TABLE 4.1. We label them as $Z_2[0, 0]A$, $Z_2[0, 0]B$, $Z_2[0, 0]C$ and $Z_2[0, 0]D$ states. They all have gapped spectra of spinons.

The ansatz of two other $U(1)$ SLs are shown in FIG. 4.2. They both have π-

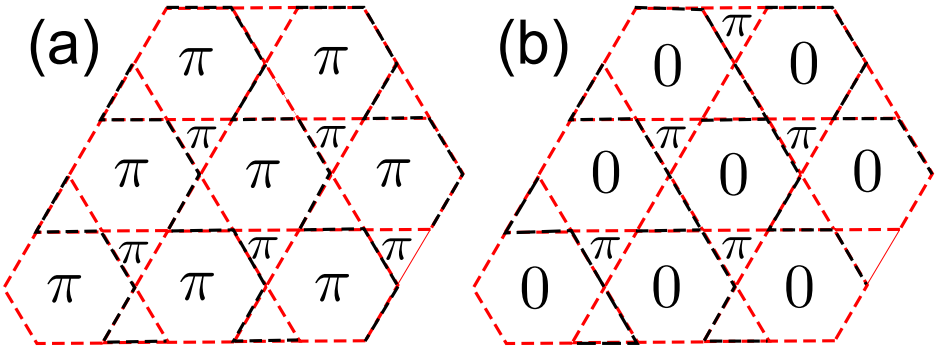

Figure 4.2: (color online) Mean-field ansatz of (a) $U(1)$ SL-$[\pi,\pi]$ state and (b) $U(1)$ SL-$[\pi,0]$ state, with 1st n.n. real hopping terms $H_{MF} = \chi_1 \sum_{<ij>\alpha}(\nu_{ij} f^\dagger_{i\alpha} f_{j\alpha} + h.c.)$. Colors again denote the sign structure of mean-field bonds: red dashed lines have $\nu_{ij} = 1$ and black dashed lines have $\nu_{ij} = -1$.

flux piercing through a triangle basic plaquette. Following the above notations of hopping phase in [triangle,honeycomb] motifs, with either π-flux or 0-flux through the honeycomb plaquette, they are called $U(1)$ SL-$[\pi,\pi]$ state and $U(1)$ SL-$[\pi,0]$ state. There are three Z_2 SLs in the neighborhood of both $U(1)$ SL states, *i.e.* #3, #17, #19 around $U(1)$ SL-$[\pi,\pi]$ state and #4, #18, #20 around $U(1)$ SL-$[\pi,0]$ state. All these six Z_2 SLs have gapless spinon spectra, inherited from the two gapless $U(1)$ SLs featured by a doubly-degenerate flat band and a Dirac cone at Brillouin-zone center. This is in contrast to the numerically observed gap in two-spinon spectrum[240], thus we can also rule out these 6 Z_2 SLs for the HKLM ground state.

Another $U(1)$ SL state is the so called $U(1)$-Dirac SL or $U(1)$ SL-$[0,\pi]$ state. Its mean-field ansatz is shown by the 1st n.n. bonds in FIG. 4.1(b) and clearly π-flux pierces through certain triangle plaquette with no flux through the honeycomb plaquette. According to variational Monte Carlo studies[77, 169], this $U(1)$-Dirac SL have substantially lower energy compared to many other competing phases, in particular the uniform RVB state. Therefore we shall focus on those Z_2 SLs in the

neighborhood of the $U(1)$-Dirac SL in our search of the HKLM ground state. We need to mention that although unlikely, the four Z_2 SLs in the neighborhood of uniform RVB state, or $U(1)$ SL-$[0,0]$ state is potentially possible to be the HKLM ground state.

4.3.2 $Z_2[0,\pi]\beta$ state as a promising candidate for the HKLM ground state

How to find those Z_2 SLs in the neighborhood of, or continuously connected to the $U(1)$-Dirac SL? Naively, we expect the mean-field ansatz of these Z_2 SLs can be obtained from that of $U(1)$-Dirac SL by adding an infinitesimal perturbation. To be specific, we require an infinitesimal spinon pairing term on top of the $U(1)$-Dirac SL mean-field ansatz (4.9) to break the IGG from $U(1)$ to Z_2 through Higgs mechanism. Mathematically, we need to find those Z_2 SL states whose PSG is a subgroup of the $U(1)$-Dirac SL's PSG[130]. Such Z_2 SL states are defined to be in the neighborhood of $U(1)$-Dirac SL. Similar criterion applies to the neighboring Z_2 SL states of any $U(1)$ or $SU(2)$ SL state.

We find out all four Z_2 SLs in the neighborhood of $U(1)$-Dirac SLs in Ref. [129]. They are states $\#6, \#2, \#14, \#16$ in TABLE 4.1, labeled as $Z_2[0,\pi]\alpha$, $Z_2[0,\pi]\beta$, $Z_2[0,\pi]\gamma$ and $Z_2[0,\pi]\delta$ states respectively. Since the effective theory of a $U(1)$-Dirac SL is an 8-component Dirac fermion coupled with dynamical $U(1)$ gauge field[169, 83], we can find out all symmetry-allowed mass terms that can open up a gap in the Dirac-like spinon spectrum. Following detailed calculations in Ref. [129], we can see that among the four Z_2 SLs around the $U(1)$-Dirac SL, only one state, *i.e.* $Z_2[0,\pi]\beta$ (state

#2 in TABLE 4.1) can generate a mass gap in the spinon spectrum while in other 3 states the Dirac cone in spinon spectrum is protected by symmetry. The mean-field ansatz of $Z_2[0,\pi]\beta$ SL state up to 2nd n.n. is shown in FIG. 4.1(b):

$$\begin{aligned} H_{MF} = \textstyle\sum_i (\lambda_3 \sum_\alpha f^\dagger_{i\alpha} f_{i\alpha} + \lambda_1 f^\dagger_{i\uparrow} f^\dagger_{i\downarrow} + h.c.) \\ + \chi_1 \textstyle\sum_{<ij>\alpha} \nu_{ij} (f^\dagger_{i\alpha} f_{j\alpha} + h.c.) + \\ \textstyle\sum_{<<ij>>} \nu_{ij} (\chi_2 \sum_\alpha f^\dagger_{i\alpha} f_{j\alpha} + \Delta_2 \sum_{\alpha\beta} \epsilon^{\alpha\beta} f^\dagger_{i\alpha} f^\dagger_{j\beta} + h.c.) \end{aligned} \tag{4.10}$$

where $\epsilon^{\alpha\beta}$ is the anti-symmetric tensor. We only list up to 2nd n.n. mean-field amplitudes because as shown in TABLE 4.1 (see also Ref. [129]), this $Z_2[0,\pi]\beta$ state only needs 2nd n.n. pairing terms to realize a Z_2 SL. We can always choose a proper gauge so that mean-field parameters $\chi_{1,2}$ and Δ_2 are all real. The sign structure of $\nu_{ij} = \pm 1$ are shown in FIG. 4.1(b), with red denoting $\nu_{ij} = 1$ and other colors representing $\nu_{ij} = -1$. As discussed in Ref. [129], the 2nd n.n. singlet-pairing term $\Delta_2 \neq 0$ not only break the $U(1)$ gauge symmetry down to Z_2, but also opens up a mass gap in the spinon spectrum. The on-site chemical potential $\lambda_{1,3}$ are self-consitently determined by the following constraint:

$$\begin{aligned} \textstyle\sum_i \langle f^\dagger_{i\uparrow} f^\dagger_{i\downarrow} \rangle = \sum_i \langle f_{i\uparrow} f_{i\downarrow} \rangle = 0, \\ \textstyle\sum_i (\sum_{\alpha=\uparrow,\downarrow} f^\dagger_{i\alpha} f_{i\alpha} - 1) = 0. \end{aligned} \tag{4.11}$$

For further n.n. mean-field ansatz see discussions in Ref. [129].

4.4 Conclusion

To summarize, motivated by the strong evidence of a Z_2 SL as the HKLM ground state in recent DMRG study[240], we classify all possible Z_2 SL states in Schwinger-

fermion mean-field approach using PSG. We found 20 different Schwinger-fermion mean-field states of Z_2 SLs on kagome lattice, among which 6 states are unlikely due to vanishing 1st n.n. mean-field amplitude. In other 14 Z_2 SLs only 5 possess a gapped spinon spectrum, which is observed in the DMRG result[240]. Among these five symmetric Z_2 SL states four are in the neighborhood of uniform RVB (or $U(1)$ SL-$[0,0]$) state, while the other one, *i.e.* $Z_2[0,\pi]\beta$ is in the neighborhood of $U(1)$-Dirac SL state. Previous variational Monte Carlo study[169] showed that $U(1)$-Dirac SL has a substantially lower energy in comparison to the uniform RVB state. Therefore we propose this $Z_2[0,\pi]\beta$ state with mean-field ansatz (4.10) shown in FIG. 4.1(b) as the HKLM ground state numerically detected in Ref. [240]. Our work provides important insight for future numeric study of Gutzwiller projected wavefunctions.

#	η_{12}	Λ_s	u_α	u_β	u_γ	$\tilde{u}_\gamma$	Label	Gapped?
1	$+1$	τ^2,τ^3	τ^2,τ^3	τ^2,τ^3	τ^2,τ^3	τ^2,τ^3	$Z_2[0,0]A$	Yes
2	-1	τ^2,τ^3	τ^2,τ^3	τ^2,τ^3	τ^2,τ^3	0	$Z_2[0,\pi]\beta$	**Yes**
3	$+1$	0	τ^2,τ^3	0	0	0	$Z_2[\pi,\pi]A$	No
4	-1	0	τ^2,τ^3	0	0	τ^2,τ^3	$Z_2[\pi,0]A$	No
5	$+1$	τ^3	τ^2,τ^3	τ^3	τ^3	τ^3	$Z_2[0,0]B$	Yes
6	-1	τ^3	τ^2,τ^3	τ^3	τ^3	τ^2	$Z_2[0,\pi]\alpha$	No
7	$+1$	0	0	τ^2,τ^3	0	0	-	-
8	-1	0	0	τ^2,τ^3	0	0	-	-
9	$+1$	0	0	0	τ^2,τ^3	0	-	-
10	-1	0	0	0	τ^2,τ^3	0	-	-
11	$+1$	0	0	τ^2	τ^2	0	-	-
12	-1	0	0	τ^2	τ^2	0	-	-
13	$+1$	τ^3	τ^3	τ^2,τ^3	τ^3	τ^3	$Z_2[0,0]D$	Yes
14	-1	τ^3	τ^3	τ^2,τ^3	τ^3	0	$Z_2[0,\pi]\gamma$	No
15	$+1$	τ^3	τ^3	τ^3	τ^2,τ^3	τ^3	$Z_2[0,0]C$	Yes
16	-1	τ^3	τ^3	τ^3	τ^2,τ^3	0	$Z_2[0,\pi]\delta$	No
17	$+1$	0	τ^2	τ^3	0	0	$Z_2[\pi,\pi]B$	No
18	-1	0	τ^2	τ^3	0	τ^3	$Z_2[\pi,0]B$	No
19	$+1$	0	τ^2	0	τ^2	0	$Z_2[\pi,\pi]C$	No
20	-1	0	τ^2	0	τ^2	τ^3	$Z_2[\pi,0]C$	No

Table 4.1: Mean-field ansatz of 20 possible Z_2 SLs on a kagome lattice. In our notation of mean-field amplitudes $\langle x,y,s|0,0,u\rangle \equiv [x,y,s]$, this table summarizes all symmetry-allowed independent mean-field bonds up to 3rd n.n., *i.e.* 1st n.n. bond $u_\alpha = [0,0,v]$, 2nd n.n. bond $u_\beta = [0,1,w]$, 3rd n.n. bonds $u_\gamma = [1,0,u]$ and $\tilde{u}_\gamma = [1,-1,u]$ as shown in FIG. 4.1(a). Λ_s denote the on-site chemical potential terms to enforce the constraint (4.11). $\tau^{0,3}$ denotes hopping while $\tau^{1,2}$ denotes pairing terms.#2 or $Z_2[0,\pi]\beta$ state is the most promising candidate of Z_2 SL for the HKLM ground state.

Chapter 5

Z_2 spin liquid and chiral antiferromagnetic phase in the Hubbard model on a honeycomb lattice

5.1 Introduction

A novel state of matter, quantum spin liquid (SL), has been recently discovered in organic spin-1/2 triangular lattice experimental systems[192, 90, 239]. This class of organic Mott insulators is in the vicinity of the Mott transition and can be driven into a Fermi liquid by applying pressure. A quantum SL is the ground state of a Mott insulator which does not break physical symmetries, and cannot be adiabatically connected to a band insulator. After Anderson's proposal of resonating valence bond

(RVB) states[8], a lot of theoretical and experimental efforts have been made to show the existence of such novel phases of matter with fractionalized excitations[153]. For example, various exact or quasi-exact solvable models[180, 138, 226, 102] hosting SL ground states have been constructed. The exciting experimental progress on the triangular lattice organics raises an interesting question: can SL be naturally realized in a Mott insulator close to the Mott transition?[143, 120] If this is true, it can serve as a guideline in searching SLs in experimental systems. Physical intuition suggests this is likely to be the case because in the neighborhood of the Mott transition, quantum fluctuations of spins are strong which can suppress the classical spin ordering.

A recent remarkable numerical study[136] for the nearest neighbor Hubbard model on the honeycomb lattice

$$H = -t \sum_{<ij>\sigma} c^{\dagger}_{i\sigma} c_{j\sigma} + U \sum_{i} c^{\dagger}_{i\uparrow} c_{i\uparrow} c^{\dagger}_{i\downarrow} c_{i\downarrow} \tag{5.1}$$

provides another evidence of this guideline, where an insulating phase respecting all physical symmetry is found in the neighborhood of the Mott transition. This phase has attracted quite some theoretical attention[210, 237] because it cannot be explained as a band insulator due to the honeycomb lattice structure. It should be a SL with fractionalized excitations. There are many different SLs on the honeycomb lattice, characterized by different topological orders[225]. Which SL is realized in the simulated Hubbard model? And in a general context, is there a systematic way to identify the SLs in the neighborhood of a Mott transition? We provide our answers to these questions in this letter.

In Ref. [136], it is shown that this SL phase has a full energy gap, and is likely to be smoothly connected (*i.e.* through a continuous phase transition) to both the

semi-metal phase for small U/t and an antiferromagnetic (AF) phase for large U/t. These three conditions strongly restrict the candidate SL phases.

There have been two popular approaches to describe SL phases: Schwinger-fermion[19, 108, 3, 227] and Schwinger-boson[13, 180], in which the low energy spin excitations are fermionic and bosonic spinons respectively. The fermionic approach is more natural to be used in the viicinity of a continuous Mott transition, whereas the bosonic model is more natural when close to a magnetic transition[1]. The possible underlying relation between the two seemingly very different approaches has been a long-standing puzzle.

In Schwinger-fermion representation, we classify all possible 128 different Z_2 spin liquids using projective symmetry group (PSG)[225]. In the vicinity of the Mott transition in simulated Hubbard model[136], we will show that there is only one natural SL among them, a Z_2 state coined the sublattice pairing state (SPS) which has a full energy gap and can be smoothly connected to the semi-metal phase. Moreover, Schwinger-boson method has been used to describe the magnetic phase transition[210] in the same system. It was found that only one SL phase, the 0-flux state, can be smoothly connected to an antiferromagnetically (AF) ordered phase. The 0-flux state is also a Z_2 state with a full energy gap. However, it is not clear whether this 0-flux state can be smoothly connected to the semi-metal phase. Can SPS be related to the 0-flux state? In this chapter, we will demonstrate that remarkably, SPS and 0-flux state are identical by an explicit duality transformation in the low energy effective

[1]This is because close to a Mott transition, physically the low energy spinons should be the electrons which lose their charge coherence. And bosonic spinon condensation can easily explain the transition into a magnetic ordered phase.

theory. This is the first identification of a state in both the Schwinger fermion and the Schwinger boson methods.

We will also show that the magnetically ordered phase connected to SPS is rather unusual and *not* the simple Neel phase, because it breaks the $SU(2)$ spin-rotation symmetry completely and has three Goldstone modes. We name this phase chiral-antiferromagnetic (CAF) phase. Aside from the usual AF spin order parameter $\vec{N} = (-1)^{i_s}\vec{S}_i$ where $i_s = 0, 1$ for A and B sublattices respectively, in CAF phase there is another vector-chirality spin order parameter $\vec{n} = \sum_{<<ij>>} \nu_{ij}\vec{S}_i \times \vec{S}_j$ whose expectation value satisfies $\langle\vec{n}\rangle \perp \langle\vec{N}\rangle$. $\nu_{ij} = +1(-1)$ if one goes from site i to j in a clockwise(counterclockwise) manner, as shown by the arrows in FIG. 5.1(b). Since the usual AF phase should exist in the large U/t limit[63], our results suggest a hidden phase transition, which might happen in the "Neel" phase of the previously mentioned numerical study[136] or at a larger U/t not studied before. We therefore propose the schematic phase diagram as shown in Fig.5.2(a).

This chapter is organized in the following way. In section 5.2 we give a brief exposition of $SU(2)$ Schwinger-fermion approach to spin liquid states and projective symmetry group (PSG) classification of different spin liquids. Following the mathematical classification of all Z_2 spin liquids using PSG in Ref. [128], we discuss the possible gapped Z_2 spin liquids continuously connected to a semimetal phase in section 5.3. We find out there is only one natural candidate, the sublattice pairing state (SPS). A mean-field study of SPS in J_1-J_2 Heisenberg model is also given in Ref. [128]. In section 5.4 we discuss the continuous phase transition between SPS and a magnetically ordered phase and reveal a hidden order parameter of this chiral-antiferromagnetic

(CAF) phase aside from Neel order parameter. In section 5.5 we identify our SPS state with the 0-flux state in Schwinger-boson mean-field approach[210] through an explicit duality transformation. Finally we summarize our results in section 5.6.

5.2 Schwinger-fermion approach and projective symmetry group (PSG)

In the large U limit at half-filling, the charge flucutation in Hubbard model (5.1) is severely suppressed and the low-energy spin fluctuations are described by $S = 1/2$ Heisenberg model[133]

$$H_{spin} = -\frac{4t^2}{U} \sum_{<ij>} \mathbf{S}_i \cdot \mathbf{S}_j + O(\frac{t^3}{U^2}) \tag{5.2}$$

In Schwinger-fermion approach, a spin-1/2 operator at site i is represented by:

$$\vec{S}_i = \frac{1}{2} f^\dagger_{i\alpha} \vec{\sigma}_{\alpha\beta} f_{i\beta}. \tag{5.3}$$

A Heisenberg spin Hamiltonian $H = \sum_{<ij>} J_{ij} \vec{S}_i \cdot \vec{S}_j$ is represented as $H = \sum_{<ij>} -\frac{1}{2} J_{ij} \big(f^\dagger_{i\alpha} f_{j\alpha} f^\dagger_{j\beta} f_{j\beta}$ $\frac{1}{2} f^\dagger_{i\alpha} f_{i\alpha} f^\dagger_{j\beta} f_{j\beta} \big)$. Because this representation enlarges the Hilbert space, states need to be constrained in the physical Hilbert space, i.e., one f-fermion per site:

$$f^\dagger_{i\alpha} f_{i\alpha} = 1, \qquad\qquad f_{i\alpha} f_{i\beta} \epsilon_{\alpha\beta} = 0. \tag{5.4}$$

Introducing mean-field parameters $\eta_{ij}\epsilon_{\alpha\beta} = -2\langle f_{i\alpha} f_{j\beta} \rangle$, $\chi_{ij}\delta_{\alpha\beta} = 2\langle f^\dagger_{i\alpha} f_{j\beta} \rangle$, where $\epsilon_{\alpha\beta}$ is fully antisymmetric tensor, after Hubbard-Stratonovich transformation, the

Lagrangian of the spin system can be written as[225]

$$L = \sum_i \psi_i^\dagger \partial_\tau \psi_i + \sum_{<ij>} \frac{3}{8} J_{ij} \big[\frac{1}{2} \mathrm{Tr}(U_{ij}^\dagger U_{ij}) - (\psi_i^\dagger U_{ij} \psi_j + h.c.) \big] + \sum_i a_0^l(i) \psi_i^\dagger \tau^l \psi_i \tag{5.5}$$

where two-component fermion notation $\psi_i = (f_{i,\uparrow}, f_{i,\downarrow}^\dagger)^T$ is introduced for reasons that will be explained shortly. U_{ij} is a matrix of mean-field amplitudes:

$$U_{ij} = \begin{pmatrix} \chi_{ij}^\dagger & \eta_{ij} \\ \eta_{ij}^\dagger & -\chi_{ij} \end{pmatrix}. \tag{5.6}$$

$a_0^l(i)$ are the local Lagrangian multipliers that enforces the constraints Eq.(5.4).

In terms of ψ, Schwinger-fermion representation has an explicit $SU(2)$ gauge redundancy: a transformation $\psi_i \to W_i \psi_i$, $U_{ij} \to W_i U_{ij} W_j^\dagger$, $W_i \in SU(2)$ leaves the action invariant. This redundancy is originated from representation Eq.(5.3): this local $SU(2)$ transformation leaves the spin operators invariant[3] and thus does not change physical Hilbert space.

One can try to solve Eq.(5.5) by mean-field (or saddle-point) approximation. At mean-field level, U_{ij} and a_0^l are treated as complex numbers, and a_0^l must be chosen such that constraints Eq.(5.4) are satisfied at the mean field level: $\langle \psi_i^\dagger \tau^l \psi_i \rangle = 0$. The mean-field ansatz can be written as:

$$H_{MF} = -\sum_{<ij>} \psi_i^\dagger u_{ij} \psi_j + \sum_i \psi_i^\dagger a_0^l \tau^l \psi_i. \tag{5.7}$$

where $u_{ij} = \frac{3}{8} J_{ij} U_{ij}$. A local $SU(2)$ gauge transformation modify $u_{ij} \to W_i u_{ij} W_j^\dagger$ but does not change the physical spin state described by the mean-field ansatz. By construction the mean-field amplitudes do not break spin rotation symmetry, and the

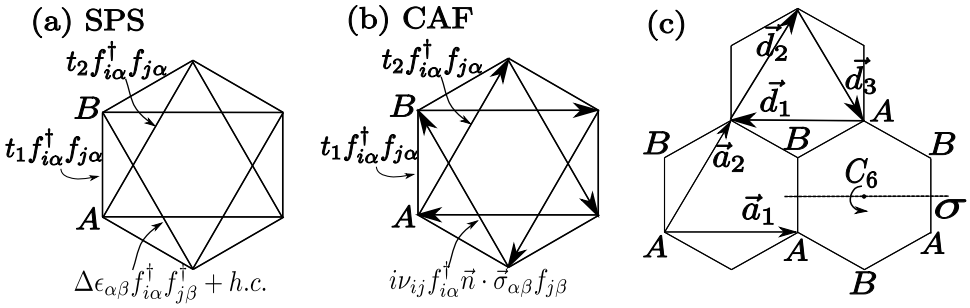

Figure 5.1: Mean-field ansatz of (a) SPS phase and (b) CAF phase in terms of f-fermion. $\nu_{ij} = 1$ if $i \to j$ is along the arrow direction. (c)The honeycomb lattice and its Bravais lattice vector $\vec{a}_{1,2}$. $\vec{d}_{1,2,3}$ are the three vectors used in Eq.5.21. Two generators of symmetry group are also shown: 60° rotation C_6 the horizontal mirror σ.

mean field solutions describe spin liquid states if translational symmetry is preserved. Different $\{u_{ij}\}$ ansatz may be in different spin liquid phases. The mathematical language to classify different spin liquid phases is PSG[225].

PSG is the manifestation of topological order in the Schwinger-fermion representation: spin liquid states described by different PSG's are different phases. It is defined as the collection of all combinations of symmetry group and $SU(2)$ gauge transformations that leave $\{u_{ij}\}$ invariant (as a^l_0 are determined self-consistently by $\{u_{ij}\}$, these transformations also leave a^l_0 invariant). The invariance of a mean-field ansatz $\{u_{ij}\}$ under an element of PSG $G_U U$ can be written as

$$\begin{aligned} G_U U(\{u_{ij}\}) &= \{u_{ij}\}, \\ U(\{u_{ij}\}) &\equiv \{\tilde{u}_{ij} = u_{U^{-1}(i),U^{-1}(j)}\}, \\ G_U(\{u_{ij}\}) &\equiv \{\tilde{u}_{ij} = G_U(i) u_{ij} G_U(j)^\dagger\}, \\ G_U(i) &\in SU(2). \end{aligned} \tag{5.8}$$

Here $U \in SG$ is an element of symmetry group (SG) of the spin liquid state. SG on

a honeycomb lattice is generated by time reversal $\boldsymbol{T}$, reflection $\boldsymbol{\sigma}$, $\pi/3$ rotation C_6 and translations T_1, T_2 as illustrated in FIG. 5.1 (see also Ref. [128]). G_U is the gauge transformation associated with U such that $G_U U$ leaves $\{u_{ij}\}$ invariant.

There is an important subgroup of PSG, Invariant Gauge Group (IGG), which is composed of all the pure gauge transformations in PSG: $IGG \equiv \{\{W_i\}|W_i u_{ij} W_j^\dagger = u_{ij}, W_i \in SU(2)\}$. One can always choose a gauge in which the elements in IGG is site-independent. In this gauge, IGG can be global Z_2 transformations: $\{W_i = \tau^0, W_i = -\tau^0\}$, the global $U(1)$ transformations: $\{W_i = e^{i\theta\tau^3}, \theta \in [0, 2\pi]\}$, or the global $SU(2)$ transformations: $\{W_i = e^{i\theta\hat{n}\cdot\vec{\tau}}, \theta \in [0, 2\pi], \hat{n} \in S^2\}$, and we dub them Z_2, $U(1)$ and $SU(2)$ state respectively.

The importance of IGG is that it controls the low-energy gauge fluctuations. Beyond mean-field level, fluctuations of U_{ij} and a_0^l need to be considered and the mean-field state may or may not be stable. The low-energy effective theory is described by fermionic spinon band structure coupled with a dynamical gauge field of IGG. For example, Z_2 state with gapped spinon dispersion can be a stable phase because the low-energy Z_2 dynamical gauge field can be in the deconfined phase[213, 106]. But for a $U(1)$ state with gapped spinon dispersion, the $U(1)$ gauge fluctuations would generally drive the system into confinement due to monopole proliferation[160], and the mean-field state would be unstable. And an $SU(2)$ state with gapped spinon dispersion should also be in the confined phase because there is no known IR stable fixed point of pure $SU(2)$ gauge theory in 2+1 dimension. Because the purpose of this chapter is to search for stable spin liquid phases that has a Schwinger fermion mean-field description, we will focus on Z_2 states.

If $G_U U \in PSG$ and $g \in IGG$, by definition we have $gG_U U \in PSG$. This means that the mapping $h : PSG \to SG : f(G_U U) = U$ is a many-to-one mapping. In fact it is easy to show that mapping h induces group homomorphism[225]:

$$PSG/IGG = SG. \tag{5.9}$$

Mathematically PSG is an extension of SG by IGG.

Our definition of PSG requires a mean-field ansatz $\{u_{ij}\}$. With Eq.(5.9), one can define algebraic-PSG which does not require ansatz $\{u_{ij}\}$. An algebraic-PSG is simply defined as a group satisfying Eq.(5.9). Obviously a PSG (realizable by an ansatz) must be an algebraic-PSG, but the reverse may not be true, because sometimes an algebraic-PSG cannot be realized by any mean-field ansatz.

To classifying all possible Z_2 Schwinger-fermion mean-field states, we need to find all possible PSG group extensions of the SG with a Z_2 IGG. Here SG is the direct product of the space group of honeycomb lattice and the time-reversal Z_2 group. In Ref. [128] we show the general constraints that must be satisfied for such a group extension. In Ref. [128], using these constraints, we find there are in total 160 Z_2 algebraic-PSGs on honeycomb lattice. And at most 128 PSGs of them can be realized by an ansatz $\{u_{ij}\}$. These 128 PSGs completely classifies all Schwinger-fermion mean-field ansatz of Z_2 spin liquids on a honeycomb lattice.

5.3 Z_2 spin liquids on a honeycomb lattice and the SPS phase

Among the 128 states, can one further identify the candidate states for the spin liquid discovered in the numerical study[136]? The answer is yes. Numerically the spin liquid phase is found close to the Mott transition and it seems to be connected to the semimetal phase by a continuous phase transition. What are the Z_2 Schwinger-fermion states in the neighborhood of the semi-metal phase?

Are there Schwinger-fermion mean-field states that can be connected to the semi-metal phase via a continuous phase transition? Physically a continuous Mott transition is associated with the loss of charge coherence of the electronic quasi-particles. The spinons in the Schwinger-fermion approach exactly describe these quasiparticles whose charge coherence has been lost[51, 82]. The natural resulting SL phase is nothing but the state with a spinon band structure identical to the electronic one on the metallic side. In the present case this SL is the uniform Resonating-Valence-Bond (u-RVB) state with a Dirac gapless spinon dispersion[82]. The nature of the Mott transtion between the SM phase and the u-RVB SL (referred to as algebraic spin liquid (ASL) in Ref. [82]) was studied by Hermele[82]. However numerically it was shown that the SL phase is fully gapped. How to resolve this discrepancy?

This discrepancy is related to the stability issue of the ASL. The u-RVB (or ASL) ansatz can be simply expressed as a graphene-like nearest neighbor hopping of f-fermions:

$$H_{MF}^{uRVB} = \chi \sum_{<ij>} f_{i\alpha}^{\dagger} f_{j\alpha}, \tag{5.10}$$

where χ is real. The low energy effective theory of ASL is 2+1D $SU(2)$ QCD with $N_f = 2$ flavors of fermions[82], *i.e.* QCD_3. In the large-N_f limit QCD_3 has a stable IR fixed point with gapless excitations and can be a stable ASL phase[10]. However the $N_f = 2$ case remains unclear. When $N_f = 0$ the pure gauge QCD_3 is in a confined phase[64, 159]. This indicates a critical N_c and when $N_f < N_c$ confinement occurs[10]. Although no controlled estimate of N_c is available, a self-consistent solution of the Schwinger-Dyson equations[10] suggests $N_c \approx \frac{64}{\pi^2}$, indicating $N_f = 2$ u-RVB (or ASL) state may not be a stable phase.

We find that the above-mentioned discrepancy can be resolved if we assume the ASL is not a stable phase but has one or more relavant couplings λ in the renormalization group sense. λ may be a four-fermion interaction. If λ is irrelevant at the Mott transition point (λ is dangerously irrelevant in this case), the Mott transition is still continuous and controlled by the fixed point studied in Ref. [82]. We present the schematic RG flow in Fig.5.2(b), and propose this scenario for the Mott transition in the simulated Hubbard model.

If this scenario is correct, the mean-field ansatz of the Z_2 spin liquid should be connected to the u-RVB ansatz by a continuous Higgs condensation driven by the λ-flow, which breaks the $SU(2)$ IGG down to Z_2. During this transition, the u-RVB ansatz $\{u_{ij}^{uRVB}\} \to \{u_{ij}^{uRVB} + \delta u_{ij}\}$ and the δu_{ij} amplitudes play the role of the Higgs boson. We define a Z_2 state to be around (or in the neighborhood of) the u-RVB when the Z_2 state can be obtained by an infinitesimal change $\{u_{ij}^{uRVB}\} \to \{u_{ij}^{uRVB} + \delta u_{ij}\}$. Therefore this scenario dictates *the PSG of the Z_2 state to be a subgroup of the PSG of the ASL*. We propose this group theoretical observation as a systematic way of

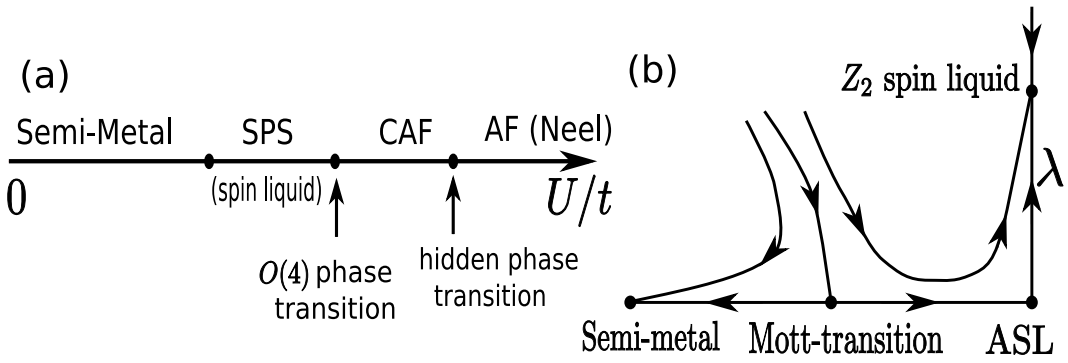

Figure 5.2: (a)Proposed schematic phase diagram of the Hubbard model on the honeycomb lattice. (b)Schematic RG flow of the Mott transition.

identifying the SLs close to a continuous Mott transition: *the PSGs of these SL are subgroups of the PSG of the "parent" SL whose spinon band structure is identical to the fermi liquid*.

In Ref. [128] we classify all these possible PSG subgroups with the Z_2 IGG, which allows us to construct all possible Z_2 states around the u-RVB state. This technique was firstly developed by Wen[225]. We find that among the 128 Z_2 states, there are totally 24 gauge inequivalent Z_2 PSGs satisfying this condition, as listed in Table 5.1 in Ref. [128].

Can these 24 Z_2 SL states have a full energy gap? We find not all of them can have a gapped spinon spectrum. This can be understood starting from a Dirac dispersion of the u-RVB state. To gap out the Dirac nodes, at least one mass term in the low-energy effective theory of a given Z_2 state must be allowed by symmetry. In Ref. [128] we show that only 4 of the 24 Z_2 states allow mass term in the low energy theory. Thus only these 4 states are fully gapped Z_2 spin liquids around u-RVB state. The other 20 states have symmetry protected gapless spinon dispersions.

These four states are state #16,#17,#19, and #22 in Table 5.1 in Ref. [128].

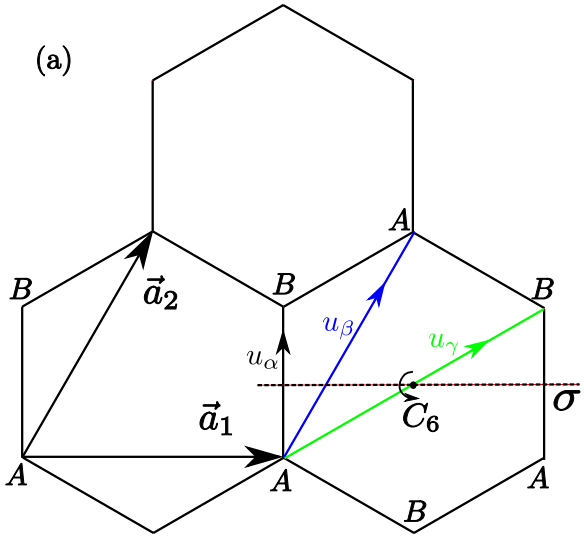

Figure 5.3: (color online) Honeycomb lattice and generators of symmetry group. u_α, u_β and u_γ are representatives of 1st, 2nd and 3rd nearest neighbor (n.n.) mean-field amplitudes.

We can generate their mean-field ansatzs by these PSGs. We find that up to the 3rd neighbor mean-field amplitudes $u_{(\alpha,\beta,\gamma)}$ as shown in Fig.5.3, only one of these four states can be realized, which is state #19. As shown in Ref. [128], mean-field ansatzs up to the 3rd neighbor of the other three states actually have a $U(1)$ IGG. Only after introducing longer-range mean-field bonds can these three states have a Z_2 IGG. In particular, state #16 requires 5th neighbor, state #17 requires 4th neighbor and state #22 requires 9th neighbor amplitudes, while state #19 only requires 2nd neighbor amplitudes. Because the t/U expansion of the Hubbard model give a rather short-ranged spin interaction for the SL phase found in numerics[136] ($t/U \sim 1/4$), the other three states are unlikely to be realized in a Hubbard model on honeycomb lattice.

SPS is a fully-gapped Z_2 SL on the honeycomb lattice. Its mean-field fermionic

spinon band structure, after choosing a proper gauge, is given as follows: (Fig.5.1 a)

$$H_{SPS}^{MF} = t_1 \sum_{<ij>} f_{i\alpha}^{\dagger} f_{j\alpha} + t_2 \sum_{<<ij>>} f_{i\alpha}^{\dagger} f_{j\alpha} - \mu \sum_{i} f_{i\alpha}^{\dagger} f_{i\alpha} + \Delta \sum_{<<ij>>} \epsilon_{\alpha\beta} f_{i\alpha}^{\dagger} f_{j\beta}^{\dagger} + h.c. \tag{5.11}$$

where $t_{1,2}$ are real numbers. In the Schwinger-fermion approach, f-spinons are coupled to an $SU(2)$ gauge field[3, 225]. However due to non-zero t_2 and Δ, the $SU(2)$ gauge symmetry is reduced to Z_2 through Higgs mechanism. Thus at low energy f-spinons are coupled to a dynamical Z_2 gauge field and stay in the deconfined phase. A Schwinger-fermion mean-field study of J_1-J_2 Heisenberg model using SPS ansatz is presented in Ref. [128].

5.4 Continuous phase transition from SPS to CAF phase

We start from discussing the continuous phase transition from SPS to CAF phase in the Schwinger-fermion approach. How to describe an AF order in this approach? In Ref. [168], it is shown that the easy-plane AF order on a honeycomb lattice is described by a quantum spin Hall (QSH) band structure of spinons (spin quantized along z-axis) coupled with a dynamical $U(1)$ gauge field. QSH effect binds the gauge fluctuation to S^z spin density fluctuation, and the Goldstone mode of the easy-plane Neel order is nothing but photon of the $U(1)$ gauge field. Monopole quantum number[168] of $U(1)$ gauge field shows the spin order is antiferromagnetic.

In the present spin rotation symmetric system, we consider the phase described

by a fluctuating $O(3)$ QSH order parameter $\vec{n}$, coupled with a $U(1)$ gauge field a_μ. Its mean-field ansatz is: (Fig. 5.1b)

$$H_{CAF}^{MF} = t_1 \sum_{<ij>} f_{i\alpha}^\dagger f_{j\alpha} + t_2 \sum_{<<ij>>} f_{i\alpha}^\dagger f_{j\alpha} - \mu \sum_i f_{i\alpha}^\dagger f_{i\alpha} + \vec{n} \cdot \sum_{<<ij>>} i\nu_{ij} f_{i\alpha}^\dagger \vec{\sigma}_{\alpha\beta} f_{j\beta}. \quad (5.12)$$

There are three gapless modes in this phase: two $\hat{n}$ fluctuating modes and one photon mode. The photon mode is in-plane spin wave of AF order $\vec{N}$ ($\vec{N} \perp \hat{n}$)[168], and the spin $SU(2)$ symmetry is completely broken. Because $\hat{n}$ has the same symmetry as QSH order, Eq.(5.12) is the representation of CAF phase in Schwinger-fermion method. The operation $C_6 \cdot \boldsymbol{T}$ ($\boldsymbol{T}$: time-reversal, C_6: defined in Fig.5.1c) leaves both order parameters invariant, indicating that the magnetic order in CAF phase is still collinear.

Comparing Eq.(5.12) with Eq.(5.11), s-wave pairing Δ of spinons in SPS phase is replaced by the $O(3)$ QSH order $\vec{n}$ in the CAF phase. If we group these orders together into a 5-component vector $\vec{V} = (\mathrm{Re}\Delta, \mathrm{Im}\Delta, \vec{n})$, as pointed out in Ref. [65], fluctuations of $\vec{V}$ has a Wess-Zumino-Witten (WZW) Berry's phase[1]. Physically it means that a skyrmion (anti-skyrmion) of $\hat{n}$ in two spatial dimension actually carries fermion charge $2(-2)$. The hedgehog instanton of $\hat{n}$ in 2+1 dimension thus creates a charge-2 s-wave fermion pair. Therefore a continuous phase transition between a QSH insulator and an s-wave superconductor on the honeycomb lattice becomes possible[65].

To discuss the CAF-SPS phase transition, it is convenient to introduce the CP^1 representation of the $\hat{n}$ order parameter: $\hat{n} = w^\dagger \vec{\sigma} w$, where $w = (w_1, w_2)^T$ are two

complex numbers satisfying $|w_1|^2 + |w_2|^2 = 1$. This representation has a $U(1)$ gauge redundancy and thus w-bosons couple to a $U(1)$ gauge field A_μ. After integrating out the f-spinons (see Ref. [128] for details), we obtain the effective Lagrangian[2]:

$$\begin{aligned} L =&|(\partial_\mu - \mathrm{i}A_\mu)w|^2 + r|w|^2 + s|w|^4 + \frac{1}{2g_a^2}f_{\mu\nu}^2 \\ &+ \frac{1}{2g_A^2}F_{\mu\nu}^2 + \frac{\mathrm{i}}{\pi}\epsilon_{\mu\nu\lambda}A_\mu\partial_\nu a_\lambda, \end{aligned} \tag{5.13}$$

where $f_{\mu\nu} = \partial_\mu a_\nu - \partial_\nu a_\mu$ and $F_{\mu\nu} = \partial_\mu A_\nu - \partial_\nu A_\mu$ are gauge field strengths. The last term, a mutual Chern-Simons (CS) term, is nothing but the WZW term in the gauge representation: it is well-known that a skyrmion of $\hat{n}$ is a 2π A_μ gauge flux, which also carries 2 units of a_μ gauge charge due to the WZW term.

What are the phases described by the effective Lagrangian Eq.(5.13)? When $r < 0$, w-boson condenses and $\hat{n}$ is ordered, corresponding to CAF phase. Here the mutual CS term does not qualitatively modify the low-energy dynamics due to the Higgs mechanism of A_μ. When $r > 0$, w-bosons are gapped and $\hat{n}$ is disordered, remarkably, Eq.(5.13) describes the Z_2 SPS phase. The identification of a $U(1)$ mutual CS theory and a Z_2 gauge theory has been studied before[75, 109]. Here with the WZW term, we are able to further identify the PSG of the Z_2 theory.

This identification is easily shown by studying the the monopoles of a_μ and A_μ in Eq.(5.13). In $\hat{n}$ disordered phase, monopole events of both a_μ and A_μ are allowed. We denote their monopole creation operators as $V_a^\dagger$ and $V_A^\dagger$ respectively. The mutual CS term clearly dictates that an a_μ monopole creates 2 units of A_μ gauge charge, and vice versa. These events mean that $f_\alpha^\dagger f_\beta^\dagger$ and $w_\alpha^\dagger w_\beta^\dagger$ pairing terms exist, which

[2]The constraint $|w_1|^2 + |w_2|^2 = 1$ can be enforced by a Lagrangian multiplier λ. (5.13) can be obtained by the saddle point expansion of λ.

break the $U(1)$ gauge group down to Z_2. The WZW term indicates that the f-spinon pairing is s-wave, and thus the system is in SPS phase.

Mutual CS term also dictates that f-spinon and w-boson satisfy mutual semion statistics. Namely they see each other as a π-flux and are dual degrees of freedom. We can focus on either set of dual variables, $f(V_A^\dagger)$ or $w(V_a^\dagger)$, to write down the effective theory. Because the phase transition from SPS to CAF phase is described by w-boson condensation in Eq.(5.13), we will use $w(V_a^\dagger)$ variables in the next section.

5.5 Duality between Schwinger-fermion and Schwinger-boson representations

In this section we focus on the dual variables of f-spinons: the w-bosons. The SPS phase is then a Z_2 phase with w-bosons as Z_2 charges, but f-spinons as visons. In this formulation SPS-CAF phase transition is naturally presented as a Higgs condensation of w-bosons.

First we need to represent the order parameters of the CAF phase in terms of w. The QSH order is $\hat{n} = w^\dagger \vec{\sigma} w$, but what is the Neel order parameter? Neel order in CAF phase corresponds to the monopole of a_μ, namely a pairing of w-boson. There are two spin-1 bosonic pairing order parameters satisfying this requirement, *i.e.* the real and imaginary part of $(i\sigma_y w^*)^\dagger \vec{\sigma} w$:

$$\hat{n}_1 + i\hat{n}_2 = (i\sigma_y w^*)^\dagger_\alpha \vec{\sigma}_{\alpha\beta} w_\beta. \tag{5.14}$$

It is easy to verify that $\hat{n} = \hat{n}_1 \times \hat{n}_2$, so there are only two independent vectorial order parameters. The issue is, which one is the Neel order parameter $\vec{N}$: $\hat{n}_1$ or $\hat{n}_2$?

A $U(1)$ gauge transformation $w \to e^{i\theta}w$ generates a rotation in the $\hat{n}_1, \hat{n}_2$ plane. By fixing a proper gauge, we can always choose $\hat{n}_1$ as the Neel order. We will work within this gauge $\vec{N} = \hat{n}_1$ throughout the phase transition. Such a gauge fixing breaks the $U(1)$ gauge redundancy down to Z_2: $w \to \pm w$.

The physical symmetries of the QSH (or vector spin chirality) and the Neel order parameters completely determine the transformation rules of the w-boson up to a Z_2 gauge redundancy:

$$\begin{aligned}
T_1, T_2 : &\quad \hat{n} \to \hat{n}, &\quad \vec{N} \to \vec{N}, &\quad w \to w, \\
\boldsymbol{T} : &\quad \hat{n} \to \hat{n}, &\quad \vec{N} \to -\vec{N}, &\quad w \to iw^*, \\
\sigma : &\quad \hat{n} \to -\hat{n}, &\quad \vec{N} \to -\vec{N}, &\quad w \to i\sigma_y w^*, \\
C_6 : &\quad \hat{n} \to \hat{n}, &\quad \vec{N} \to -\vec{N} &\quad w \to iw.
\end{aligned} \tag{5.15}$$

where time-reversal transformation $\boldsymbol{T}$ is anti-unitary. The reason why there are no further arbitrariness on the transformation rules of w can be easily understood by the following construction. If we write w-boson as an SU(2) matrix:

$$U = \begin{pmatrix} w_1 & w_2^* \\ w_2 & -w_1^* \end{pmatrix}, \tag{5.16}$$

then the most general $O(4)$ transformation leaving $|w_1|^2 + |w_2|^2 = 1$ is $U \to V_L U V_R$, where V_L and V_R are both $SU(2)$ rotations (V_L is spin rotation), and $O(4) \sim SU(2)_L \times SU(2)_R$. In this representation, the vectors $\hat{n}_1, \hat{n}_2, \hat{n}$ are the 1st, 2nd and 3rd columns of a 3 by 3 rotation matrix R:[117]

$$R^{ab} = \frac{1}{2}\mathrm{Tr}(U^\dagger \sigma^a U \sigma^b) \tag{5.17}$$

Clearly, to leave R invariant, the transformations $V_{L,R}$ must be ± 1.

These symmetry transformation rules allow us to reveal the connection between the SPS state here and the 0-flux state in the Schwinger-boson representation obtained by Wang[210]. In Wang's work, the Neel order is represented by the z-boson as $\vec{N} = z^\dagger \vec{\sigma} z$ in the effective theory. From Eq.(5.17), we can easily construct the duality transformation between the w-boson and z-boson representations: $U_w = U_z V_R$, $V_R = e^{i\frac{\pi}{4}\sigma_y}$, namely:

$$w = \frac{1}{\sqrt{2}}(z - i\sigma^y z^*) \qquad \text{or} \qquad z = \frac{1}{\sqrt{2}}(w + i\sigma^y w^*) \tag{5.18}$$

Under duality transformation:

$$\begin{aligned} \vec{N} &= \mathrm{Re}[(i\sigma_y w^*)^\dagger \vec{\sigma} w] = z^\dagger \vec{\sigma} z, \\ \hat{n} &= w^\dagger \vec{\sigma} w = -\mathrm{Re}[(i\sigma_y z^*)^\dagger \vec{\sigma} z]. \end{aligned} \tag{5.19}$$

From Eq.(5.15),(5.18), we can obtain transformation rules of z-bosons:

$$\begin{aligned} T_1, T_2 &: && z \to z, \\ \boldsymbol{T} &: && z \to \sigma_y z, \\ \sigma &: && z \to i\sigma_y z^*, \\ C_6 &: && z \to \sigma_y z^*, \end{aligned} \tag{5.20}$$

which are exactly the transformation rules found by Wang[210] for 0-flux state up to a Z_2 gauge arbitrariness. This explicitly confirms that the z-bosons constructed in Eq.(5.18) are the same z-bosons discussed by Wang, and the SPS phase here is identical to the 0-flux phase in Schwinger-boson description.

Following the discussion in Ref. [210], we can write down the general symmetry-

allowed effective theory for the phase transition in terms of z-boson:

$$\begin{aligned} L =&|\partial_\tau z|^2 + c^2|\nabla z|^2 + m^2|z|^2 + u(|z|^2)^2 \\ &+ \lambda_H\ (i\sigma_y z^*)^\dagger \big[\sum_i (\vec{d_i}\cdot\nabla)^3\big] z + h.c. \end{aligned} \tag{5.21}$$

Here λ_H is the Higgs coupling which reduces the gauge degrees of freedom in the z-boson formulation down to Z_2. $\vec{d_1} = -\vec{a}_1$,$\vec{d_2} = \vec{a}_2$, and $\vec{d_3} = \vec{a}_1 - \vec{a}_2$ as shown in FIG. 5.1. For instance, the single time derivative term $z^\dagger\partial_\tau z$ is forbidden by σ, and $z^T(-i\sigma_y)\partial_\tau z$ is forbidden by C_6. The Higgs coupling can also be written as a pairing of w-bosons: $\lambda_H\ (i\sigma_y w^*)^\dagger \big[\sum_i (\vec{d_i}\cdot\nabla)^3\big] w + h.c.$ By naive power counting λ_H is irrelevant, therefore we have an $O(4)$ critical point between the CAF (z-condensed) phase and the SPS (z-gapped) phase. The critical behavior of this transition is well-studied[30, 29, 89].

5.6 Summary

In this study, our main prediction is the CAF phase. Unlike usual AF (Neel) phase, CAF phase has two order parameters: Neel order $\vec{N}$ and QSH order $\hat{n}$. As CAF phase is likely to be the magnetically ordered phase adjacent to the SL phase found in the numeric study[136], in the following we propose explicit numerical methods to detect the CAF phase.

One can directly measure QSH order by $\langle\vec{n}(x)\cdot\vec{n}(0)\rangle$ correlation function, or the spin vector-chirality correlation $\langle(\nu_{i+x,j+x}\vec{S}_{i+x}\times\vec{S}_{j+x})\cdot(\nu_{ij}\vec{S}_i\times\vec{S}_j)\rangle$. Since QSH order is odd under $\sigma\cdot\boldsymbol{T}$ while Neel order is $\sigma\cdot\boldsymbol{T}$-even, one does not expect a long range correlation of QSH order in a usual Neel phase. Therefore, the long range QSH

correlation is an intrinsic signature of CAF phase. In addition, one can check that the QSH vector is normal to the Neel vector. For example, one can pin the Neel order by an infinitesimal (in thermodynamic limit) staggered magnetic field along z-axis, and the measured QSH order parameters should only have x, y components. Experimentally such an exotic SL may be realized in candidate systems such as expanded graphene-like system in group IV elements[187, 26] and fermions in optical lattices[45, 99].

#	$g_{\boldsymbol{T}}$	$g_{\boldsymbol{\sigma}}$	g_{C_6}	g_1	g_2
1	τ^0	τ^0	τ^0	τ^0	τ^0
2	τ^0	τ^0	$i\tau^3$	τ^0	τ^0
3	τ^0	τ^0	$i\tau^3$	$e^{\mathrm{i}2\pi/3\tau^1}$	$e^{-\mathrm{i}2\pi/3\tau^1}$
4	τ^0	$\mathrm{i}\tau^3$	$\mathrm{i}\tau^3$	τ^0	τ^0
5	τ^0	$\mathrm{i}\tau^3$	$\mathrm{i}\tau^3$	τ^0	τ^0
6	τ^0	$\mathrm{i}\tau^3$	$\mathrm{i}\tau^1$	τ^0	τ^0
7	τ^0	$\mathrm{i}\tau^3$	$e^{\mathrm{i}\pi/6\tau^1}$	τ^0	τ^0
8	τ^0	$\mathrm{i}\tau^3$	$e^{\mathrm{i}\pi/3\tau^1}$	τ^0	τ^0
9	τ^0	$\mathrm{i}\tau^3$	$\mathrm{i}\tau^1$	$e^{\mathrm{i}2\pi/3\tau^3}$	$e^{-\mathrm{i}2\pi/3\tau^3}$
10	τ^0	$\mathrm{i}\tau^3$	$e^{\mathrm{i}2\pi/3\tau^1}$	$\mathrm{i}(\frac{\tau^1}{\sqrt{3}}-\sqrt{\frac{2}{3}}\tau^2)$	$\mathrm{i}(\frac{\tau^3}{\sqrt{2}}-\frac{\tau^2}{\sqrt{6}}-\frac{\tau^1}{\sqrt{3}})$
11	$\mathrm{i}\tau^3$	τ^0	τ^0	τ^0	τ^0
12	$\mathrm{i}\tau^3$	τ^0	$\mathrm{i}\tau^3$	τ^0	τ^0
13	$\mathrm{i}\tau^3$	τ^0	$\mathrm{i}\tau^1$	τ^0	τ^0
14	$\mathrm{i}\tau^3$	τ^0	$\mathrm{i}\tau^1$	$e^{\mathrm{i}2\pi/3\tau^3}$	$e^{-\mathrm{i}2\pi/3\tau^3}$
15	$\mathrm{i}\tau^3$	$\mathrm{i}\tau^3$	τ^0	τ^0	τ^0
16	$\mathrm{i}\tau^3$	$\mathrm{i}\tau^3$	$\mathrm{i}\tau^3$	τ^0	τ^0
17	$\mathrm{i}\tau^3$	$\mathrm{i}\tau^3$	$\mathrm{i}\tau^1$	τ^0	τ^0
18	$\mathrm{i}\tau^3$	$\mathrm{i}\tau^3$	$\mathrm{i}\tau^1$	$e^{\mathrm{i}2\pi/3\tau^3}$	$e^{-\mathrm{i}2\pi/3\tau^3}$
19	$\mathrm{i}\tau^3$	$\mathrm{i}\tau^1$	$\mathrm{i}\tau^1$	τ^0	τ^0
20	$\mathrm{i}\tau^3$	$\mathrm{i}\tau^1$	$\mathrm{i}\tau^2$	τ^0	τ^0
21	$\mathrm{i}\tau^3$	$\mathrm{i}\tau^1$	τ^0	τ^0	τ^0
22	$\mathrm{i}\tau^3$	$\mathrm{i}\tau^1$	$\mathrm{i}\tau^3$	τ^0	τ^0
23	$\mathrm{i}\tau^3$	$\mathrm{i}\tau^1$	$e^{\mathrm{i}\pi/6\tau^3}$	τ^0	τ^0
24	$\mathrm{i}\tau^3$	$\mathrm{i}\tau^1$	$e^{\mathrm{i}\pi/3\tau^3}$	τ^0	τ^0

Table 5.1: A summary of all 24 different PSG's with $IGG = \{\pm\tau^0\}$ around the u-RVB ansatz. They correspond to 24 different Z_2 spin liquids near the u-RVB state.

Chapter 6

Majorana fermions in nodal singlet superconductors with coexisting non-collinear magnetic orders

6.1 Introduction

A Majorana fermion is an electrically neutral fermion whose antiparticle is itself. High energy physicists have been looking for this hypothetical particle in *e.g.* neutrino physics and dark matter, but so far a confirmation for these speculations is still lacking[233]. On the other hand, in recent years Majorana fermions have attracted more and more attention of condensed matter physicists[146, 76, 164]. To be specific, Majorana fermions can be realized by zero-energy bound states in the vortex core (or on the edge) of certain two-dimensional superconductors. A particularly unusual property of these vortices is that instead of usual bosonic or fermionic statistics,

they obey non-Abelian statistics[140, 147, 52, 176, 91, 201] as a manifestation of nontrivial topological order[218, 216] in such systems. Due to this feature MBSs have been proposed to serve as topologically-protected qubits in fault-tolerant quantum computation[101, 35, 146]. A variety of systems have been proposed to realize MBSs, such as even-denominator fractional quantum Hall liquids[140, 147, 176, 131], $p + \mathrm{i}p$ superconductors[176, 91, 201] and superfluids[66, 33], s-wave-superconductor-strong-topological-insulator interface[55], s-wave Rashba superconductor[184, 185, 4] and spin-orbit-coupled nodal superconductors[183].

In this work we propose another realization of MBSs in non-centrosymmetric singlet superconductors with nodal excitations, such as d-wave superconductors. We show that when with a coexisting non-collinear magnetic order with a wavevector connecting two nodes with opposite momenta, there will be MBSs in the vortex core or the edge of such superconductors. We demonstrate our proposal explicitly by two examples. The 1st one is a $d + \mathrm{i}d$ superconductor with coexisting 1×3 coplanar magnetic order on the triangular lattice. We show it's likely to be realized in a doped t-J_2 model on triangular lattice. In particular this example is relevant for a material: superconducting sodium cobaltate $\mathrm{Na}_x\mathrm{CoO}_2 \cdot y\mathrm{H}_2\mathrm{O}$ with doping concentration $x_c \approx 0.25$[246]. The 2nd example is a $d_{x^2-y^2}$ superconductor with coexisting $\mathbf{Q} = (Q_0, Q_0)$ coplanar magnetic order on the square lattice. We also show this state might be realized in a doped $t - J_1 - J_2 - J_3$ model on square lattice. Experimentally the phase diagram of a wide range of strongly-correlated materials, from cuprates to heavy-fermion compounds, are featured by d-wave superconductivity[206, 158] in proximity of[119] or even coexisting with[158, 193] magnetic orders. Therefore our

proposal opens a window for discovering non-Abelian MBSs in strongly-correlated unconventional superconductors with gap nodes.

6.2 General discussions on the mechanism

The low-energy excitations of a nodal singlet superconductor are massless Dirac fermions with linear dispersion around the nodes. First we discuss the mechanism of creating a sinlge MBS by adding a proper mass term to these Dirac fermions. In the mean-field level the quadratic Hamiltonian with singlet pairing terms can be expanded around nodal points $\{\mathbf{q}_i\}$. We can write the low-energy effective Hamiltonian as $H_{eff} = \sum_{\mathbf{k}} \sum_i (c^\dagger_{\mathbf{q}_i+\mathbf{k},\uparrow}, c_{-\mathbf{q}_i-\mathbf{k},\downarrow}) \mathcal{H}^i_{\mathbf{k}} (c_{\mathbf{q}_i+\mathbf{k},\uparrow}, c^\dagger_{-\mathbf{q}_i-\mathbf{k},\downarrow})^T$ where $\mathcal{H}^i_{\mathbf{k}}$ are 2×2 Hermitian matrices linear in small momenta $\mathbf{k}$. Now let's focus on one gap node at $\mathbf{q}_0$ and without loss of generality we have

$$\sum_{\mathbf{k}} \begin{pmatrix} c_{\mathbf{q}_0+\mathbf{k},\uparrow} \\ c^\dagger_{-\mathbf{q}_0-\mathbf{k},\downarrow} \end{pmatrix}^\dagger \begin{bmatrix} \xi_{\mathbf{q}_0+\mathbf{k},\uparrow} & \Delta_{\mathbf{q}_0+\mathbf{k}} \\ \Delta^*_{\mathbf{q}_0+\mathbf{k}} & -\xi_{-\mathbf{q}_0-\mathbf{k},\downarrow} \end{bmatrix} \begin{pmatrix} c_{\mathbf{q}_0+\mathbf{k},\uparrow} \\ c^\dagger_{-\mathbf{q}_0-\mathbf{k},\downarrow} \end{pmatrix}$$
$$= H^0_{eff} = \sum_{\mathbf{k}} v(k_1 + \mathrm{i}k_2) d^\dagger_{\mathbf{k}\uparrow} d^\dagger_{-\mathbf{k}\downarrow} + \ h.c. \tag{6.1}$$

which is formally the same as a spin-triplet $p+\mathrm{i}p$ superconductor. We defined Dirac fermions $(d_{\mathbf{k}\uparrow}, d^\dagger_{-\mathbf{k}\downarrow})^T = U_0 (c_{\mathbf{q}_0+\mathbf{k},\uparrow}, c^\dagger_{-\mathbf{q}_0-\mathbf{k},\downarrow})^T$ where U_0 is an $SU(2)$ matrix. v is a constant and (k_1, k_2) are two-dimensional momenta in a certain coordinate system. As pointed out in Ref. [176] the effective Hamiltonian (6.1) can be decoupled into two independent spinless $p+\mathrm{i}p$ superconductors in the isospin basis $d_{\mathbf{k},e/o} \equiv$

$(d_{\mathbf{k}\uparrow} \pm d_{\mathbf{k}\downarrow})/\sqrt{2}$:

$$H^0_{eff} = \sum_{\mathbf{k}} v(k_1 + \mathrm{i}k_2)(d^\dagger_{\mathbf{k},e} d^\dagger_{-\mathbf{k},e} - d^\dagger_{\mathbf{k},o} d^\dagger_{-\mathbf{k},o}) + \ h.c.$$

Now let's add a magnetic mass to the effective Hamiltonian (6.1) with $m > 0$

$$\begin{aligned} \delta H^0 = m \sum_{\mathbf{k}} c^\dagger_{\mathbf{q}_0+\mathbf{k},\uparrow} c_{-\mathbf{q}_0+\mathbf{k},\downarrow} + \ h.c. = m \sum_{\mathbf{k}} d^\dagger_{\mathbf{k}\uparrow} d_{\mathbf{k}\downarrow} \\ + \ h.c. = m \sum_{\mathbf{k}} (d^\dagger_{\mathbf{k},e} d_{\mathbf{k},e} - d^\dagger_{\mathbf{k},o} d_{\mathbf{k},o}) \end{aligned} \tag{6.2}$$

Remarkably this term drives one spinless $p + \mathrm{i}p$ superconductor of $\{d_{\mathbf{k},e}\}$ fermions into non-Abelian weak-pairing phase and the other spinless $p + \mathrm{i}p$ superconductor of $\{d_{\mathbf{k},o}\}$ fermions into Abelian strong-pairing phase[176]. Each weak-paired $p + \mathrm{i}p$ superconductor contributes one single zero-energy MBS in the vortex core while a strong-paired one contributes none. Therefore we obtain one single MBS from $\{d_{\mathbf{k},e}\}$ fermions by introducing a magnetic mass term to nodal Dirac fermions (6.1). Our proposal is in analogy to a doubled-layer $\nu = 1/2$ fractional quantum Hall system, where a phase transition from an Abelian (331) state to a non-Abelian (Moore-Read pfaffian) state can be driven by a tunneling term between layers[84, 177, 176]. In the electron basis apparently (6.2) corresponds to a non-collinear (coplanar) magnetic order with wavevector $2\mathbf{q}_0$. After a Fourier transformation we have

$$\begin{aligned} \delta H^0 = m \sum_{\mathbf{r}} e^{-\mathrm{i}\,2\mathbf{q}_0\cdot\mathbf{r}} c^\dagger_{\mathbf{r},\uparrow} c_{\mathbf{r},\downarrow} + \ h.c. = \\ 2m \sum_{\mathbf{r}} \left[S^x_{\mathbf{r}} \cos(2\mathbf{q}_0 \cdot \mathbf{r}) + S^y_{\mathbf{r}} \sin(2\mathbf{q}_0 \cdot \mathbf{r}) \right] \end{aligned}$$

where $S^a_{\mathbf{r}} = \sum_{\alpha,\beta=\uparrow,\downarrow} c^\dagger_{\mathbf{r},\alpha} \sigma^a_{\alpha,\beta} c_{\mathbf{r},\alpha}/2, \ a = x, y, z$ is the electron spin operator on lattice site $\mathbf{r}$ and $\sigma^{x,y,z}$ are Pauli matrices. In general these non-collinear magnetic order can be realized in frustrated spin models. We expect that residual spin-spin interactions

between nodal Dirac fermions might induce the desired non-collinear magnetic order coexisting with superconductivity. In the following we shall demonstrate the above general discussions by two examples on triangular and square lattices.

It is crucial to require the magnetic order to be *non-collinear*: a collinear magnetic mass term such as

$$\begin{aligned} H_{col} &= m\sum_{\mathbf{k}}(c^{\dagger}_{\mathbf{q}_0+\mathbf{k},\uparrow}c_{-\mathbf{q}_0+\mathbf{k},\downarrow}+c^{\dagger}_{\mathbf{q}_0+\mathbf{k},\downarrow}c_{-\mathbf{q}_0+\mathbf{k},\uparrow})+\ h.c. \\ &= 2m\sum_{\mathbf{r}} S^x_{\mathbf{r}}\cos(2\mathbf{q}_0\cdot\mathbf{r}) \end{aligned}$$

will not only drive $\{d_{\mathbf{k},o}\}$ fermions associated with $(c_{\mathbf{q}_0+\mathbf{k},\uparrow}, c^{\dagger}_{-\mathbf{q}_0-\mathbf{k},\downarrow})$ into weak-pairing phase, but also another branch of $\{d'_{\mathbf{k},o}\}$ fermions (with opposite spin) associated with another Nambu pair $(c_{-\mathbf{q}_0+\mathbf{k},\uparrow}, c^{\dagger}_{\mathbf{q}_0-\mathbf{k},\downarrow})$. As a result there would be two weak-paired spinless $p+\mathrm{i}p$ superconductors and hence two MBSs in the vortex core or the edge. To be precise, on the edge there will be two counter-propagating Majorana modes, one from Nambu pair $(c_{\mathbf{q}_0+\mathbf{k},\uparrow}, c^{\dagger}_{-\mathbf{q}_0-\mathbf{k},\downarrow})$ and the other from $(c_{-\mathbf{q}_0+\mathbf{k},\uparrow}, c^{\dagger}_{\mathbf{q}_0-\mathbf{k},\downarrow})$: the two branches will scatter with each other and open up a gap in the edge spectrum. As a result there will be no MBS in the gapped edge spectrum of a superconductor with coexisting collinear magnetic order, as shown in FIG. 6.3 for a specific case on triangular lattice.

6.3 $d+\mathrm{i}d$ superconductor with coplanar 1×3 magnetic order on triangular lattice

In the 1st example we consider a $d+\mathrm{i}d$ superconductor on the triangular lattice. Let's start with 2nd nearest neighbor (NN) $d+\mathrm{i}d$ pairing order parameter[246],

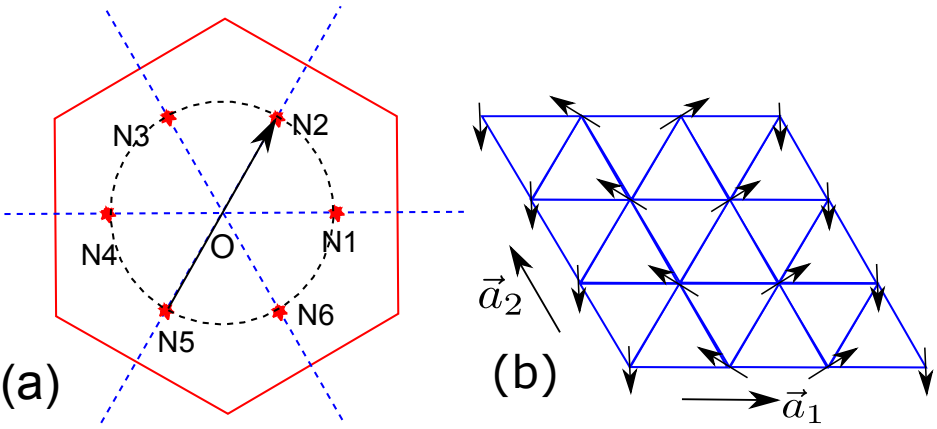

Figure 6.1: (color online) (a) The 1st BZ of triangular lattice and the gap nodes $\{N_i\}$ of 2nd NN $d+\mathrm{i}d$ pairing gap function (6.3) inside 1st BZ. The dashed circle indicates the Fermi surface crossing the 6 gap nodes. The arrow represents the momentum of the magnetic order, which adds a magnetic mass to the nodal Dirac fermion and creates the single MBS. (b) The spin configuration of the 1×3 magnetic order in a $S=1/2$ Heisenberg J_2 model on the triangular lattice. $\vec{a}_{1,2}$ represent two Bravais primitive vectors. Their corresponding reciprocal vectors are $\vec{b}_{1,2}$ with the convention $\vec{a}_i\cdot\vec{b}_j=\delta_{i,j}$.

i.e. $\Delta_{ij}=\Delta_2 e^{2\mathrm{i}\theta_{ij}}$ if $\langle\langle i,j\rangle\rangle$ is a 2nd NN pair, where θ_{ij} is the angle of $\mathbf{r}_i-\mathbf{r}_j$. With momentum denoted as $\mathbf{k}=k_1\vec{b}_1+k_2\vec{b}_2$ (see FIG. 6.1), the gap function in momentum space

$$\Delta^{(2)}_{\mathbf{k}}=2\Delta_2\big[\cos(k_1-k_2)+e^{\mathrm{i}2\pi/3}\cos(2k_1+k_2)$$
$$+e^{\mathrm{i}4\pi/3}\cos(k_1+2k_2)\big] \tag{6.3}$$

has 7 gap nodes inside the 1st Brillouin zone (BZ): zone center O and $N_i,\ i=1,\cdots,6$ as shown in FIG. 6.1(a). Such a 2nd-NN paired state is expected to be realized in a doped t-J_2 model on triangular lattice[212]. Such a $d+\mathrm{i}d$ superconductor is featured by quantized spin-Hall conductance[176] associated winding number W of unit vector $\hat{n}_{\mathbf{k}}=(\mathrm{Re}\Delta^{(2)}_{\mathbf{k}},-\mathrm{Im}\Delta^{(2)}_{\mathbf{k}},\xi_{\mathbf{k}})/E_{\mathbf{k}}$ where $\xi_{\mathbf{k}}$ represents the kinetic energy and $E_{\mathbf{k}}=\sqrt{\xi^2_{\mathbf{k}}+|\Delta^{(2)}_{\mathbf{k}}|^2}$. When the Fermi surface lies inside the dashed circle in

FIG. 6.1(a) we have $W = -2$ and there are two counter-clockwise-propagating chiral fermions on the edge the superconductor. Each of them is charge neutral but carries spin 1/2. When the Fermi surface encloses the dashed circle and six gap nodes $\{N_i\}$ we have $W = 4$[246] and there are four clockwise-propagating chiral fermions on the edge carrying only spin. When the Fermi surface crosses the 6 nodes $\{N_i\}$ with a proper doping concentration, however the winding number W is not well-defined since the superconductor has gapless nodal excitations in the bulk. The question is, can we introduce a proper mass term to these nodal Dirac fermions so that a gap is opened, and the corresponding state can have a winding number $W = +1$ (the same as a $p + \mathrm{i}p$ superconductor[176]) and hence single MBS in the vortex core/edge? The answer is yes. A magnetic mass (6.2) with a momentum pointing from N_{i+3} to N_i shown in FIG. 6.1 will do. We shown the edge spectrum of such a superconductor with non-collinear magnetic order in FIG. 6.2. As we expected there is a single MBS crossing $k = 0$. The corresponding spin configuration is shown in FIG. 6.1(b). On the other hand, as discussed earlier for a generic case, a collinear magnetic order with the same ordering vector will not create a MBS in the edge spectrum, although it does open up a gap in the bulk dispersion as shown in FIG. 6.3. This means not all mass terms can create MBS by opening up a gap for the nodal Dirac fermions.

Now another question rises: can the 1×3 non-collinear magnetic order be possibly realized on the triangular lattice? Notice that in the superconducting phase of doped $t - J_2$ model, when the Fermi surface crosses the 6 nodes $\{N_i\}$, the low-energy physics are described by nodal Dirac fermions interacting through a residual J_2 interaction. The classical ground states of J_2 model is well-known to have[100, 98]

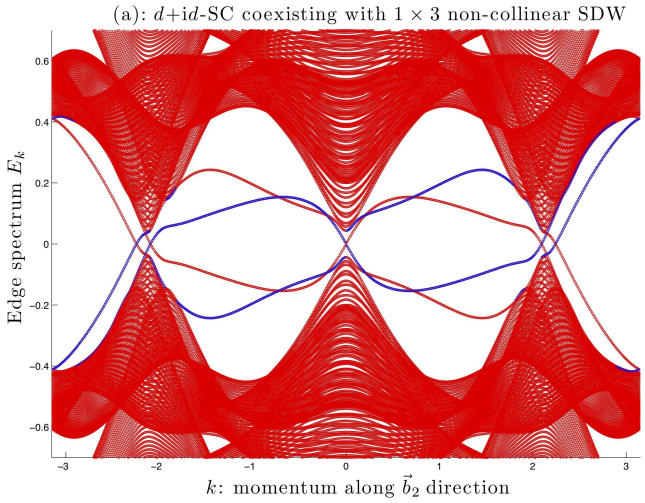

Figure 6.2: (color online) The edge spectra with momentum k along $\vec{b}_2$ direction of a 2nd-NN $d+\mathrm{i}d$ superconductor coexisting with 1×3 non-collinear (in-plane) magnetic order as shown in FIG. 6.1(b). Among the in-gap edge states separated from the bulk continuum, blue lines represent edge states on one edge, while red lines represents edge states on the other edge. Note there is one single counter-clockwise-propagating zero-energy MBS at $k = 0$ localized on the edges. We use the hopping parameters in Ref. [246], *i.e.* $(t_1, t_2, t_3) = (-202, 39, 25)$ MeV, $\Delta_2 = 150$ MeV and magnetic mass $m = 100$ MeV.

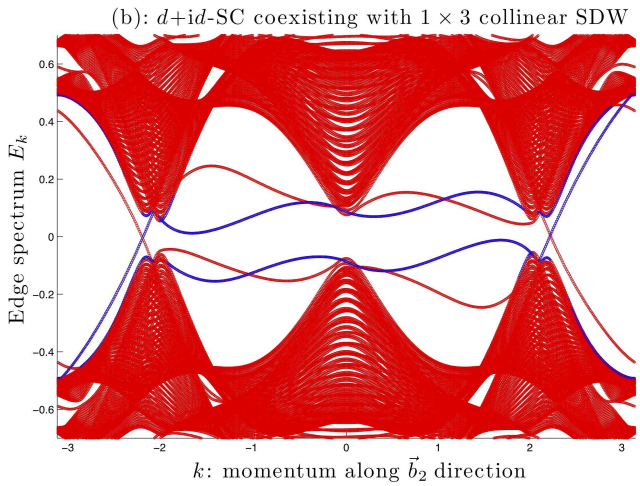

Figure 6.3: (color online) The edge spectra with momentum k along $\vec{b}_2$ direction of a 2nd-NN $d + \mathrm{i}d$ superconductor coexisting with 1×3 collinear magnetic order with magnetization along $\hat{z}$ direction. Notations and parameters are the same as in FIG. 6.2. Note that there are no MBSs in the spectrum.

3×3 non-collinear magnetic order, *i.e.* on each of the three "sublattices" connected by 2nd-NN bonds the spins exhibit in 120 degree coplanar order. There is a large ground state degeneracy at classical level from the relative spin orientations of the three "sublattices", which is lifted by quantum fluctuations through ordering-due-to-disorder mechanism[208, 81, 28]. The ultimate quantum ground state is nothing but a 1×3 ordered one as shown in FIG. 6.1(b). We further carry out a Schwinger-boson mean-field study[1] of spin-S Heisenberg J_2 model and find that when S is larger than a critical value $\kappa_c/2 \approx 0.17$ (such as spin-1/2), the system will develop exactly the 1×3 non-collinear order as shown in FIG. 6.1(b). This suggests the coexistence of 2nd NN $d + \mathrm{i}d$ pairing and non-collinear magnetic order 6.1(b) in a doped t-J_2 model and hence the MBS in the vortex core/edge.

Finally we want to discuss possible experimental realizations. Sodium cobaltate

[1]Yuan-Ming Lu and Ziqiang Wang, to appear.

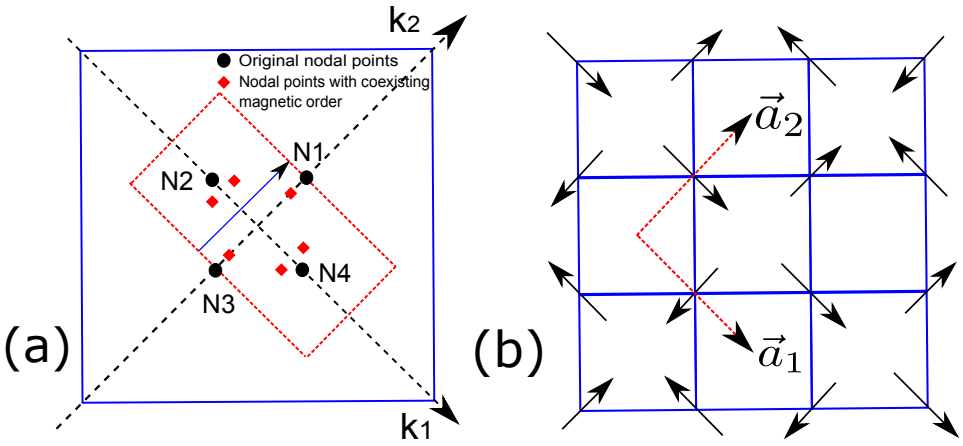

Figure 6.4: (color online) (a) The 1st BZ of square lattice. Black circles denote the four nodal points $\{N_i\}$, *i.e.* the intersections between the Fermi surface and nodal lines of NN $d_{x^2-y^2}$ pairing gap function. After a non-collinear magnetic order with momentum $(\pi/2, \pi/2)$ (shown by the arrow) is introduced, the Brillouin zone is reduced to the red rectangle and the nodal excitations shift to the momenta denoted by red diamonds. (b) The spin configuration of (Q_0, Q_0) magnetic order with $Q_0 = \pi/2$. $\vec{a}_{1,2}$ represent two primitive vectors we've chosen. Their corresponding reciprocal vectors are $\vec{b}_{1,2}$ with $\vec{a}_i \cdot \vec{b}_j = \delta_{i,j}$. Notice along $\vec{a}_2$ direction the unit cell is doubled by the magnetic order.

Na_xCoO_2 is a layered triangular lattice electron system which becomes a water-intercalated superconductor at low temperature with doping concentration $x \approx 0.3$[203]. NMR measurements[56, 245, 244] suggest singlet pairing and there are signatures of nodal excitations at doping $x_c \approx 0.26$. A 2nd-NN $d + \mathrm{i}d$ pairing order parameter with gap nodes $\{N_i\}$ in FIG. 6.1(a) could explain all these facts. On the other hand this suggests an effective J_2 interaction which could lead to 2nd-NN $d + \mathrm{i}d$ pairing. Therefore Na_xCoO_2 with doping concentration around x_c is a possible candidate to realize such a "magnetic superconductor" with non-Abelian MBS.

6.4 $d_{x^2-y^2}$ superconductor with (Q_0, Q_0) coplanar magnetic order on square lattice

The 2nd example is a more familiar one: a NN $d_{x^2-y^2}$ paired superconductor on the square lattice. We consider only NN hopping (amplitude t). Writing momentum as $\mathbf{k} = k_1\vec{b}_1 + k_2\vec{k}_2$ (see FIG. 6.4) the mean-field Hamiltonian has a band structure $\xi_{\mathbf{k}} = -2t\big[\cos(k_1+k_2)+\cos(k_1-k_2)\big] - \mu$ and gap function $\Delta_{\mathbf{k}} = 2\Delta\big[\cos(k_1+k_2) - \cos(k_1-k_2)\big]$. The four nodal points are shown in FIG. 6.4(a)

$$N_{1,3}: \ k_2 = \pm q_0, k_1 = 0; \quad N_{2,4}: \ k_1 = \pm q_0, k_2 = 0.$$

with $q_0 = \arccos(-\frac{\mu}{4t})$. Now adding a magnetic mass *e.g.* with momentum $\mathbf{Q}_0 = 2q_0\vec{b}_2$ will gap out the $(c_{N_3,\uparrow}, c^\dagger_{N_1,\downarrow})$ branch and create a single MBS. In FIG. 6.4 we show the particular case when $\mu = -2\sqrt{2}t$ and $q_0 = \pi/4$. The spin configuration of such a non-collinear magnetic order is shown in FIG. 6.4(b). In this specific case, such a commensurate magnetic order will not gap out all nodal excitations since the Hamiltonian is still invariant under time reversal followed by a lattice translation[21]. As shown in FIG. 6.4(a) when the non-collinear magnetic order is present, the original four nodal points (each being two-fold degenerate with spin $\uparrow, \downarrow$) denoted by black circles are split into 6 nodes (each being non-degenerate) denoted by red diamonds. The disappearing Dirac nodes is gapped out by magnetic mass and enters the weak-pairing phase. Therefore despite the bulk gapless excitations in this particular case $q_0 = \pi/4$, we expect the non-Abelian MBS on the edge to be stable against impurities[183]. The corresponding edge spectra is shown in FIG. 6.5, which confirms the existence of MBS on the edge. In a generic doping when q_0 is an arbitrary number, the corre-

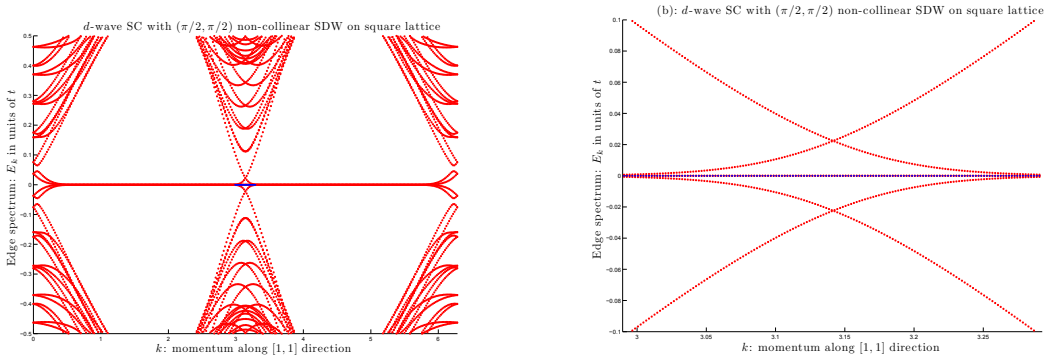

Figure 6.5: (color online) (a) *Left panel:* Edge spectrum of a NN $d_{x^2-y^2}$ superconductor with $(\pi/2, \pi/2)$ non-collinear magnetic order shown by FIG. 6.4(b) on square lattice, dispersing with momentum k_2 along $[1, 1]$ direction. Although there are bulk gapless excitations, there is a zero-energy MBS at $k_2 = \pi$, in the almost flat band as shown by the blue line. Parameters are chosen as $\Delta = 0.7t$ and $m = 0.4t$. (b) *Right panel:* Edge spectrum of FIG. 6.5 zoomed in around $k_2 = \pi$. The almost flat (non-dispersing) band crossing $k_2 = \pi$ corresponds to the MBS (at $k_2 = \pi$) localized around one edge, as shown by the blue line.

sponding incommensurate non-collinear magnetic order might open up a gap for all nodal excitations and leave the edge states as the only low-energy modes.

In fact, such a non-collinear magnetic order with momenta $\mathbf{Q}_0 = Q_0\vec{b}_{1,2}$ can also be realized in a microscopic Heisenberg J_1-J_2-J_3 model. The classical ground state of J_1-J_2-J_3 is a non-collinear one with momenta $\mathbf{Q}_0 = Q_0\vec{b}_{1,2}$ where $\cos(Q_0) = -J_1/(2J_2 + 4J_3)$, in the parameter range $4J_3 + 2J_2 \geq J_1$ and $J_3 \geq J_2/2$[170, 48]. There are numerical evidences that such phases survive in the quantum $S = 1/2$ Heisenberg J_1-J_2-J_3 model in a wide parameter range[196, 197]. Therefore we expect such an exotic non-Abelian phase, *i.e.* a d-wave superconductor with coexisting $\mathbf{Q}_0 = Q_0\vec{b}_{1,2}$ non-collinear magnetic order might be realized in a doped t-J_1-J_2-J_3 model.

6.5 Summary

In this work we propose another possible realization of Majorana fermions in solid state physics. We show that in general when singlet superconductivity with nodal excitations coexists with non-collinear magnetic order with a proper wavevector, there will be non-Abelian MBS in the vortex core (or on the edge) of such a superconductor. We show such an exotic phase might be realized by extended t-J models on different lattices. Relevant experimental realizations are also discussed. This proposal reveals a new possibility to discover MBS in strongly-correlated electron systems, where phase coexistence are observed in many different materials.

Chapter 7

Symmetry protected fractional Chern insulators and fractional topological insulators

7.1 Introduction

Phases of matters in condensed matter systems can almost always be characterized by the Landau-Ginzburg symmetry breaking theory[110, 111]. Experimental discovery of integer and fractional quantum Hall states in 2-D electron gas under a strong external magnetic field[105, 207] has provided striking counter examples of this paradigm. The fractional quantum Hall liquids are particularly fascinating in the sense that their low energy excitations are quasi-particles carrying fractional electric charge[114] and obeying anyonic statistics[12]. Although these liquid phases do not break physical symmetries, they are still different quantum phases. One measurable

difference is their edge states: despite the fact that these liquids are all insulators in the bulk, they all possess certain edge metallic modes[223]. In general different bulk phases host different edge states which can be detected by various experimental probes such as electric transport[222].

A few years after the experimental discovery of integer quantum Hall effect(IQHE), Haldane showed that the essence of it is *not* the external magnetic field[68], by explicitly writing down a lattice model Hamiltonian of IQHE with zero net magnetic field. However, it takes more than two decades for people to show that similar statement is true even for FQHE. Recently in a series of model studies[204, 202, 149, 191, 148], fractional quantum hall states have been shown to be the ground states of interacting lattice models, in the absence of an external magnetic field. It is found that the ground state is likely to respect the full lattice symmetry. Here we call these fractional ground states spin-polarized "fractional Chern insulators" (FCI) to distinguish from the traditional fractional quantum Hall states in an external magnetic field. These proposed lattice models share a common feature: a partially filled nearly flat two-dimensional band with non-trivial band topology.

The concept of band topology originates from the well-known TKNN index (or Chern number) of an IQH insulator[205]. In the past few years, this concept has been generalized to time-reversal symmetric systems, and triggers the theoretical and experimental discoveries of topological insulators in spin-orbital coupled compounds in both two and three spatial dimensions[165, 76, 141]. In two dimension (2D), a time-reversal symmetric band insulator is characterized by a Z_2 topological index. Experimentally, HgTe quantum heterostructure has been shown to be a 2D topological

insulator[107]. In the simplest limit, 2D topological insulator can be viewed as a direct product of the up-spin and down-spin wavefunctions hosting opposite TKNN index.

It is then quite natural to ask whether similar time-reversal-invariant (TRI) versions of fractional topological insulators (FTI) exist or not[122]. In the simplest limit when spin along z-direction is conserved, it can be understood as the direct product of wavefunctions of the up spin and down spin with opposite FQHE. Clearly this direct product is a fully gapped stable phase. In addition it must have non-trivial ground state degeneracy on a torus even in the presence of a small S_z conservation breaking perturbation, because the ground state degeneracy cannot be lifted by an arbitrary local perturbation. So there is no question that in principle this fractionalized phase could exist. One important open question is that whether TRI FTI can exist in a reasonable Hamiltonian.

In order to realize the fractional topological insulators (FTI) in experiments, one should find a compound with a nearly flat topological non-trivial band so that correlation effect is strong. Naively this is unnatural because usually a flat band is realized by spatially localized orbitals which do not support topological non-trivial hopping terms. However, a very recent theoretical investigation[236] of transition metal oxide interface indicates that a nearly flat topological non-trivial band can be naturally realized in the e_g orbital double-layer perovskite grown along [111] direction. Exact diagonalization in the same work shows that fractional quantum hall state can be realized in principle when the nearly flat band is partially filled. Because the temperature scale of the FCI/FTI physics in this system is controlled by short-range Coulomb interaction, it can be a high-temperature effect.

Fractional quantum Hall states, especially the non-Abelian ones, have been shown to be very useful building blocks of quantum computers. If high temperature FCI/FTI physics can be realized experimentally, it will certainly have deep impact in condensed matter physics, including the efforts on topological quantum computation[146].

Motivated by the recent progresses on FCI/FTI physics, in this paper we try to address several important issues: *what are the many-particle wavefunctions of FCIs/FTIs? Can there exist more than one FCI/FTI phases with the same filling fraction? If the answer is positive, can we classify these quantum phases (or ground state wavefunctions)?*

Historically, Laughlin's wavefunctions of FQH states in a magnetic field[114] have been shown to be one of the most important theoretical progress in many-particle physics. It allows people to understand a lot of properties of FQH liquids in a compact fashion, including the fractionalized quasi-particle excitations[12], topological ground state degeneracies[70, 218], as well as constructing the low energy effective theories[59, 243, 171]. Here in the case of FCI systems, analytical understanding of the ground state wavefunctions will help us extract various measurable information in a similar way.

Recently there was interesting work to construct FCI wavefunctions by proposing a one-to-one mapping between the lattice problem and the magnetic field problem[163]. We would like to emphasize that the wavefunction problem for FCI is related to that for the magnetic field case, yet they are very different from each other. This is because the lattice symmetry of FCI is fundamentally different from the continuum case of 2-D electron gas. In fact, the recently discovered FCI states preserve all the lattice point

group symmetry as well as translational symmetry[1]. Here in this paper, we point out that as a consequence of the lattice symmetry, there exist many different quantum FCI phases, all respecting the full lattice symmetry, even at the same filling fraction with the same quantum Hall conductance. These different FCI phases are distinct in the bulk in a more subtle way. One hand-waving statement is that the bulk quasi-particle excitations of these phases carry different lattice quantum numbers. These distinct FCI phases cannot adiabatically connect with each other without a phase transition while the lattice symmetry is respected. Similar phenomena of distinct topologically ordered phases protected by symmetry is known in the context of quantum spin liquids[225] and other low dimensional topological phases[27].

Now we outline the content of this paper. We start with the spin-polarized FCI at filling $\nu = \frac{1}{m}$ (m is an odd number). In section 7.2 the $SU(m)$ parton construction of the fractional quantum Hall states (or spin-polarized FCI states) is introduced on a lattice, which is a natural generalization of the continuum case[114, 95]. We argue that a general the FCI wavefunction could break the $SU(m)$ gauge group down to Z_m, and consequently the low-energy dynamics is described by $SU(m)$ Chern-Simons-Higgs theory. We explicitly write down the form of the electronic FCI wavefunctions which will be useful for future variational Monte Carlo study. We construct quasiparticle excitations of such a FCI state. To demonstrate how lattice symmetry restricts the structure of the wavefunctions, we introduce the concept of projective symmetry group (PSG)[225] which serves as the mathematical language to classify different symmetry

[1]Because the wavefunction constructed in Ref. [163] is based on one-dimensional Wannier function which explicitly select a special direction of the lattice, the constructed wavefunctions do not obviously respect the lattice point group symmetry.

protected FCI phases. Due to the limited length, we won't discuss explicit examples of FCI states on specific lattices. Interested readers can find detailed examples in Ref. [127]. We also propose spin-polarized FCI states with non-Abelian quasiparticles, which might be realized in nearly flat bands with Chern number $C > 1$. Such non-Abelian FCIs might be used to build a universal quantum computer[53, 146].

In section 7.3 we demonstrate that our parton construction can be used to compute the topological ground state degeneracy, and to find the conformal field theory for the edge excitations. This is particularly important for the Z_m states, which belong to a new class of FQH wavefunctions.

In section 7.4 we generalize our efforts to construct ground state wavefunctions of TRI FTI. When the mixing between the up and down spins is weak, it is natural to generalize our spin polarized results to this case. For filling fraction $\nu = \frac{2}{m}$ (on average $\nu = \frac{1}{m}$ for each spin), we present classes of $SU(m)^{\uparrow} \times SU(m)^{\downarrow}$ and $Z_m^{\uparrow} \times Z_m^{\downarrow}$ wavefunctions and discuss their properties including quasi-particle statistics and ground state degeneracies. We also propose a new parton construction formalism which allows one to write down generic electron wavefunctions for TRI FTI states in the absence of spin conservation. We can deform such a generic TRI FTI wavefunction in the absence of spin conservation into a S^z-conserved TRI FTI wavefunction (where spin-$\uparrow$ and spin-$\downarrow$ decouple) by continuously tuning a parameter.

7.2 $SU(m)$ parton construction of spin-polarized Z_m fractional Chern insulator states

7.2.1 A brief review of Laughlin's FQH state from $SU(m)$ parton construction

Soon after the experimental discovery of fractional quantum Hall (FQH) effects[207], Laughlin proposed a series of variational wavefunctions[114] which were shown[69] numerically to be a very good description of FQH states at odd-denominator filling fraction $\nu = 1/m$. Later this idea of constructing trial wavefunctions was generalized to other filling fractions[67, 73, 94]. An important lesson we can learn from Laughlin's wavefunction is that with a fixed filling fraction (or a fixed number of flux quanta through the sample), the many-body wavefunction tends to vanish as fast as possible when two electrons approach each other so that the repulsive Coulomb energy between electrons could be minimized. As an example, Laughlin's state at $\nu = 1/3$ is nothing but the cube of the wavefunction for a filled lowest Landau level of partons with charge $e/3$: $\Phi_{\nu=1/3}(\{\mathbf{r}_i\}) = \left[\Phi'_{\nu=1}(\{\mathbf{r}_i\})\right]^3 = \prod_{i<j}(z_i - z_j)^3 \exp[-\sum_{i=1}^{N} |z_i|^2/(4l_B^2)]$ in the disc geometry choosing symmetric gauge, where $z_i = x_i + \mathrm{i}y_i$ are complex coordinates, $l_B = \sqrt{\hbar/|eB|} = l'_B/\sqrt{3}$ is the electron magnetic length and l'_B is the parton magnetic length. We can construct this wavefunction by splitting an electron into three fermionic *partons*:

$$c(\mathbf{r}) = f_1(\mathbf{r}) f_2(\mathbf{r}) f_3(\mathbf{r}) \tag{7.1}$$

and the electron wavefunction is obtained through the following projection

$$\Phi_e(\{\mathbf{r}_i\}) = \langle 0| \prod_{i=1}^{N} f_1(\mathbf{r}_i) f_2(\mathbf{r}_i) f_3(\mathbf{r}_i) |MF\rangle \tag{7.2}$$

where $|0\rangle$ represents the parton vacuum and $|MF\rangle$ can be any mean-field state of the three partons $f_{1,2,3}$. When each of the three partons occupy the lowest Landau level (LLL) one immediately obtains the Laughlin's state $\Phi_{\nu=1/3}(\{\mathbf{r}_i\})$. Naturally from (7.1) we can see each parton carries $U(1)$ electric charge $e_0 = e/3$ where e stands for the electron charge. Since each kind of parton occupies a LLL, the electromagnetic response of the FQH state $\Phi_{\nu=1/3}(\{\mathbf{r}_i\}) = \left[\Phi'_{\nu=1}(\{\mathbf{r}_i\})\right]^3$ is characterized by Hall conductivity $\sigma_{xy} = 3 \cdot (\frac{1}{3})^2 \cdot \frac{e^2}{h} = \frac{1}{3}\frac{e^2}{h}$. This reproduces the correct filling fraction and many-body Chern number. Note that electron operator $c(\mathbf{r})$ in (7.1) is invariant under any *local* $SU(3)$ transformation on the three partons $(f_1, f_2, f_3)^T$. The mean-field Hamiltonian density describing the Laughlin state is[224]

$$\mathcal{H}_{MF} = \frac{1}{2m^*} \sum_{\alpha=1}^{3} f_\alpha^\dagger(\mathbf{r}) \big(-\mathrm{i}\nabla - e_0 \mathbf{A}(\mathbf{r}) \big)^2 f_\alpha(\mathbf{r}) \tag{7.3}$$

where m^* is the effective mass of each parton. This mean-field Hamiltonian preserves the $SU(3)$ gauge symmetry and partons will also couple to an $SU(3)$ internal gauge field. Its effective theory is the $SU(3)_1$ Chern-Simons gauge theory, which explains the 3-fold topological ground state degeneracy on a torus[220]. These f partons are nothing but charge charge $-e/3$ quasihole excitations[114] of Laughlin state. Indeed after projection (7.2) the three species of partons $f_{1,2,3}$ becomes indistinguishable thanks to the internal $SU(3)$ symmetry: each f parton creates a charge $-e/3$ quasihole upon acting on the ground state $|MF\rangle$. It is straightforward to verify that the

following wavefunction

$$\Phi_e(\{\mathbf{r}_i\}|\mathbf{w}_{1,2,3}) = \tag{7.4}$$
$$\langle 0|f_1(\mathbf{w}_1)f_2(\mathbf{w}_2)f_3(\mathbf{w}_3)\prod_{i=1}^{N-1} f_1(\mathbf{r}_i)f_2(\mathbf{r}_i)f_3(\mathbf{r}_i)|MF\rangle$$

reproduces the Laughlin wavefunction with three quasiholes at $\mathbf{w}_{1,2,3}$ up to a constant factor. Hence these partons are indeed charge $\pm e/3$ anyons obeying fractional statistics with statistical angle $\theta_{1/3} = \frac{\pi}{3}$.

7.2.2 Z_m FCI state and its quasiparticles from $SU(m)$ parton construction

Since the three seemingly-different partons $f_{1,2,3}$ are essentially the same quasihole excitations with the same quantum numbers, physically it is attempting to include the tunneling terms $f_\alpha^\dagger f_\beta,\ \alpha \neq \beta$ in the mean-field Hamiltonian. By mixing different partons, these terms will break the internal $SU(3)$ gauge symmetry down to a a subgroup of $SU(3)$, which is Z_3, the center of the $SU(3)$ group, in the most generic case where $f_\alpha^\dagger f_\beta$, $\forall\ \alpha \neq \beta$ terms are present. In general the projected Z_3 wavefunction (7.2) is always different from its parent projected $SU(3)$ wavefunction. For a 2-D electron gas in a magnetic field, however, people usually focus on the LLL within which the many-body wavefunction is an analytic function (*e.g.* in the symmetric gauge on a disc). It is straightforward to show that as long as the mixing terms act inside the Hilbert space of LLL, the corresponding electron wavefunction (7.2) for a Z_3 state remains the same as that of its parent $SU(3)$ state. This is because the parton wavefunction describes a state with LLL fully filled. Mixing between different

partons within the LLL Hilbert space only gives a unitary transformation of basis and does not modify the parton wavefunction. For a lattice model, it is natural to consider mixing terms acting between all bands (rather than within the filled bands), and the corresponding electron wavefunction of a Z_3 state will be a different wavefunction from that of its parent $SU(3)$ state. For a filling fraction $\nu = 1/m$, our discussion straightforwardly generalizes to the corresponding Z_m (the center of the $SU(m)$ group) state and its parent $SU(m)$ state.

To our knowledge, the Z_m parton states of FQHE have not been proposed before. For this new class of wavefunctions, several natural questions need to be answered. What are the quasi-particles in the Z_m state? What is the low-energy effective theory of the Z_m state? Will it preserves the topological properties, including ground state degeneracy and edge states? We answer these questions in this paper and find the topological properties of the Z_m states are identical to the $SU(m)$ states. Their difference lies in the projective symmetry group, which is protected by lattice symmetry. In general, Z_m states and $SU(m)$ states both serve as candidate ground states for the FCI states of a $\nu = 1/m$ filled band with Chern number one.

To begin with, let us consider the quasi-particle excitations in a Z_m state. The physical quasiparticle excitations in a Z_m state are constructed by inserting fluxes in the mean-field ansatz of $f_\alpha^\dagger f_\alpha$ terms and simultaneously creating vortices (or defects) in the Higgs condensates $\langle f_\alpha^\dagger f_\beta \rangle,\ \alpha \neq \beta$. In 2-D, because $\pi_1(SU(m)/Z_m) = Z_m$, these defects are the point-like vortices carrying Z_m gauge fluxes. Because the Z_m flux can be considered to be localized in a single plaquette, one can effectively interpret it as a overall $U(1)$ gauge flux of all the f-partons. Namely when a f-parton winds

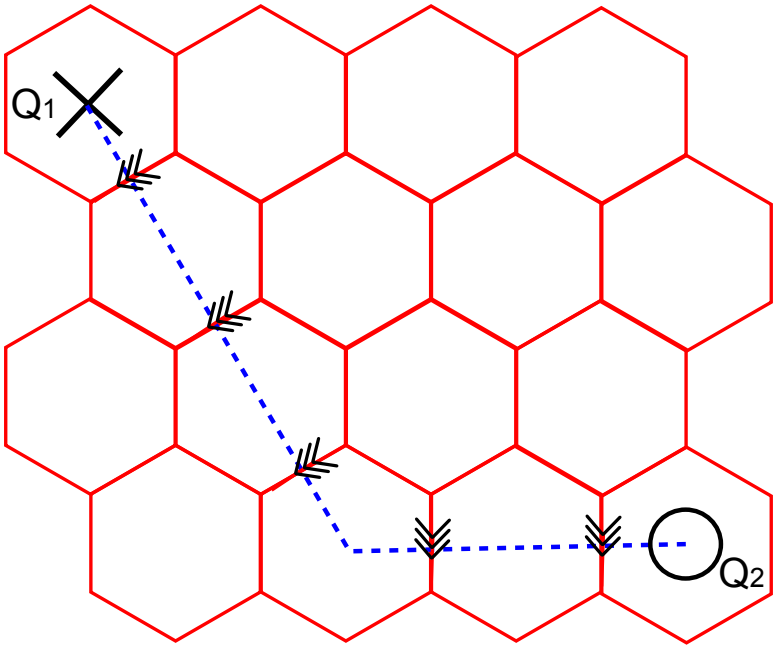

Figure 7.1: (color online) A pair of anyonic quasiparticle and its antiparticle in a Z_m state on the honeycomb lattice. The dashed line denotes the string of $e^{\mathrm{i}2\pi k/m}$ phase shift connecting the two plaquettes where quasiparticle Q_1 and its antiparticle Q_2 are located. On top of the ground state mean-field ansatz, any mean-field bond crossing the string should pick up a phase shift $e^{\mathrm{i}2\pi k/m}$. Here we only demonstrate the phase shift of nearest-neighbor (NN) mean-field amplitudes by triple arrows in the figure.

around a fundamental vortex, it experiences a $2\pi/m$ flux. Due to the Chern numbers of the filled parton bands, this vortex also binds with a single f-parton gauge charge and thus carries electric charge e/m. Because this object carries both flux and gauge charge, the fractional statistical angle $\theta = \pi/m$ results. These are exactly the same charge and statistics a quasihole carries in the $SU(m)$ state. We conclude that the topological properties of quasiparticles are the same in both the Z_m and its $SU(m)$ parent state.

Following the above discussions, we can write down the wavefunctions with low-energy anyonic excitations in a Z_m state. At filling fraction $\nu = 1/m$, in order to

create one quasiparticle Q_1 at $\mathbf{w}_1$ and its antiparticle Q_2 at $\mathbf{w}_2$, we need to insert $2\pi k/m$ flux in a plaquette $P_{\mathbf{w}_1}$ at position $\mathbf{w}_1$ and $-2\pi k/m$ flux in a plaquette $P_{\mathbf{w}_2}$ at position $\mathbf{w}_2$ with $k = 1, \cdots, m$. Q_1 carries $2\pi k/m$ flux and ek/m charge while Q_2 carries $-2\pi k/m$ flux and $-ek/m$ charge. Both Q_1 and Q_2 have statistical angle $\theta = k^2\pi/m$ and their mutual statistical angle is $\theta' = -k^2\pi/m$. They are realized by creating $e^{\mathrm{i}2\pi k/m}$ phase shift for all mean-field amplitudes on the string connecting two plaquettes $P_{\mathbf{w}_1}$ and $P_{\mathbf{w}_2}$, on top of the mean-field ansatz for the ground state. An example of such a pair of quasiparticle and its antiparticle in a Z_m state on honeycomb lattice is shown in FIG. 7.1. The corresponding electron wavefunction is obtained by the projection on this new mean-field ansatz for excited state.

The ground state degeneracy of a Z_m FCT state at $\nu = 1/m$ on a torus can also be understood once we know its quasiparticle statistics[218, 153]. Consider the following tunneling process $\mathcal{T}_1$: a pair of quasiparticle (with flux $2\pi/m$ and charge e/m) and its antiparticle (with flux $-2\pi/m$ and charge $-e/m$) are created and the quasiparticle is dragged around the non-contractable loop X_1 along x_1 direction on the torus before it is finally annihilated with it anti-particle. This tunneling process will leave a string of $e^{\mathrm{i}2\pi/m}$ phase shift (as shown in FIG. 7.1) along this loop X_1, therefore has the same physical effects as adiabatically inserting a $2\pi/m$ flux in the non-contractable loop X_2 along x_2 direction on the torus. Notice that when the quasiparticle-anti-quasiparticle pair carries flux $\pm 2\pi k/m$ and charge $\pm ke/m$ the corresponding tunneling process is realized by $\mathcal{T}_1^k$. Similarly we can define a tunneling process $\mathcal{T}_2$ by dragging the fundamental quasiparticle around non-contractible loop X_2 once, which is physically equivalent to inserting $2\pi/m$ flux in non-contractible loop X_1. In the thermodynamic

limit, the Hilbert space of degenerate ground states should be expanded by these tunneling processes[153]. The two tunneling operators satisfy the following "magnetic algebra":

$$\mathcal{T}_1\mathcal{T}_2 = \mathcal{T}_2\mathcal{T}_1 e^{2\pi/m} \tag{7.5}$$

This is straightforward to understand from Aharonov-Bohm effect point of view. Another way to understand it is because the tunneling process $\mathcal{T}_2^{-1}\mathcal{T}_1^{-1}\mathcal{T}_1\mathcal{T}_2$ can de continuously deformed into two linking loops[218] and corresponds to a phase of $2\theta_{1/m}$, where $\theta_{1/m} = \pi/m$ is the statistical angle of the fundamental quasiparticle. All degenerate ground states can be labeled by *e.g.* eigenvalues of unitary operators $\mathcal{T}_1$ and $\mathcal{T}_2^m$ (since they commute with each other). In this basis $\mathcal{T}_2$ acts like a ladder operator and changes the eigenvalue of $\mathcal{T}_1$ by a phase $e^{\mathrm{i}2\pi/m}$. In this way one can see the ground state degeneracy of a Z_m state on torus is m-fold. We can easily generalize this discussion to a genius-g Riemann surface with g pairs of non-contractible loops and the corresponding ground state degeneracy is m^g-fold. This is consistent with the ground state degeneracy calculated from the low-energy effective theory as will be shown in section 7.3 in a formal way.

Because the discussion on low-energy effective theory the Z_m state involves more technical details, we postpone it to Section 7.3, where we compute its ground state degeneracy and extract the edge conformal field theory. We'll show that the ground state degeneracy of a Z_m state is the same as that of a $SU(m)$ state: m^g-fold on a genus-g Riemann surface. We'll also show that the Z_m state and $SU(m)$ state share the same edge conformal field theory.

7.2.3 Regarding lattice symmetries

In the numerical simulations of FCI phases[191, 149], only the m-fold topological degeneracy of $\nu = 1/m$ FCI is observed on torus. This indicates that the FCI wavefunctions respect the full lattice symmetry, since otherwise there should be extra degeneracies due to lattice symmetry breaking. This motivates us to write down the fully symmetric FCI wavefunctions.

In the following we outline the general strategy to construct fully symmetric FCI states on a lattice in the parton approach. Here we focus on spin-polarized FCI states with filling fraction $\nu = 1/m$ through $SU(m)$ parton construction. The electron operator is given by

$$c(\mathbf{r}) = \prod_{\alpha=1}^{m} f_\alpha(\mathbf{r}) \tag{7.6}$$

where $\mathbf{r}$ is the coordinate of a lattice site. For simplicity we assume there is only one orbital per lattice site. As mentioned earlier, this parton construction has a local $SU(m)$ symmetry since the electron operator $c(\mathbf{r})$ is invariant under any local transformation $f_\alpha(\mathbf{r}) \to \sum_\beta G_{\alpha\beta}(\mathbf{r}) f_\beta(\mathbf{r})$ where $G(\mathbf{r}) \in SU(m)$. A generic parton men-field ansatz is written as

$$H^{MF} = \sum_{\mathbf{r},\mathbf{r}'} \sum_{\alpha\beta} f^\dagger_\alpha(\mathbf{r}) M_{\alpha\beta}(\mathbf{r}|\mathbf{r}') f_\beta(\mathbf{r}') \tag{7.7}$$

where $M(\mathbf{r}|\mathbf{r}') = M^\dagger(\mathbf{r}'|\mathbf{r})$ is a $m \times m$ matrix. Under a local $SU(m)$ gauge transformation $\{G(\mathbf{r})\}$ it transforms as $M(\mathbf{r}|\mathbf{r}') \to G(\mathbf{r}) M(\mathbf{r}|\mathbf{r}') G^\dagger(\mathbf{r}')$. Again once we obtain a mean-field state $|MF\rangle$ with the right filling number from (7.7), the corresponding electron wavefunction is obtained through

$$\Phi_e(\{\mathbf{r}_i\}) = \langle 0| \prod_{i=1}^{N} c(\mathbf{r}_i)|MF\rangle = \langle 0| \prod_{i=1}^{N} \prod_{\alpha=1}^{m} f_\alpha(\mathbf{r}_i)|MF\rangle, \tag{7.8}$$

whose explicit form is a Slater determinant as given later in (7.10).

Notice that not all parton mean-field ansatz correspond to a $\nu = 1/m$ FCI state. Let's start from a $SU(m)$ mean-field state $H_\alpha^{MF} = \sum_\alpha f_\alpha^\dagger(\mathbf{r}) T(\mathbf{r}|\mathbf{r}') f_\alpha(\mathbf{r}')$ where each flavor of the parton has the same filling number as the electron. For $\nu = 1/m$ FCI states in topological nearly flat bands, the filling fraction is such that on average there is one electron (hence one parton with each flavor) per m unit cells. If the mean-field ansatz (7.7) has explicit lattice translation symmetry, however, the corresponding state with $\nu = 1/m$ filling would most likely be a gapless metallic state[2] since only a fraction $(1/m)$ of the lowest band is filled. How to construct a gapped mean-field ansatz of FCI with filling fraction $1/m$?

The answer lies in the $SU(m)$ gauge structure of the parton construction (7.6). Briefly speaking, the mean-field state itself can explicitly break lattice symmetries (such as lattice translation) by inserting fluxes in each plaquette, as long as the mean-field ansatz is invariant under a symmetry operation followed by an $SU(3)$ gauge rotation. By inserting *e.g.* $2\pi/m$ flux in each plaquette one can enlarge the unit cell by m times. Therefore the corresponding mean-field state with filling $\nu = 1/m$ corresponds to a state filling lowest m bands of mean-field ansatz (7.7). Although the mean-field Hamiltonian (7.7) explicitly breaks lattice symmetry, the corresponding electron wavefunction (7.8) preserves all the lattice symmetries. If each of the m

[2]When there are parton mixing terms which breaks the gauge symmetry from $SU(m)$ down to Z_m, one can construct a gapped state with filling $\nu = 1/m$ by just filling the lowest parton band, since there is on average one parton (including all flavors) in each unit cell. However, the Hall conductance of such a state is $\sigma_{xy} = \frac{C}{m^2}\frac{e^2}{h}$ where C is the Chern number of lowest parton band. Unless this lowest parton band has Chern number $C = m$ (which is unlikely), this gapped state at filling $\nu = 1/m$ will have a Hall conductance different from $\sigma_{xy} = e^2/(mh)$ and is not a good candidate for the FCI states realized in recent numerical studies.

lowest bands have a Chern number +1, the mean-field state filling these m bands would have Chern number $+m$, and the corresponding Hall conductivity is

$$\sigma_{xy} = m \cdot (\frac{1}{m})^2 \cdot \frac{e^2}{h} = \frac{1}{m}\frac{e^2}{h}, \tag{7.9}$$

because each parton carries $U(1)$ electric charge e/m. This gives the correct electromagnetic response of a $\nu = 1/m$ spin-polarized FCI state. The technique of enlarging the unit cell by m times without physically breaking any lattice symmetry will be generalized to the case of time-reversal-invariant FTI state with filling fraction $\nu = 2/m$, as will be discussed in section 7.4.

Following this strategy, we always require the parton mean-field ansatz of $\nu = 1/m$ FCI state breaks lattice translation symmetry explicitly and enlarges the unit cell by m times, so that the resultant mean-field state is an insulator. We require the partons to fill the lowest m bands of the mean-field spectrum and the corresponding electron state after projection would still be gapped. Now that the number of momentum points of each band in the (reduced) 1st Brillouin zone equals the electron number

N, we can see the electron wavefunction (7.8) is nothing but a Slater determinant

$$\Phi_e(\{\mathbf{r}_i\})_{Z_m} = \det \tag{7.10}$$

$$\begin{bmatrix}
\phi_{\mathbf{k}_1^1}(\mathbf{r}_1^1)\cdots\phi_{\mathbf{k}_N^1}(\mathbf{r}_1^1)\cdots\cdots\phi_{\mathbf{k}_1^m}(\mathbf{r}_1^1)\cdots\phi_{\mathbf{k}_N^m}(\mathbf{r}_1^1) \\
\phi_{\mathbf{k}_1^1}(\mathbf{r}_2^1)\cdots\phi_{\mathbf{k}_N^1}(\mathbf{r}_2^1)\cdots\cdots\phi_{\mathbf{k}_1^m}(\mathbf{r}_2^1)\cdots\phi_{\mathbf{k}_N^m}(\mathbf{r}_2^1) \\
\cdots\cdots\cdots \\
\phi_{\mathbf{k}_1^1}(\mathbf{r}_1^2)\cdots\phi_{\mathbf{k}_N^1}(\mathbf{r}_1^2)\cdots\cdots\phi_{\mathbf{k}_1^m}(\mathbf{r}_1^2)\cdots\phi_{\mathbf{k}_N^m}(\mathbf{r}_1^2) \\
\phi_{\mathbf{k}_1^1}(\mathbf{r}_2^2)\cdots\phi_{\mathbf{k}_N^1}(\mathbf{r}_2^2)\cdots\cdots\phi_{\mathbf{k}_1^m}(\mathbf{r}_2^2)\cdots\phi_{\mathbf{k}_N^m}(\mathbf{r}_2^2) \\
\cdots\cdots\cdots \\
\cdots\cdots\cdots\cdots\cdots \\
\cdots\cdots\cdots\cdots\cdots \\
\cdots\cdots\cdots\cdots\cdots \\
\phi_{\mathbf{k}_1^1}(\mathbf{r}_1^m)\cdots\phi_{\mathbf{k}_N^1}(\mathbf{r}_1^m)\cdots\cdots\phi_{\mathbf{k}_1^m}(\mathbf{r}_1^m)\cdots\phi_{\mathbf{k}_N^m}(\mathbf{r}_1^m) \\
\phi_{\mathbf{k}_1^1}(\mathbf{r}_2^m)\cdots\phi_{\mathbf{k}_N^1}(\mathbf{r}_2^m)\cdots\cdots\phi_{\mathbf{k}_1^m}(\mathbf{r}_2^m)\cdots\phi_{\mathbf{k}_N^m}(\mathbf{r}_2^m) \\
\cdots\cdots\cdots
\end{bmatrix}$$

where $\phi_{\mathbf{k}_j^n}(\mathbf{r}_i^\alpha)$ represents the eigenvector of mean-field Hamiltonian (7.7). To be specific, $\phi_{\mathbf{k}_j^n}(\mathbf{r}_i^\alpha)$ corresponds to the f_α parton component in momentum-$\mathbf{k}_j$ single-particle eigenvector of the bottom-up n-th band. Here $\alpha, n = 1, \cdots, m$ and $i, j = 1, \cdots, N$ where N is the total electron number at filling fraction $\nu = 1/m$. Note that for an $SU(m)$ mean-field ansatz (7.15) in the absence of mixing terms, the lowest m bands are all degenerate and we have $\phi_{\mathbf{k}^n}(\mathbf{r}^\alpha) = \phi_{\mathbf{k}}(\mathbf{r})\delta_{n,\alpha}$. The corresponding electron

wavefunction (7.10) reduces to the product of m copies of a Slater determinant:

$$\Phi_e(\{\mathbf{r}_i\})_{SU(m)} = \Big\{ \det \begin{bmatrix} \phi_{\mathbf{k}_1}(\mathbf{r}_1)\cdots\phi_{\mathbf{k}_N}(\mathbf{r}_1) \\ \phi_{\mathbf{k}_1}(\mathbf{r}_2)\cdots\phi_{\mathbf{k}_N}(\mathbf{r}_2) \\ \cdots\cdots\cdots \\ \phi_{\mathbf{k}_1}(\mathbf{r}_N)\cdots\phi_{\mathbf{k}_N}(\mathbf{r}_N) \end{bmatrix} \Big\}^m \tag{7.11}$$

where $\phi_{\mathbf{k}_j}(\mathbf{r}_i)$ is the momentum-$\mathbf{k}_j$ single-particle eigenvector of parton mean-field Hamiltonian $H_\alpha^{MF} = f_\alpha^\dagger(\mathbf{r})T(\mathbf{r}|\mathbf{r}')f_\alpha(\mathbf{r}')$ with $\forall\alpha = 1,\cdots,m$. This is a lattice version of Laughlin's state in free space[114]. However once we add lattice-symmetry-preserving parton mixing terms which breaks gauge symmetry from $SU(m)$ to Z_m, the electron wavefunction (7.10) of a Z_m FCI state, as well as its projective symmetry group which will be introduced shortly, will immediately become different from its parent $SU(m)$ state (7.11). We emphasize again that only when the unit cell is enlarged by m times, we will have the same number of momentum points $\mathbf{k}_j$ as the electron number N. The mean-field amplitudes can be determined by variational Monte Carlo study of the energetics of electronic wavefunctions (7.10).

Considering flux insertion in order to enlarge the unit cell in mean-field ansatz (7.7), there is another question: can there be more than one way of inserting fluxes into each plaquette without breaking physical lattice symmetries? If yes, how to classify different mean-field ansatz (7.7)? The answer of the 1st question is yes and to answer the 2nd question, we need to introduce a mathematical structure: projective symmetry group (PSG)[225] in order to characterize different ways of flux insertion and corresponding different "universality classes" of symmetric FCI states. In the following we give a brief introduction to the idea of PSG.

Note that there is a many-to-one correspondence between parton mean-field states and physical electron states due to the above projection operation: any two parton mean-field states related to each other by an $SU(m)$ gauge transformation $\{G(\mathbf{r})\}$ correspond to the same electron state. As a result, although the physical electron state preserves all lattice symmetry, its parton mean-field ansatz may or may not explicitly preserve these lattice symmetries. More precisely, in a generic case the parton mean-field ansatz (7.7) should be invariant under a combination of lattice symmetry operation U and a corresponding gauge transformation $\{G_U(\mathbf{r}) \in SU(m)\}$:

$$M(U(\mathbf{r})|U(\mathbf{r}')) = G_U(U(\mathbf{r}))M(\mathbf{r}|\mathbf{r}')G_U^\dagger(U(\mathbf{r}')) \tag{7.12}$$

Different universality classes of parton mean-field ansatzs are characterized by different PSGs[225], *i.e.* different $SU(m)$ gauge transformations $\{G_U\}$ associated with symmetry operations U:

$$PSG = \{G_U(\mathbf{r})U|U \in \text{ symmetry group}\} \tag{7.13}$$

The low-energy gauge fluctuation of a mean-field ansatz is controlled by its invariant gauge group[225] (IGG)

$$IGG = \{G_{\boldsymbol{e}} \in SU(m)|G_{\boldsymbol{e}}M(\mathbf{r}|\mathbf{r}')G_{\boldsymbol{e}}^\dagger = M(\mathbf{r}|\mathbf{r}'), \forall\ \mathbf{r}, \mathbf{r}'\}$$

where $\boldsymbol{e}$ represents the identity operator of the (lattice) symmetry group (SG). In other words, IGG is a subgroup of the internal gauge group (which is $SU(m)$ here) that keeps the mean-field ansatz (7.7) invariant. Hereafter we would call a parton mean-field state with *e.g.* $IGG = SU(m)$ state an $SU(m)$ state. We can see that the IGG of mean-field ansatz (7.7) always contains the following Z_m group as a subgroup:

$$Z_m = \{e^{\mathrm{i}\frac{2\pi a}{m}} \cdot I_{m\times m}|a = 1, 2, \cdots, m\} \tag{7.14}$$

where $I_{m\times m}$ is the $m \times m$ identity matrix. This Z_m group is the center of the $SU(m)$ group. A mean-field ansatz $\{M(\mathbf{r}|\mathbf{r}')\}$ with $IGG = Z_m$ is called a Z_m state. The low-energy theory of this Z_m state will be described by fermionic partons f_α interacting with Z_m gauge fields.

The classification of PSGs with $IGG = SU(m)$ (which we call $SU(m)$ PSGs in this paper) are easy to carry out. The only gauge invariant quantities of a $SU(m)$ ansatz is the gauge-invariant flux through each plaquette, which must belong to the center of the $SU(m)$ gauge group, namely the Z_m group in Eq.7.14, because otherwise the $SU(m)$ gauge group would be broken and IGG cannot be $SU(m)$. Two $SU(m)$ states have the same PSG if and only if they have the same Z_m gauge flux in each given plaquette. Therefore distinct $SU(m)$ PSGs have different Z_m gauge flux pattern and vise versa.

The classification of PSGs with $IGG = Z_m$ (which we call Z_m PSGs in this paper) involves more technical details and we leave this analysis for the honeycomb lattice model[68] and the checkerboard lattice model[202, 149] in Ref. [127].

7.2.4 Possible non-Abelian states by partially filling a nearly flat band with Chern number $C > 1$

It has been shown[216, 220] that in $SU(m)$ parton construction, when each parton species fills n Landau levels, the effective theory of the corresponding electron state is the $SU(m)_n$ Chern-Simons theory and the system has non-Abelian quasiparticle excitations when $n > 1$. Moreover, the non-Abelian quasiholes of this state can be used as topologically-protected qubits in a universal quantum computer[146] as long

as $m > 2$. This motivates us to propose possible realization of non-Abelian FCI states realized in a partially-filled nearly flat band with Chern number $C > 1$. When this band is partially filled with a filling fraction *e.g.* $\nu = 1/m$, the Hall conductance of the corresponding FCI state would be $\sigma = \frac{C}{m}\frac{e^2}{h}$. If the lowest m parton bands all have Chern number C instead of $+1$, the $SU(m)$ FCI state obtained by filling m lowest parton bands indeed has Hall conductance $\sigma = m\frac{Ce_0^2}{h} = \frac{C}{m}\frac{e^2}{h}$ with $e_0 = e/m$. This $SU(m)$ FCI state can be a promising candidate for $\nu = 1/m$-filled nearly flat band with $C > 1$.

Take the $C = 2$ case as an example. In Ref. [127] using $SU(3)$ parton construction, we show two examples of $SU(3)$ FCIs, one on honeycomb lattice and the other on checkerboard lattice, both have 3 lowest parton bands with Chern number $+2$. These two $SU(3)$ FCIs with $\nu = 1/3$ and $\sigma = \frac{2}{3}\frac{e^2}{h}$ are non-Abelian FCIs. Their low-energy effective theory of these $SU(3)$ states is $SU(3)_2$ Chern-Simons theory[220], featured by 6-fold ground state degeneracy on the torus and non-Abelian quasiparticle excitations. These results indicate that once a nearly flat band with Chern number $C > 1$ is found, by partially filling it one may realize non-Abelian FCIs, which have the potential to build a universal quantum computer[53, 146].

7.3 Effective theory of spin-polarized Z_m FCI states: ground state degeneracy and edge excitations

As mentioned earlier, the partons in our construction not only couples to the external electromagnetic gauge field, but also couples to an internal gauge field. These

internal gauge fields "glue" the partons together to form an electron. Since the parton mean-field state is essentially a Chern insulator of partons with a band gap, its low-energy physical properties (*e.g.* its ground state degeneracy on a manifold with no boundary, such as torus[218, 220]) are completely determined by fluctuations of internal gauge fields. The topological properties of a $SU(m)$ state has been studied before[220, 224]. In this section we will analyze the low-energy effective theory of spin-polarized Z_m FCI state (7.7) from $SU(m)$ parton construction. We'll try to answer the following questions: what is the ground state degeneracy of the Z_m FCI state? Is it the same as or different from that of a $SU(m)$ FCI state? How to describe the gapless edge states of a Z_m FCI state?

7.3.1 Effective theory of spin-polarized Z_m FCI states: when Chern-Simons encounters Higgs

We start from an $SU(m)$ mean-field state which has been shown[220] to describe the $\nu = 1/m$ Laughlin state in the continuum limit. Its mean-field ansatz is

$$M_{\alpha,\beta}(\mathbf{r}|\mathbf{r}') = \delta_{\alpha,\beta}\, T(\mathbf{r}|\mathbf{r}') \tag{7.15}$$

In other words, there is no hopping between partons of different species and the m species of partons have exactly the same band structure. As shown in (7.11) its electron wavefunction is a lattice version of Laughlin state[114]. Apparently this mean-field state doesn't break the $SU(m)$ gauge symmetry which leaves the electron operator (7.6) invariant. Since here the partons couple to both $U(1)$ and $SU(m)$

gauge fields, the Lagrangian writes

$$L_{SU(m)} = \tag{7.16}$$
$$\int \mathrm{d}t \Big\{ \sum_\alpha \sum_{\mathbf{r}} f^\dagger_\alpha(\mathbf{r},t) \Big[\mathrm{i}\partial_t f_\alpha(\mathbf{r},t) - \sum_{\mathbf{r}'} t(\mathbf{r}|\mathbf{r}') f_\alpha(\mathbf{r}',t) \Big]$$
$$- \sum_{\alpha,\mathbf{r},\mathbf{r}'} f^\dagger_\alpha(\mathbf{r},t) T(\mathbf{r}|\mathbf{r}') \cdot$$
$$e^{-\mathrm{i}e_0 \int_{\mathbf{r}}^{\mathbf{r}'} \vec{A}(\mathbf{x},t)\cdot \mathrm{d}\vec{\mathbf{x}}} \mathcal{P} \big[e^{-\mathrm{i}\int_{\mathbf{r}}^{\mathbf{r}'} \vec{a}(\mathbf{x},t)\cdot \mathrm{d}\vec{\mathbf{x}}} \big] f_\alpha(\mathbf{r}',t),$$

where $\mathcal{P}$ means path-ordered integral. A_μ and a_μ are $U(1)$ and $SU(m)$ gauge fields respectively. Strictly speaking they are both defined on the link of a lattice here. To linear order the above action can be written as

$$L_{SU(m)} = \tag{7.17}$$
$$\int \mathrm{d}t \Big\{ \sum_\alpha \sum_{\mathbf{r}} f^\dagger_\alpha(\mathbf{r},t) \Big[\mathrm{i}\partial_t f_\alpha(\mathbf{r},t) - \sum_{\mathbf{r}'} T(\mathbf{r}|\mathbf{r}') f_\alpha(\mathbf{r}',t) \Big]$$
$$- e_0 \sum_{\mathbf{r}} J^{U(1)}_\mu(\mathbf{r},t) A^\mu(\mathbf{r},t)$$
$$- \sum_{\mathbf{r}} \big(J^{SU(m)}_\mu \big)_{\alpha,\beta}(\mathbf{r},t)\ a^\mu_{\alpha,\beta}(\mathbf{r},t) \Big\}$$

where $A^\mu(\mathbf{r})$ stands for electromagnetic $U(1)$ gauge field while $a^\mu(\mathbf{r})$ represents the internal $SU(m)$ gauge field. $e_0 = e/m$ is the electric charge of each parton. Here $J^{U(1)}(\mathbf{r})$ and $J^{SU(m)}_\mu(\mathbf{r})$ are conserved $U(1)$ and $SU(m)$ parton currents respectively. To be precise, $J^{U(1)}_0 = \sum_\alpha f^\dagger_\alpha f_\alpha$ and $(J^{SU(m)}_0)_{\alpha\beta} = f^\dagger_\alpha f_\beta$. In the long-wavelength limit the spatial components of the parton currents in momentum space (with momentum $\mathbf{q}$) writes:

$$\overrightarrow{J^{U(1)}_{\mu,\mathbf{q}}} = \sum_{\mathbf{k}} \vec{\nabla}_{\mathbf{k}} T_{\mathbf{k}} \sum_\alpha f^\dagger_{\alpha,\mathbf{k}-\mathbf{q}/2} f_{\alpha,\mathbf{k}+\mathbf{q}/2}$$
$$(\overrightarrow{J^{SU(m)}_{\mu,\mathbf{q}}})_{\alpha,\beta} = \sum_{\mathbf{k}} \vec{\nabla}_{\mathbf{k}} T_{\mathbf{k}} f^\dagger_{\alpha,\mathbf{k}-\mathbf{q}/2} f_{\beta,\mathbf{k}+\mathbf{q}/2}$$

Since the partons form a band insulator, the band gap allows us to safely integrate out the partons and obtain an effective action $L[A, a]$ for the gauge fields. Let's assume all the filled m lowest parton bands have Chern number $+1$. Upon integrating out partons $\{f_\alpha, f_\alpha^\dagger\}$, the effective Lagrangian density writes

$$\begin{aligned}\mathcal{L}_{SU(m)}[A, a] &= \tfrac{me_0^2}{4\pi}\epsilon_{\mu\nu\lambda}A_\mu\partial_\nu A_\lambda \\ &+\tfrac{1}{4\pi}\epsilon_{\mu\nu\lambda}\mathrm{Tr}\big(a_\mu\partial_\nu a_\lambda + \tfrac{\mathrm{i}}{3}a_\mu a_\nu a_\lambda\big)\end{aligned} \tag{7.18}$$

the first term corresponds to the quantized Hall conductance $\sigma_{xy} = me_0^2/h$, while the second term, *i.e.* a $SU(m)_1$ Chern-Simons term describes the low-energy gauge fluctuations. As shown in Ref. [127], the Chern-Simons theory of $SU(m)$ gauge field a_μ can be reduced to Chern-Simons theory of $U(1)$ gauge fields $a_\mu^I,\ I = 1, \cdots, m-1$. The gauge field configuration is given by $(a_\mu)_{\alpha,\beta} = \sum_{I=1}^{m-1} a_\mu^I g_{\alpha,\beta}^I$ where g^I are $m \times m$ matrices defined in Ref. [127]. In the $a_0 = 0$ gauge, a_1 and a_2 are conjugate variables since the Lagrangian density for internal gauge fields a_μ writes

$$\mathcal{L}_{SU(m)_1}[a] = \frac{1}{4\pi}\sum_{I=1}^{m-1} I(I+1)\Big(a_1^I\partial_t a_2^I - a_2^I\partial_t a_1^I\Big)$$

According to uncertainty principle, a_1^I and a_2^I cannot be determined simultaneously and we choose to fix the configuration of a_2^I. Aside from these $U(1)$ gauge symmetries, there are also discrete symmetries associated with essentially all permutations between partons (for details see Ref. [127]). Taking all these into account we can obtain the ground state degeneracy as the number of gauge-inequivalent configurations of $\{a_\mu^I\}$. As shown in Ref. [127], the m-fold degenerate ground states correspond to

the following gauge field configurations:

$$a_2^I = 0,\ (I = 1, 2, \cdots, m-2);$$
$$a_2^{m-1} = \tfrac{2\pi}{L_2}\tfrac{k}{m}, \quad k = 1, \cdots, m. \tag{7.19}$$

Physically this means once we insert $2\pi k/m$ flux in the hole along x_1 direction of the torus for each parton, the original ground state is transformed into a different degenerate ground state. This is a "small" gauge transformation for the partons since they transform as

$$f_\alpha \to \exp\Big[\mathrm{i}\sum_{i=1,2} x_2 \sum_{I=1}^{m-1} a_2^I g_{\alpha\beta}^I\Big] f_\beta \tag{7.20}$$

Now we add Higgs terms $M_{\alpha,\beta}(\mathbf{r}|\mathbf{r}')$ which break the original $SU(m)$ gauge symmetry down to Z_m. Does the corresponding Z_m state have the same ground state degeneracy as an $SU(m)$ state? The answer is positive. In the long-wavelength limit we introduce the Higgs fields $\phi_{\alpha\beta}$ which carry no electric $U(1)$ charge but carry the internal gauge charge. As an example, the $f_1^\dagger(\mathbf{r})M_{1,m}(\mathbf{r}|\mathbf{r}')f_m(\mathbf{r}')$ terms in the lattice model will introduce Higgs field $\phi_{1,m}(x_1, x_2)$ in the long-wavelength limit. The Higgs field $\phi_{1,m}$ carries a^I charge $+1$ for $I = 1, \cdots, m-2$ and a^{m-1} charge $+m$. Likewise, for example, $\phi_{2,m}$ carries a^1 charge -1, a^I charge $+1$ for $I = 2, \cdots, m-2$ and a^{m-1} charge $+m$. In general for a Higgs field $\phi_{\alpha,\beta} = \phi_{\beta,\alpha}^*$, $\alpha < \beta$ associated with mixing term $f_\alpha^\dagger f_\beta$ has a_μ^I charge $Q_{\alpha,\beta}^I$ where

$$Q_{\alpha,\beta}^I = \begin{cases} 0, & I \le \alpha - 2 \ \text{ or } I \ge \beta \\ \alpha - 1, & I = \alpha - 1 \\ +1, & \alpha \le I \le \beta - 2 \\ \beta, & I = \beta - 1 \end{cases} \tag{7.21}$$

In the end one can see that the condensation of Higgs field can be viewed as adding a potential in the phase space of gauge field configurations to $SU(m)_1$ Chern-Simons action (7.19). To be specific, once we integrate out partons with the presence of Higgs fields the effective Lagrangian density for internal gauge fields becomes

$$\mathcal{L}_{eff}[a^I, \phi_{\alpha,\beta}] = \mathcal{L}_{SU(m)_1}[a]$$
$$+\mathcal{L}_{Higgs}\Big[(\partial_\mu - \mathrm{i}\sum_I Q^I_{\alpha,\beta} a^I_\mu)\phi_{\alpha,\beta}\Big]$$

Note that the above action is invariant under the following "large" gauge transformations

$$(a^I_1, a^I_2) \to (a^I_1 + \tfrac{2\pi p_1}{L_1}, a^I_2 + \tfrac{2\pi p_2}{L_2}),$$
$$\phi_{\alpha,\beta} \to \phi_{\alpha,\beta} \exp\Big[\mathrm{i}2\pi \sum_I Q^I_{\alpha,\beta}\big(\tfrac{p_1 x_1}{L_1} + \tfrac{p_2 x_2}{L_2}\big)\Big]$$

where $p_{1,2}$ are integers so that $\phi_{\alpha,\beta}$ is a single-valued function on the torus. Besides there are other large gauge transformations as listed in Ref. [127]. And all the discrete symmetries associated with permutations between partons are present, such as $P_{1,2}$

$$f_1 \longleftrightarrow f_2,\ a^1_\mu \to -a^1_\mu,\ \phi_{1,2} \longleftrightarrow \phi_{2,1}.$$

Upon integrating out the fluctuations of Higgs fields $\delta\phi_{\alpha,\beta}$ around their mean-field values $\bar{\phi}_{\alpha,\beta}$ in $\mathcal{L}_{eff}[a^I, \phi_{\alpha,\beta}]$ we have

$$\mathcal{L}_{Z_m}[a] = \mathcal{L}_{SU(m)_1}[a] - V[a^I_1, a^I_2]$$

The exact shape of potential $V[a^I_1, a^I_2]$ depends on *e.g.* magnitudes of Higgs fields $\phi_{\alpha,\beta}$, but it has certain robust features determined by the gauge charges $Q^I_{\alpha,\beta}$ of Higgs fields $\phi_{\alpha,\beta}$ which condense[218]. More precisely, *this potential is periodic in*

a_μ *configuration space*, with periodicity $2\pi/L_1$ for $a_1^I,\ I \leq m-2$ and $2\pi/L_2$ for $a_2^I,\ I \leq m-2$. It also has periodicity $2\pi/(mL_1)$ for a_1^{m-1} and $2\pi/(mL_2)$ for a_2^{m-2}. The minima of this potential sits exactly on the configurations shown in (7.19) of the m-fold degenerate ground states of $SU(m)_1$ Chern-Simons theory. Besides these features associated with large gauge transformations, the potential $V[a_1^I, a_2^I]$ are not invariant under the discrete symmetries associated with parton permutations such as $P_{1,2}$. This is essentially because the introduced mixing terms (or Higgs condensation) breaks the $SU(m)$ gauge symmetry. The action (7.22) actually describes the motion of particles in a magnetic field[220, 46] and a periodic potential: the I-th particle associated with a_μ^I experiences a magnetic field of $I(I+1)$ flux quanta piercing through the torus. Due to the periodicity of potential $V[a_1^I, a_2^I]$, the m-fold ground state degeneracy (as calculated in Ref. [127]) is still present when the gauge symmetry is broken from $SU(m)$ down to Z_m by introducing mixing terms between different partons (or Higgs fields).

This can be understood physically: by threading a $2\pi k/m$ flux of gauge field a_μ^{m-1} in the hole along x_1 direction on the torus, one creates a vortex (or 2π phase winding) in the $\phi_{I,m},\ I = 1, \cdots, m-1$ condensates in the non-contractible loop along the x_1 direction. This operation exactly corresponds to the tunneling process $\mathcal{T}_2^k$ mentioned in section 7.2 and will cost zero energy in the thermodynamic limit. Therefore the presence of Higgs fields will not lift the m-fold ground state degeneracy in the thermodynamic limit.

We've shown that the ground state degeneracy of a Z_m FCI state is m on a torus. The above analysis for the torus case can be easily generalized to study the ground

state degeneracy on a genus-g Riemann surface. There are g pairs of non-contractible loops $\{A_a, B_a | a = 1, \cdots, g\}$ on a genus-g Riemann surface where each pair is just like the two non-contractible loops on a torus. Thus one can straightforwardly show that the ground state degeneracy of a Z_m FCI state is m^g on a genus-g Riemann surface.

7.3.2 Edge states of spin-polarized Z_m FCI states

One of the hallmark of FQH states is the presence of chiral edge modes[214, 222] localized on the boundary of the sample. The topological order in a FQH state is also encoded in its edge spectrum[223]. The edge states of an $SU(m)$ FCI state is known to be described by $U(1)^m/SU(m)$ coset theory[220, 224]. How is the edge state in a Z_m FCI different from that of an $SU(m)$ state? In this section we demonstrate that the edge excitations of spin-polarized Z_m FCIs are still described by $U(1)^m/SU(m)$ coset theory and has the same edge counting as Laughlin state. We focus on the Abelian states with filling fraction $\nu = 1/m$, m being an odd integer.

Edge excitations are collective modes of electrons that propagate on the edge of the sample. For a 2D electron gas in a magnetic field $B\hat{z}$, it can be seen as edge electrons drift[223] along the direction perpendicular to the in-plane electric field $\mathbf{E}$ with a drift velocity $v = cE/B$. Once we quantize this drift motion of electrons we obtain the effective theory of edge states, which is a 1+1-D conformal field theory with central charge $c = 1$ (for Abelian FQH liquids). For example the edge state of a filled Landau level can be represented by a chiral fermion field $\psi(z)$ whose scaling dimension is $h_\psi = 1/2$, where $z = x + \mathrm{i}t$ and x is the coordinate along the edge. Parton construction also provides a representation of the chiral edge states in $\nu = 1/m$ FCI

states. In the $SU(m)$ parton construction each parton fills one Landau level, so each has an edge mode described by a chiral fermion (actually a fermionic chiral parton) ψ_i. The question is, not all the excitations generated by these fermionic chiral partons ψ_i are real physical excitations. The physical excitations after projection (7.8) must be invariant under $SU(m)$ gauge transformations, and have to be local with respect to the electron operator[224]. In the following we will show how to construct the physical edge excitations in both an $SU(m)$ state and a Z_m state.

First note that in our $SU(m)$ construction the partons fill m lowest bands, each of which have Chern number $+1$ (in the Abelian case). As a result, there are m branches of independent chiral edge modes, each described by a free chiral fermion ψ_i. Each chiral fermion forms a representation of $U(1)$ Kac-Moody algebra (which is a conformal field theory) with the following operator product expansion (OPE)[36]

$$\psi_i^\dagger(z)\psi_i(w) = \frac{1}{z-w} + :\partial\psi_i(w)\psi_i(w): + O(z-w) \tag{7.22}$$

Here $:\hat{O}:$ denotes the normal ordering of operator $\hat{O}$. Even in the Z_m parton mean-field state, the chiral fermion modes ψ_i on the edge are related to the partons by a unitary transformation

$$\psi_i = \sum_\alpha S_i^\alpha f_\alpha \tag{7.23}$$

obtained by diagonalizing the mean-field band with boundaries. The electron operator (7.6) is invariant under any similar transformation S_i^α with unit determinant ($\det S_i^\alpha = 1$). Therefore we have

$$\Psi_e(z) =: \prod_{\alpha=1}^{m} f_\alpha(z) :=: \prod_{i=1}^{m} \psi_i(z) : \tag{7.24}$$

which is exactly the same as in an $SU(m)$ FCI state[224].

The physical edge excitations are all invariant under $SU(m)$ gauge transformations and should be generated by the electron operators[224] Ψ_e and $\Psi_e^\dagger$. As a result, we conclude that the edge excitations of a Z_m FCI is described by the same conformal field theory as the $SU(m)$ state. More precisely, the edge excitations are still described by $U(1)^m/SU(m)$ coset theory[61]. The OPE of electron operators can be worked out easily from (7.22) and (7.24)

$$\begin{aligned}\Psi_e^\dagger(z)\Psi_e(0) &= \tfrac{1}{z^m} + \tfrac{\rho(0)}{z^{m-1}} + O(z^{2-m}), \\ \Psi_e(z)\Psi_e^\dagger(0) &= \tfrac{1}{z^m} - \tfrac{\rho(0)}{z^{m-1}} + O(z^{2-m}).\end{aligned} \tag{7.25}$$

where we defined the following $SU(m)$ gauge-invariant parton density operator

$$\hat{\rho}(z) \equiv \sum_{i=1}^{m} :\psi_i^\dagger(z)\psi_i(z): = \sum_\alpha f_\alpha^\dagger(z) f_\alpha(z) \tag{7.26}$$

The higher-order terms in OPE (7.25) are all descendants of either the electron operators $\{\Psi_e, \Psi_e^\dagger\}$ or the density operator $\hat{\rho}$. For example the next term in OPE (7.25) is $z^{2-m}\hat{O}_2(0)$ where $\hat{O}_2 = \sum_i :\partial\psi_i^\dagger\psi_i: + :\hat{\rho}^2:$. In other words, the electron operators and density operators create the whole Hilbert space while higher-order terms from the OPE don't bring in any new physical states.

One can verify that the electron operators and density operators form a closed algebra and the OPEs between them don't further create new operators:

$$\begin{aligned}\hat{\rho}(z)\Psi_e^\dagger(0) &= \tfrac{\Psi_e^\dagger(0)}{z} + O(z), \\ \hat{\rho}(z)\Psi_e(0) &= -\tfrac{\Psi_e(0)}{z} + O(z), \\ \hat{\rho}(z)\hat{\rho}(0) &= \tfrac{1}{z^2} + O(1).\end{aligned}$$

In the following we show how to construct the edge state with momentum k. All the edge "phonon" modes in spin-polarized Z_m FCI states are generated by density operator (7.26):

$$k = 0: \quad |GS\rangle,$$

$$k = 1: \quad \hat{\rho}_{k=1}|GS\rangle,$$

$$k = 2: \quad \hat{\rho}_{k=1}\hat{\rho}_{k=1}|GS\rangle, \quad \hat{\rho}_{k=2}|GS\rangle,$$

$$k = 3: \quad \hat{\rho}_{k=1}\hat{\rho}_{k=1}\hat{\rho}_{k=1}|GS\rangle, \quad \hat{\rho}_{k=1}\hat{\rho}_{k=2}|GS\rangle, \hat{\rho}_{k=3}|GS\rangle,$$

$$\cdots\cdots\cdots$$

where $|GS\rangle$ represents the mean-field ground state. The physical electron state are again obtained by projection (7.8) on mean-field states. We can see such construction gives us the $\{1, 1, 2, 3, 5, \cdots\}$ counting of edge states with increasing momentum (or angular momentum) along the edge, the same as in Laughlin's state.

7.4 Parton construction of time-reversal-invariant FTI states

7.4.1 $SU(m)^{\uparrow} \times SU(m)^{\downarrow}$ parton construction of TRI FTI states

In our previous construction of Z_m FCI states, we focused on spin-polarized FCI states. Taking into account spin degrees of freedom, nearly flat bands with time-reversal-invariant (TRI) $\mathbb{Z}_2$ index[202] can exist. When a pair of bands carrying $\mathbb{Z}_2$ index are partially filled, can a fractionalized topological phase preserving both time reversal and lattice symmetries be realized? In principle the answer is yes. As a direct

generalization of spin-polarized $SU(m)$ and Z_m FCI states, when the pair of nearly flat $\mathbb{Z}_2$ bands are filled partially with $\nu = 2/m$, by $SU(m)^{\uparrow} \times SU(m)^{\downarrow}$ parton approach we can construct a TRI fractionalized phase which we term as $SU(m)^{\uparrow} \times SU(m)^{\downarrow}$ and $Z_m^{\uparrow} \times Z_m^{\downarrow}$ FTIs. In a simple way, the $SU(m)^{\uparrow} \times SU(m)^{\downarrow}$ ($Z_m^{\uparrow} \times Z_m^{\downarrow}$) FTI with $\nu = 2/m$ is a direct product of a spin-polarized $SU(m)$ (Z_m) FCI state with $\sigma_{xy} = e^2/(mh)$ for spin $\uparrow$ and its time-reversal counterpart: a spin-polarized $SU(m)$ (Z_m) FCI state with $\sigma_{xy} = -e^2/(mh)$ for spin $\downarrow$. In a TRI $SU(m)^{\uparrow} \times SU(m)^{\downarrow}$ ($Z_m^{\uparrow} \times Z_m^{\downarrow}$) FTI there are no mixing terms $f^{\dagger}_{\alpha,\uparrow} f_{\beta,\downarrow}$ between partons with different spins and thus the total spin is a conserved quantity. As in the case of spin-polarized $SU(m)$ and Z_m FCI states, we still use the technique of enlarging the unit cell by m times, to guarantee that the ground state with the correct filling fraction is an insulator with a band gap. As a fully gapped topological phase, this phase is stable at least when the electronic mixing between spin $\uparrow$ and spin $\downarrow$ is weak.

The mean-field ansatz of a generic spin-conserved FTI is written as

$$\begin{gathered} H_0^{MF} = \textstyle\sum_{\mathbf{r},\mathbf{r}'} \sum_{\sigma,\sigma'} f^{\dagger}_{\alpha,\sigma}(\mathbf{r}) \tilde{M}_{\alpha,\beta}(\mathbf{r},\sigma|\mathbf{r}',\sigma') f_{\beta,\sigma'}(\mathbf{r}'), \\ \tilde{M}_{\alpha,\beta}(\mathbf{r},\sigma|\mathbf{r}',\sigma') = \\ \delta_{\sigma,\sigma'} \Big[M_{\alpha,\beta}(\mathbf{r}|\mathbf{r}') \delta_{\sigma,\uparrow} + M^{*}_{\alpha,\beta}(\mathbf{r}|\mathbf{r}') \delta_{\sigma,\downarrow} \Big] \end{gathered} \tag{7.27}$$

where $\sigma, \sigma' = \uparrow, \downarrow$ are the spin indices. $M_{\alpha,\beta}(\mathbf{r}|\mathbf{r}')$ can be any mean-field ansatz of a $SU(m)$ (or Z_m) FCI state constructed in section 7.2 and demonstrated in section **??**, and the corresponding FTI state is a $SU(m)^{\uparrow} \times SU(m)^{\downarrow}$ ($Z_m^{\uparrow} \times Z_m^{\downarrow}$) FTI. Apparently (7.27) is invariant under time-reversal symmetry while preserving all the lattice symmetry.

Again the N-electron wavefunction (with $N/2$ electrons for each spin here in the

S^z-conserved case) is obtained by projection on mean-field state $|MF\rangle = |MF_\uparrow\rangle \otimes |MF_\downarrow\rangle$

$$\Phi_e(\{\mathbf{r}_i^\uparrow\};\{\mathbf{r}_j^\downarrow\}) = \langle 0| \prod_{i=1}^{N/2} c_\uparrow(\mathbf{r}_i^\uparrow) \prod_{j=1}^{N/2} c_\downarrow(\mathbf{r}_j^\downarrow)|MF\rangle, \tag{7.28}$$

which is simply a product of two Slater determinants (7.10) for spin up and down partons. Since in the $SU(m)^\uparrow \times SU(m)^\downarrow$ ($Z_m^\uparrow \times Z_m^\downarrow$) FTI the spin-$\uparrow$ and spin-$\downarrow$ parts are essentially decoupled, it is nothing but a direct product of two spin-polarized $SU(m)$ (Z_m) FCI states which are the time-reversal conjugates of each other. Following our discussion in section 7.3, the ground state degeneracy of this $SU(m)^\uparrow \times SU(m)^\downarrow$ ($Z_m^\uparrow \times Z_m^\downarrow$) FTI is m^2 on a torus and there are quasiparticle excitations (with both spin) with electric charge $\pm e/m$.

The $SU(m)^\uparrow \times SU(m)^\downarrow$ (or $Z_m^\uparrow \times Z_m^\downarrow$) FTI wavefunctions constructed above explicitly conserve the both the $\uparrow$ and $\downarrow$ electrons. However, in a spin-orbit coupled system where the S_z conservation is not a symmetry, the true ground state wavefunction must involve mixings between the two spin species. Of course it is possible that this true ground state is in the same universality class as those spin-conserved FTI states, because they are gapped stable topological phases. Nevertheless it is still interesting to explicitly write down a FTI state without spin-conservation.

There is a natural question that needs to be answered in the current formalism: when spin mixing terms $f_{\alpha,\uparrow}^\dagger f_{\beta,\downarrow}$ are present in the parton mean-field Hamiltonian Eq.7.27, is the corresponding electronic state Eq.7.28 a TRI FTI without spin conservation? The answer is negative. Below we study the properties of this state in details.

The mean-field Hamiltonian including spin mixings between partons is

$$H^{MF} = H_0^{MF} + \sum_{\alpha\beta} \left[f^\dagger_{\alpha,\uparrow}(\mathbf{r}) \tilde{M}_{\alpha,\beta}(\mathbf{r},\uparrow|\mathbf{r}',\downarrow) f_{\beta,\downarrow}(\mathbf{r}') + h.c. \right] \tag{7.29}$$

Note that upon mixing partons with different spins, *e.g.* for a $Z_m^\uparrow \times Z_m^\downarrow$ FTI the internal gauge symmetry is further broken from $Z_m^\uparrow \times Z_m^\downarrow$ (one $Z_m^\uparrow$ for spin-$\uparrow$ parton and another independent $Z_m^\downarrow$ for spin-$\downarrow$ parton)

$$f_{\alpha,\sigma}(\mathbf{r}) \to e^{\mathrm{i}\frac{2\pi a_\sigma}{m}} f_{\alpha,\sigma}(\mathbf{r}), \quad a_\uparrow, a_\downarrow = 1, 2, \cdots, m. \tag{7.30}$$

to a single Z_m symmetry (for partons with both spin $\uparrow$ and $\downarrow$)[3]:

$$f_{\alpha,\sigma}(\mathbf{r}) \to e^{\mathrm{i}\frac{2\pi a}{m}} f_{\alpha,\sigma}(\mathbf{r}), \quad a = 1, 2, \cdots, m. \tag{7.31}$$

In this paper, we define the FTI phase as the phase of matter which is in the same universality class as the direct product of two FCI states of opposite spins while preserving the time-reversal symmetry. Following this definition, the Z_m state defined in Eq.7.29 with spin mixings is *not* a FTI state.

One clear difference between the Z_m state Eq.7.29 and the $Z_m^\uparrow \times Z_m^\downarrow$ FTI state is their quasiparticle statistics. In a $Z_m^\uparrow \times Z_m^\downarrow$ FTI state, the $Z_m^\uparrow$ fluxes and the $Z_m^\downarrow$ fluxes bind with parton charges due to the Chern numbers of the parton bands, and are anyons with statistical angles $\theta = \pm\frac{\pi}{m}$. But in a Z_m state Eq.7.29, the Z_m fluxes do not bind with parton charges, and are bosons. This indicates that the Z_m state

[3]For a $SU(m)^\uparrow \times SU(m)^\downarrow$ FTI, the internal gauge symmetry is further broken down to an overall $SU(m)$ by mixing of partons with different spins but the same flavor. The unbroken $SU(m)$ gauge field does not have a Chern-Simons term. Consequently, this state suffers from the well-known confinement problem of the dynamical $SU(m)$ gauge field and does not have a stable mean-field description. We therefore do not discuss this state in this paper.

Eq.7.29, which is described by a regular Z_m lattice gauge dynamics with bosonic flux excitations, must separate from the $Z_m^\uparrow \times Z_m^\downarrow$ FTI state by a phase transition.

Another observation that we have is that, in the $SU(m)^\uparrow \times SU(m)^\downarrow$ parton construction, the Z_m state Eq.7.29 cannot preserves both time-reversal symmetry and lattice translation symmetry simultaneously. Essentially the technique of enlarging unit cell m times by inserting fluxes fails to generate a translation symmetric wavefunction when partons with opposite spins are mixed. In a TRI $Z_m^\uparrow \times Z_m^\downarrow$ FTI state, when $2\pi/m$ fluxes are inserted in each unit cell for spin $\uparrow$ partons, an opposite $-2\pi/m$ fluxes are inserted in each unit cell for spin $\downarrow$ parton to preserve the time-reversal symmetry. After the partons with opposite spins are mixed, the gauge flux pattern of the partons no longer enjoys well-defined $\pm 2\pi/m$ value per plaquette. As a result physical translation symmetry is broken. This simple argument dictates that, *using $SU(m)^\uparrow \times SU(m)^\downarrow$ parton construction, when partons with opposite spins are mixed, either time reversal symmetry or lattice translation symmetry must be broken to form a gapped state with filling fraction $2/m$ ($\nu = 1/m$ for each spin on average).* In Ref. [127] we prove this statement by a careful PSG analysis.

The analysis in this subsection seems to suggest that it is difficult to explicitly construct a FTI wavefunctions breaking the S_z conservation. In fact, this difficulty is due to the formalism of $SU(m)^\uparrow \times SU(m)^\downarrow$ parton construction. In the next subsection, we propose another parton construction formalism which allows us to explicitly write down FTI wavefunctions with spin mixings.

7.4.2 Parton construction of generic TRI FTI states in the absence of spin conservation

In the following we demonstrate that in a new parton construction formalism, one can write down the electron wavefunctions for fully symmetric TRI FTI states breaking the S_z conservation, and with mean-field terms mixing partons with different spins. We introduce the following parton construction (m being an odd integer and θ is an arbitrary real number)

$$\begin{aligned} c_\uparrow(\mathbf{r}) &= \cos\theta \prod_{\alpha=1}^{m} f_{\alpha,\uparrow}(\mathbf{r}) + \sin\theta \prod_{\beta=1}^{m} g_{\beta,\uparrow}(\mathbf{r}), \\ c_\downarrow(\mathbf{r}) &= -\sin\theta \prod_{\alpha=1}^{m} f_{\alpha,\downarrow}(\mathbf{r}) + \cos\theta \prod_{\beta=1}^{m} g_{\beta,\downarrow}(\mathbf{r}). \end{aligned} \tag{7.32}$$

where $f_{\alpha,\sigma}$ and $g_{\beta,\sigma}$ are all fermionic partons each of which carries electric charge e/m. It's straightforward to see that the electron constructed in this way is indeed a fermion with electric charge e. The N-electron wavefunction at filling fraction $\nu = 2/m$ (with $N_\uparrow$ spin-$\uparrow$ electrons and $N_\downarrow = N - N_\uparrow$ spin-$\downarrow$ electrons) is obtained by projection

$$\Phi_e(\{\mathbf{r}_i^\uparrow\};\{\mathbf{r}_j^\downarrow\}) = \langle 0| \prod_{i=1}^{N_\uparrow} c_\sigma(\mathbf{r}_i^\uparrow) \prod_{j=1}^{N-N_\uparrow} c_\sigma(\mathbf{r}_j^\downarrow) |MF\rangle \tag{7.33}$$

where $|MF\rangle$ is the parton mean-field ground state as will be described later. $N_\uparrow$ can be any integer between 0 and total electron number N.

The mean-field ansatz can be written as

$$\begin{aligned} H^{MF} = &\sum_{\alpha,\alpha'=1}^{m} \sum_{\sigma,\sigma'=\uparrow,\downarrow} \sum_{\mathbf{r},\mathbf{r}'} \\ &\Big(f_{\alpha,\sigma}^\dagger(\mathbf{r}) M_{\alpha,\alpha'}(\mathbf{r},\sigma|\mathbf{r}',\sigma') f_{\alpha',\sigma'}(\mathbf{r}') \\ &+ g_{\alpha,\sigma}^\dagger(\mathbf{r}) M'_{\alpha,\alpha'}(\mathbf{r},\sigma|\mathbf{r}',\sigma') g_{\alpha',\sigma'}(\mathbf{r}') \Big) \end{aligned} \tag{7.34}$$

where Hamiltonian $M'_{\alpha,\alpha'}(\mathbf{r},\sigma|\mathbf{r}',\sigma')$ is the time reversal conjugate of $M_{\alpha,\alpha'}(\mathbf{r},\sigma|\mathbf{r}',\sigma')$:

$$M'_{\alpha,\alpha'}(\mathbf{r},\sigma|\mathbf{r}',\sigma') = \sigma\sigma' M^*_{\alpha,\alpha'}(\mathbf{r},-\sigma|\mathbf{r}',-\sigma') \tag{7.35}$$

We use spin index $\sigma = \pm 1$ to denote spin $\uparrow,\downarrow$. In the simplest case when $M_{\alpha,\alpha'}(\mathbf{r},\sigma|\mathbf{r}',\sigma') = \delta_{\alpha,\alpha'} M(\mathbf{r},\sigma|\mathbf{r}',\sigma')$, the mean-field ansatz has $SU(m)$ gauge symmetry or in other words $IGG = SU(m)$. As discussed earlier in section 7.2, in a generic case parton mixing terms $f^\dagger_{\alpha,\sigma} f_{\beta,\sigma'}, \alpha \neq \beta$ could exist and the IGG of the parton mean-field Hamiltonian $M_{\alpha,\alpha'}(\mathbf{r},\sigma|\mathbf{r}',\sigma')$ could be Z_m, which is the center of group $SU(m)$. Here $M_{\alpha,\alpha'}(\mathbf{r},\sigma|\mathbf{r}',\sigma')$ can be any mean-field ansatz as a solution of the PSG constraints on the lattice, so that the N-electron wavefunction obtained by projection (7.33) preserves all the lattice symmetries. More precisely, mean-field Hamiltonian $M_{\alpha,\alpha'}(\mathbf{r},\sigma|\mathbf{r}',\sigma')$ should be invariant under a symmetry operation U followed by a $SU(m)$ gauge rotation $G_U(\mathbf{r},\sigma)$ on f-partons. For example the lattice symmetry group are shown in Ref. [127] for honeycomb lattice and for checkerboard lattice for spin $\uparrow$ / $\downarrow$. The constraints for $G_U(\mathbf{r},\sigma)$ will still be those in Ref. [127] in the case when $IGG = Z_m$. Namely $G_U(\mathbf{r},\uparrow)$ and $G_U(\mathbf{r},\downarrow)$ can be any two solutions of PSG constraints. The symmetry-allowed mean-field Hamiltonian $M_{\alpha,\alpha'}(\mathbf{r},\sigma|\mathbf{r}',\sigma')$ can be obtained in the same way shown in Ref. [127]. It's easy to check that spin-mixing terms in mean-field Hamiltonian $M_{\alpha,\alpha'}(\mathbf{r},\sigma|\mathbf{r}',\sigma')$ is in general allowed by these PSG constraints.

Meanwhile time reversal symmetry is also preserved since the anti-unitary time reversal operation $\boldsymbol{T}$ is realized by complex conjugation $\mathcal{C}$ combined with the following operation

$$f_{\alpha,\sigma}(\mathbf{r}) \leftrightarrow \sigma g_{\alpha,-\sigma}(\mathbf{r}) \tag{7.36}$$

where spin index $\sigma = \pm 1$ denotes spin $\uparrow$ / $\downarrow$. One can easily check that under time reversal $\boldsymbol{T}$ the spin-1/2 electron operators indeed transform as $c_\sigma(\mathbf{r}) \to \sigma c_{-\sigma}(\mathbf{r})$. Apparently the above time reversal operation $\boldsymbol{T}$ leaves the mean-field ansatz (7.34) invariant. At filling $\nu = 2/m$ ($1/m$ filling for each spin *on average*) we still use the technique of inserting flux to enlarge the unit cell by m times. Notice that when $2\pi/m$ flux is inserted into each unit cell for f-partons, an opposite $-2\pi/m$ flux must be inserted in each unit cell for g-partons to keep the time reversal symmetry. Then we fill the lowest m bands for both f-partons and g-partons. Each filled band contains $N/2$ f-partons (or g-partons) which correspond to a filling fraction of $1/m$. It's straightforward to see the electron filling fraction of state (7.33) is indeed $\nu = 2/m$. There can be symmetry-allowed mixing terms between partons with different spins in ansatz $M_{\alpha,\alpha'}(\mathbf{r}, \sigma|\mathbf{r}', \sigma')$. The mean-field ground state in (7.33) is a direct product of f-parton state and g-parton state: $|MF\rangle = |MF^f\rangle \otimes |MF^g\rangle$.

Notice there is a real parameter $\theta \in [0, \pi/4]$ which can be continuously tuned in our parton construction (7.32). This parameter controls the many-body entanglement between spin-$\uparrow$ and spin-$\downarrow$ electrons in wavefunction (7.33). It should be considered as a variational parameter in variational Monte Carlo studies of projected wavefunctions. When $\theta = 0$ clearly there must be equal number of spin-$\uparrow$ and spin-$\downarrow$ electrons: $N_\uparrow = N_\downarrow = N/2$ since other components of the many-body wavefunction with $N_\uparrow \neq N_\downarrow$ all vanish in (7.33). In this case the electron wavefunction (7.33) is nothing but a direct product of spin-$\uparrow$ wavefunction $\Phi_\uparrow(\mathbf{r}_i^\uparrow) = \langle 0| \prod_{i=1}^{N/2} \prod_{\alpha=1}^{m} f_{\alpha,\uparrow}(\mathbf{r}_i^\uparrow)|MF^f\rangle$ and spin-$\downarrow$ wavefunction $\Phi_\downarrow(\mathbf{r}_j^\downarrow) = \langle 0| \prod_{j=1}^{N/2} \prod_{\alpha=1}^{m} g_{\alpha,\downarrow}(\mathbf{r}_j^\downarrow)|MF^g\rangle$. This corresponds to the spin-conserved limit when there is no entanglement between electrons with different

spins. If the filled lowest m bands of f-partons have a nonzero total Chern number, there will be chiral edge modes for spin-$\uparrow$ electrons and its time reversal counterpart for spin-$\downarrow$ electrons. When θ is nonzero, many-body entanglement between electrons with different spins is encoded in electron wavefunction (7.33) as long as there are spin mixing terms in mean-field Hamiltonian (7.34). And in general the many-body wavefunction components with an arbitrary number of spin-$\uparrow$ electrons $\forall\ 0 \leq N_\uparrow \leq N$ should be nonzero. In a generic case with $\theta \neq 0$ the many-body wavefunction (7.33) is very complicated and cannot be written as a Slater determinant. Now one can see the parton construction (7.32) allows us to write down generic electron wavefunctions for TRI FTI states in the absence of spin conservation. The spin-conserved TRI FTI wavefunction ($\theta = 0$) can be deformed into a generic TRI FTI state in the absence of spin conservation ($\theta \neq 0$) by continuously tuning parameter θ, while keeping the mean-field Hamiltonian (7.34) unchanged. In the process of tuning θ continuously, we expect the low-energy effective theory and quasiparticles of such a TRI FTI state to remain the same.

In the end we comment on the low-energy effective theory of such a TRI FTI state. In the simplest case when $M_{\alpha,\alpha'}(\mathbf{r},\sigma|\mathbf{r}',\sigma') = \delta_{\alpha,\alpha'}M(\mathbf{r},\sigma|\mathbf{r}',\sigma')$, the mean-field ansatz (7.34) has a $SU(m) \times SU(m)$ gauge symmetry or in other words $IGG = SU(m)^f \times SU(m)^g$. Let's assume the filled lowest band of $M(\mathbf{r},\sigma|\mathbf{r}',\sigma')$ for $\{f_{\alpha,\uparrow/\downarrow}|\alpha = 1,\cdots,m\}$ partons has a Chern number k. Then due to time reversal symmetry the filled lowest band for $\{g_{\alpha,\uparrow/\downarrow}|\alpha = 1,\cdots,m\}$ partons will have a Chern number $-k$. And its low-

energy effective theory is a $SU(m)_k \times SU(m)_{-k}$ Chern-Simons theory:

$$\begin{aligned}\mathcal{L}_{eff} = &\tfrac{k}{4\pi}\epsilon_{\mu\nu\lambda}\mathrm{Tr}\big(a_\mu\partial_\nu a_\lambda + \tfrac{\mathrm{i}}{3}a_\mu a_\nu a_\lambda\big)\\ &-\tfrac{k}{4\pi}\epsilon_{\mu\nu\lambda}\mathrm{Tr}\big(b_\mu\partial_\nu b_\lambda + \tfrac{\mathrm{i}}{3}b_\mu b_\nu b_\lambda\big)\end{aligned} \tag{7.37}$$

where a_μ is the $SU(m)$ gauge field coupled to f-partons and b_μ is the $SU(m)$ gauge field coupled to g-partons. Such a $SU(m)^f \times SU(m)^g$ TRI FTI state will host non-Abelian quasiparticles if $k > 1$.

When $k = 1$ this is an Abelian TRI FTI state with ground state degeneracy m^2 on a torus and anyonic quasiparticles. When parton mixing terms $f^\dagger_{\alpha,\sigma} f_{\beta,\sigma'},\ \alpha \neq \beta$ are present, again the IGG is reduced from $SU(m)^f \times SU(m)^g$ to ${Z_m}^f \times {Z_m}^g$ and the low-energy effective theory is described by Chern-Simons-Higgs theory, *i.e.* effective action (7.37) with a periodic potential due to Bose condensation of Higgs fields. Such an Abelian ${Z_m}^f \times {Z_m}^g$ TRI FTI has the same topological properties as an Abelian $SU(m)^f \times SU(m)^g$ FTI, such as ground state degeneracy and quasiparticle charge/statistics. In the parton construction (7.32), both $SU(m)^f \times SU(m)^g$ and ${Z_m}^f \times {Z_m}^g$ TRI FTI states are possible candidates for a symmetric TRI FTI state in the absence of spin conservation: which state is realized depends on the IGG of mean-field amplitudes $M_{\alpha,\alpha'}(\mathbf{r},\sigma|\mathbf{r}',\sigma')$ and should be determined by energetics of wavefunctions (7.33) in variational studies.

7.5 Conclusion

To summarize, we show that a large class of Abelian (and non-Abelian) fractionalized topological phases can be constructed on a lattice using parton construction.

These states preserve all the lattice symmetry and are featured by *e.g.* fractionalized excitations and topological ground state degeneracy. In the spin-polarized case when the time reversal symmetry is broken, we construct two classes of wavefunctions, $SU(m)$ states and Z_m states, with filling $\nu = 1/m$. Their low-energy physics is described by $SU(m)_1$ Chern-Simons theory and $SU(m)$ Chern-Simons-Higgs theory respectively, and they both have m-fold degenerate ground states on a torus. We explicitly construct the ground state wavefunctions, bulk quasiparticles and edge excitations on the lattice. We demonstrate our construction by several explicit examples, including non-Abelian FCIs which may be realized in a nearly flat band with Chern number $C > 1$. Furthermore, we show that when time reversal symmetry is present, classes of fractionalized phases preserving both time reversal symmetry and lattice symmetries can be constructed. These TRI FTI states are characterized by $SU(m) \times SU(m)$ or $Z_m \times Z_m$ gauge groups. Their electron wavefunctions on the lattice, which are essentially products of spin-polarized FCI states for spin $\uparrow$ and its time reversal conjugate, are provided. These are stable topological phases even when S_z conservation is not a symmetry in the electronic system. In order to explicitly construct TRI FTI wavefunctions with entanglement between opposite spins, we propose a new parton construction formalism. It allows one to write down generic electron wavefunctions of TRI FTI states, which preserve both time reversal and lattice symmetries in the absence of spin conservation. Our work provides important insight for future numeric study using variational Monte Carlo method.

Bibliography

[1] A. G. Abanov and P. B. Wiegmann. Theta-terms in nonlinear sigma-models. *Nuclear Physics B*, 570(3):685 – 698, 2000.

[2] Ian Affleck and J. Brad Marston. Large-n limit of the heisenberg-hubbard model: Implications for high-tc superconductors. *Phys. Rev. B*, 37(7):3774–, March 1988.

[3] Ian Affleck, Z. Zou, T. Hsu, and P. W. Anderson. Su(2) gauge symmetry of the large-u limit of the hubbard model. *Phys. Rev. B*, 38(1):745–, July 1988.

[4] Jason Alicea. Majorana fermions in a tunable semiconductor device. *Phys. Rev. B*, 81(12):125318–, March 2010.

[5] P. W. Anderson. Coherent excited states in the theory of superconductivity: Gauge invariance and the meissner effect. *Phys. Rev.*, 110(4):827–, May 1958.

[6] P. W. Anderson. Random-phase approximation in the theory of superconductivity. *Phys. Rev.*, 112(6):1900–, December 1958.

[7] P. W. Anderson. More is different. *Science*, 177(4047):393–396, 1972.

[8] P.W. Anderson. Resonating valence bonds: A new kind of insulator? *Materials Research Bulletin*, 8(2):153–160, February 1973.

[9] James F. Annett. Symmetry of the order parameter for high-temperature superconductivity. *Advances in Physics*, 39(2):83–126, April 1990.

[10] Thomas Appelquist and Daniel Nash. Critical behavior in (2+1)-dimensional qcd. *Phys. Rev. Lett.*, 64(7):721–, February 1990.

[11] E. Ardonne, N. Read, E. Rezayi, and K. Schoutens. Non-abelian spin-singlet quantum hall states: wave functions and quasihole state counting. *Nuclear Physics B*, 607(3):549–576, July 2001.

[12] Daniel Arovas, J. R. Schrieffer, and Frank Wilczek. Fractional statistics and the quantum hall effect. *Phys. Rev. Lett.*, 53(7):722–, August 1984.

[13] Daniel P. Arovas and Assa Auerbach. Functional integral theories of low-dimensional quantum heisenberg models. *Phys. Rev. B*, 38(1):316–, July 1988.

[14] A. Auerbach. *Interacting electrons and quantum magnetism*. Graduate Texts in Contemporary Physics. Springer, September 1994.

[15] Leon Balents. Spin liquids in frustrated magnets. *Nature*, 464(7286):199–208, March 2010.

[16] Maissam Barkeshli and Xiao-Gang Wen. Structure of quasiparticles and their fusion algebra in fractional quantum hall states. *Phys. Rev. B*, 79(19):195132–, May 2009.

[17] Maissam Barkeshli and Xiao-Gang Wen. Classification of abelian and non-abelian multilayer fractional quantum hall states through the pattern of zeros. *Phys. Rev. B*, 82(24):245301–, December 2010.

[18] G. Baskaran and P. W. Anderson. Gauge theory of high-temperature superconductors and strongly correlated fermi systems. *Phys. Rev. B*, 37(1):580–, January 1988.

[19] G. Baskaran, Z. Zou, and P. W. Anderson. The resonating valence bond state and high-tc superconductivity – a mean field theory. *Solid State Communications*, 63(11):973–976, September 1987.

[20] J. G. Bednorz and K. A. Mueller. Possible high-tc superconductivity in the ba-la-cu-o system. *Zeitschrift fur Physik B Condensed Matter*, 64(2):189–193, 1986-06-01.

[21] E. Berg, C-C. Chen, and S. A. Kivelson. Stability of nodal quasiparticles in superconductors with coexisting orders. *Phys. Rev. Lett.*, 100(2):027003–, January 2008.

[22] E. J. Bergholtz, J. Kailasvuori, E. Wikberg, T. H. Hansson, and A. Karlhede. Pfaffian quantum hall state made simple: Multiple vacua and domain walls on a thin torus. *Phys. Rev. B*, 74(8):081308–, August 2006.

[23] B. Andrei Bernevig and F. D. M. Haldane. Generalized clustering conditions of jack polynomials at negative jack parameter . *Phys. Rev. B*, 77(18):184502–, May 2008.

[24] B. Andrei Bernevig and F. D. M. Haldane. Model fractional quantum hall states and jack polynomials. *Phys. Rev. Lett.*, 100(24):246802–, June 2008.

[25] N. E. Bonesteel. Singular pair breaking in the composite fermi liquid description of the half-filled landau level. *Phys. Rev. Lett.*, 82(5):984–, February 1999.

[26] S. Cahangirov, M. Topsakal, E. Aktrk, H. ahin, and S. Ciraci. Two- and one-dimensional honeycomb structures of silicon and germanium. *Phys. Rev. Lett.*, 102(23):236804–, June 2009.

[27] Xie Chen, Z. Gu, Zheng-Xin Liu, and X. G. Wen. Symmetry protected topological orders and the cohomology class of their symmetry group. *arXiv:1106.4772v1*, 2011.

[28] Andrey V. Chubukov and Th. Jolicoeur. Order-from-disorder phenomena in heisenberg antiferromagnets on a triangular lattice. *Phys. Rev. B*, 46(17):11137–, November 1992.

[29] Andrey V. Chubukov, Subir Sachdev, and T. Senthil. Quantum phase transitions in frustrated quantum antiferromagnets. *Nuclear Physics B*, 426(3):601–643, September 1994.

[30] Andrey V. Chubukov, T. Senthil, and Subir Sachdev. Universal magnetic properties of frustrated quantum antiferromagnets in two dimensions. *Phys. Rev. Lett.*, 72(13):2089–, March 1994.

[31] O. Ciftja. Monte carlo study of bose laughlin wave function for filling factors 1/2, 1/4 and 1/6. *EPL (Europhysics Letters)*, 74(3):486–, 2006.

[32] Piers Coleman. Many body physics: Unfinished revolution. *Annales Henri Poincare*, 4(0):559–580, 2003-12-01.

[33] N. R. Cooper and G. V. Shlyapnikov. Stable topological superfluid phase of ultracold polar fermionic molecules. *Phys. Rev. Lett.*, 103(15):155302–, October 2009.

[34] S. Das Sarma, M. Freedman, and C. Nayak. Topological quantum computation. *Physics Today*, 59:32–38, July 2006.

[35] Sankar Das Sarma, Michael Freedman, and Chetan Nayak. Topologically protected qubits from a possible non-abelian fractional quantum hall state. *Phys. Rev. Lett.*, 94(16):166802–, April 2005.

[36] Philippe Di Francesco, Pierre Mathieu, and David Senechal. *Conformal field theory*. Graduate texts in contemporary physics. New York : Springer, 1997.

[37] Xiang-Mao Ding, Mark D. Gould, and Yao-Zhong Zhang. A(2)2 parafermions: a new conformal field theory. *Nuclear Physics B*, 636(3):549–567, August 2002.

[38] Xiang-Mao Ding, Mark D. Gould, and Yao-Zhong Zhang. Twisted parafermions. *Physics Letters B*, 530(1-4):197–201, March 2002.

[39] M. Dolev, M. Heiblum, V. Umansky, Ady Stern, and D. Mahalu. Observation of a quarter of an electron charge at the $\nu = 5/2$ quantum hall state. *Nature*, 452(7189):829–834, April 2008.

[40] Vladimir S. Dotsenko, Jesper Lykke Jacobsen, and Raoul Santachiara. Parafermionic theory with the symmetry z5. *Nuclear Physics B*, 656(3):259–324, April 2003.

[41] Vladimir S. Dotsenko, Jesper Lykke Jacobsen, and Raoul Santachiara. Parafermionic theory with the symmetry zn, for n odd. *Nuclear Physics B*, 664(3):477–511, August 2003.

[42] Vladimir S. Dotsenko, Jesper Lykke Jacobsen, and Raoul Santachiara. Conformal field theories with zn and lie algebra symmetries. *Physics Letters B*, 584(1-2):186–191, March 2004.

[43] Vladimir S. Dotsenko, Jesper Lykke Jacobsen, and Raoul Santachiara. Parafermionic theory with the symmetry zn for n even. *Nuclear Physics B*, 679(3):464–494, February 2004.

[44] Vladimir S. Dotsenko and Raoul Santachiara. The third parafermionic chiral algebra with the symmetry z3. *Physics Letters B*, 611(1-2):189–192, March 2005.

[45] L.-M. Duan, E. Demler, and M. D. Lukin. Controlling spin exchange interactions of ultracold atoms in optical lattices. *Phys. Rev. Lett.*, 91(9):090402–, August 2003.

[46] G. V. Dunne. Aspects of chern-simons theory. *arXiv:hep-th/9902115*, 1999.

[47] G. Evenbly and G. Vidal. Frustrated antiferromagnets with entanglement renormalization: Ground state of the spin-1/2 heisenberg model on a kagome lattice. *Phys. Rev. Lett.*, 104(18):187203–, May 2010.

[48] Jaime Ferrer. Spin-liquid phase for the frustrated quantum heisenberg antiferromagnet on a square lattice. *Phys. Rev. B*, 47(14):8769–, April 1993.

[49] Lukasz Fidkowski and Alexei Kitaev. Effects of interactions on the topological classification of free fermion systems. *Phys. Rev. B*, 81(13):134509–, April 2010.

[50] Lukasz Fidkowski and Alexei Kitaev. Topological phases of fermions in one dimension. *Phys. Rev. B*, 83(7):075103–, February 2011.

[51] Serge Florens and Antoine Georges. Slave-rotor mean-field theories of strongly correlated systems and the mott transitionin finite dimensions. *Phys. Rev. B*, 70(3):035114–, July 2004.

[52] Eduardo Fradkin, Chetan Nayak, Alexei Tsvelik, and Frank Wilczek. A chern-simons effective field theory for the pfaffian quantum hall state. *Nuclear Physics B*, 516(3):704–718, April 1998.

[53] Michael H. Freedman, Michael Larsen, and Zhenghan Wang. A modular functor which is universal for quantum computation. *Communications in Mathematical Physics*, 227:605–622, 2002. 10.1007/s002200200645.

[54] Jurg Frohlich, Bill Pedrini, Christoph Schweigert, and Johannes Walcher. Universality in quantum hall systems: Coset construction of incompressible states. *Journal of Statistical Physics*, 103(3):527–567, 2001-05-21.

[55] Liang Fu and C. L. Kane. Superconducting proximity effect and majorana fermions at the surface of a topological insulator. *Phys. Rev. Lett.*, 100(9):096407–, March 2008.

[56] Tatsuya Fujimoto, Guo-qing Zheng, Y. Kitaoka, R. L. Meng, J. Cmaidalka, and C. W. Chu. Unconventional superconductivity and electron correlations in the cobalt oxyhydrate $na_{0.35}coo_2{\cdot}yh_2o$ from nuclear quadrupole resonance. *Phys. Rev. Lett.*, 92(4):047004–, January 2004.

[57] Doron Gepner and Zongan Qiu. Modular invariant partition functions for parafermionic field theories. *Nuclear Physics B*, 285:423–453, 1987.

[58] P. H. Ginsparg. Applied conformal field theory. *arXiv:hepth/9108028*, 1991.

[59] S. M. Girvin and A. H. MacDonald. Off-diagonal long-range order, oblique confinement, and the fractional quantum hall effect. *Phys. Rev. Lett.*, 58(12):1252–, March 1987.

[60] J. Goldstone. Field theories with superconductor solutions. *Il Nuovo Cimento (1955-1965)*, 19(1):154–164, 1961-01-01.

[61] P. Goodard, A. Kent, and D. Olive. Virasoro algebras and coset space models. *Physics Letters B*, 152(1-2):88–92, February 1985.

[62] Martin Greiter, X. G. Wen, and Frank Wilczek. Paired hall states. *Nuclear Physics B*, 374(3):567–614, May 1992.

[63] C. Gros, R. Joynt, and T. M. Rice. Antiferromagnetic correlations in almost-localized fermi liquids. *Phys. Rev. B*, 36(1):381–, July 1987.

[64] David J. Gross and Frank Wilczek. Ultraviolet behavior of non-abelian gauge theories. *Phys. Rev. Lett.*, 30(26):1343–, June 1973.

[65] Tarun Grover and T. Senthil. Topological spin hall states, charged skyrmions, and superconductivity in two dimensions. *Phys. Rev. Lett.*, 100(15):156804–, April 2008.

[66] V. Gurarie, L. Radzihovsky, and A. V. Andreev. Quantum phase transitions across a p-wave feshbach resonance. *Phys. Rev. Lett.*, 94(23):230403–, June 2005.

[67] F. D. M. Haldane. Fractional quantization of the hall effect: A hierarchy of incompressible quantum fluid states. *Phys. Rev. Lett.*, 51(7):605–, August 1983.

[68] F. D. M. Haldane. Model for a quantum hall effect without landau levels: Condensed-matter realization of the "parity anomaly". *Phys. Rev. Lett.*, 61(18):2015–, October 1988.

[69] F. D. M. Haldane and E. H. Rezayi. Finite-size studies of the incompressible state of the fractionally quantized hall effect and its excitations. *Phys. Rev. Lett.*, 54(3):237–, January 1985.

[70] F. D. M. Haldane and E. H. Rezayi. Periodic laughlin-jastrow wave functions for the fractional quantized hall effect. *Phys. Rev. B*, 31(4):2529–, February 1985.

[71] B. I. Halperin. Quantized hall conductance, current-carrying edge states, and the existence of extended states in a two-dimensional disordered potential. *Phys. Rev. B*, 25(4):2185–, February 1982.

[72] B. I. Halperin. Theory of quantized hall conductance. *Helv. Phys. Acta*, 56:75–102, 1983.

[73] B. I. Halperin. Statistics of quasiparticles and the hierarchy of fractional quantized hall states. *Phys. Rev. Lett.*, 52(18):1583–, April 1984.

[74] B. I. Halperin, Patrick A. Lee, and Nicholas Read. Theory of the half-filled landau level. *Phys. Rev. B*, 47(12):7312–, March 1993.

[75] T. H. Hansson, Vadim Oganesyan, and S. L. Sondhi. Superconductors are topologically ordered. *Annals of Physics*, 313(2):497–538, October 2004.

[76] M. Z. Hasan and C. L. Kane. Colloquium: Topological insulators. *Rev. Mod. Phys.*, 82(4):3045–, November 2010.

[77] M. B. Hastings. Dirac structure, rvb, and goldstone modes in the kagomé antiferromagnet. *Phys. Rev. B*, 63(1):014413–, December 2000.

[78] Yasuhiro Hatsugai. Chern number and edge states in the integer quantum hall effect. *Phys. Rev. Lett.*, 71(22):3697–, November 1993.

[79] J. S. Helton, K. Matan, M. P. Shores, E. A. Nytko, B. M. Bartlett, Y. Qiu, D. G. Nocera, and Y. S. Lee. Dynamic scaling in the susceptibility of the spin-1/2 kagome lattice antiferromagnet herbertsmithite. *Phys. Rev. Lett.*, 104(14):147201–, April 2010.

[80] J. S. Helton, K. Matan, M. P. Shores, E. A. Nytko, B. M. Bartlett, Y. Yoshida, Y. Takano, A. Suslov, Y. Qiu, J.-H. Chung, D. G. Nocera, and Y. S. Lee. Spin dynamics of the spin-1/2 kagome lattice antiferromagnet zncu$_3$(oh)$_6$cl$_2$. *Phys. Rev. Lett.*, 98(10):107204–, March 2007.

[81] Christopher L. Henley. Ordering due to disorder in a frustrated vector antiferromagnet. *Phys. Rev. Lett.*, 62(17):2056–, April 1989.

[82] Michael Hermele. Su(2) gauge theory of the hubbard model and application to the honeycomb lattice. *Phys. Rev. B*, 76(3):035125, Jul 2007.

[83] Michael Hermele, Ying Ran, Patrick A. Lee, and Xiao-Gang Wen. Properties of an algebraic spin liquid on the kagome lattice. *Phys. Rev. B*, 77(22):224413–, June 2008.

[84] Tin-Lun Ho. Broken symmetry of two-component nu = 1/2 quantum hall states. *Phys. Rev. Lett.*, 75(6):1186–, August 1995.

[85] P. C. Hohenberg. Existence of long-range order in one and two dimensions. *Phys. Rev.*, 158(2):383–, June 1967.

[86] Kerson Huang. *Statistical Mechanics*. Wiley, 2nd edition edition, May 1987.

[87] Masatoshi Imada, Atsushi Fujimori, and Yoshinori Tokura. Metal-insulator transitions. *Rev. Mod. Phys.*, 70(4):1039–, October 1998.

[88] T. Imai, E. A. Nytko, B. M. Bartlett, M. P. Shores, and D. G. Nocera. ^{63}cu,^{35}cl, and ^{1}h nmr in the $s = 1/2$ kagome lattice zncu$_3$(oh)$_6$cl$_2$. *Phys. Rev. Lett.*, 100(7):077203–, February 2008.

[89] S. V. Isakov, T. Senthil, and Yong Baek Kim. Ordering in cs2 cu cl4 : Possibility of a proximate spin liquid. *Phys. Rev. B*, 72(17):174417–, November 2005.

[90] T. Itou, A. Oyamada, S. Maegawa, M. Tamura, and R. Kato. Quantum spin liquid in the spin-1/2 triangular antiferromagnet $etme_3sb[pd(dmit)_2]_2$. *Phys. Rev. B*, 77(10):104413–, March 2008.

[91] D. A. Ivanov. Non-abelian statistics of half-quantum vortices in p-wave superconductors. *Phys. Rev. Lett.*, 86(2):268–, January 2001.

[92] P. Jacob and P. Mathieu. Graded parafermions: standard and quasiparticle bases. *Nuclear Physics B*, 630(3):433–452, May 2002.

[93] P. Jacob and P. Mathieu. The parafermions. *Physics Letters B*, 627(1-4):224–232, October 2005.

[94] J. K. Jain. Composite-fermion approach for the fractional quantum hall effect. *Phys. Rev. Lett.*, 63(2):199–, July 1989.

[95] J. K. Jain. Incompressible quantum hall states. *Phys. Rev. B*, 40(11):8079–, October 1989.

[96] J. K. Jain. Theory of the fractional quantum hall effect. *Phys. Rev. B*, 41(11):7653–, April 1990.

[97] H. C. Jiang, Z. Y. Weng, and D. N. Sheng. Density matrix renormalization group numerical study of the kagome antiferromagnet. *Phys. Rev. Lett.*, 101(11):117203–, September 2008.

[98] Th. Jolicoeur, E. Dagotto, E. Gagliano, and S. Bacci. Ground-state properties of the s=1/2 heisenberg antiferromagnet on a triangular lattice. *Phys. Rev. B*, 42(7):4800–, September 1990.

[99] Robert Jordens, Niels Strohmaier, Kenneth Gunter, Henning Moritz, and Tilman Esslinger. A mott insulator of fermionic atoms in an optical lattice. *Nature*, 455(7210):204–207, September 2008.

[100] Shigetoshi Katsura, Tsugio Ide, and Tohru Morita. The ground states of the classical heisenberg and planar models on the triangular and plane hexagonal lattices. *Journal of Statistical Physics*, 42:381–404, 1986. 10.1007/BF01127717.

[101] A. Yu. Kitaev. Fault-tolerant quantum computation by anyons. *Annals of Physics*, 303(1):2–30, January 2003.

[102] Alexei Kitaev. Anyons in an exactly solved model and beyond. *Annals of Physics*, 321(1):2–111, January 2006.

[103] Alexei Kitaev. Periodic table for topological insulators and superconductors. *AIP Conf. Proc.*, 1134(1):22–30, May 2009.

[104] Alexei Kitaev and John Preskill. Topological entanglement entropy. *Phys. Rev. Lett.*, 96(11):110404–, March 2006.

[105] K. v. Klitzing, G. Dorda, and M. Pepper. New method for high-accuracy determination of the fine-structure constant based on quantized hall resistance. *Phys. Rev. Lett.*, 45(6):494–, August 1980.

[106] John B. Kogut. An introduction to lattice gauge theory and spin systems. *Rev. Mod. Phys.*, 51(4):659–, October 1979.

[107] Markus Konig, Steffen Wiedmann, Christoph Brune, Andreas Roth, Hartmut Buhmann, Laurens W. Molenkamp, Xiao-Liang Qi, and Shou-Cheng Zhang. Quantum spin hall insulator state in hgte quantum wells. *Science*, 318(5851):766–770, 2007.

[108] Gabriel Kotliar and Jialin Liu. Superexchange mechanism and d-wave superconductivity. *Phys. Rev. B*, 38(7):5142–, September 1988.

[109] Su-Peng Kou, Michael Levin, and Xiao-Gang Wen. Mutual chern-simons theory for z_2 topological order. *Phys. Rev. B*, 78(15):155134–, October 2008.

[110] L. D. Landau. Theory of phase transformations. i. *Phys. Z. Sowjetunion*, 11:26, 1937.

[111] L. D. Landau. Theory of phase transformations. ii. *Phys. Z. Sowjetunion*, 11:545, 1937.

[112] L. D. Landau and L. P. Pitaevskii. *Statistical Physics, Part 2*, volume 9 of *Course of Theoretical Physics*. Butterworth-Heinemann, 1980.

[113] R. B. Laughlin. Quantized hall conductivity in two dimensions. *Phys. Rev. B*, 23(10):5632–, May 1981.

[114] R. B. Laughlin. Anomalous quantum hall effect: An incompressible quantum fluid with fractionally charged excitations. *Phys. Rev. Lett.*, 50(18):1395–, May 1983.

[115] Patrick A. Lee. An end to the drought of quantum spin liquids. *Science*, 321(5894):1306–1307, 2008.

[116] Patrick A Lee. From high temperature superconductivity to quantum spin liquid: progress in strong correlation physics. *Reports on Progress in Physics*, 71(1):012501, 2008.

[117] Patrick A. Lee, Naoto Nagaosa, Tai-Kai Ng, and Xiao-Gang Wen. Su(2) formulation of the t-j model: Application to underdoped cuprates. *Phys. Rev. B*, 57(10):6003–, March 1998.

[118] Patrick A. Lee, Naoto Nagaosa, and Xiao-Gang Wen. Doping a mott insulator: Physics of high-temperature superconductivity. *Rev. Mod. Phys.*, 78(1):17–, January 2006.

[119] Patrick A. Lee, Naoto Nagaosa, and Xiao-Gang Wen. Doping a mott insulator: Physics of high-temperature superconductivity. *Rev. Mod. Phys.*, 78(1):17–85, Jan 2006.

[120] Sung-Sik Lee and Patrick A. Lee. U(1) gauge theory of the hubbard model: Spin liquid states and possible application to $\kappa - (bedt - ttf)_2cu_2(cn)_3$. *Phys. Rev. Lett.*, 95(3):036403–, July 2005.

[121] J. Leinaas and J. Myrheim. On the theory of identical particles. *Il Nuovo Cimento B (1971-1996)*, 37(1):1–23, 1977-01-01.

[122] Michael Levin and Ady Stern. Fractional topological insulators. *Phys. Rev. Lett.*, 103(19):196803–, November 2009.

[123] Michael Levin and Xiao-Gang Wen. Detecting topological order in a ground state wave function. *Phys. Rev. Lett.*, 96(11):110405–, March 2006.

[124] Hui Li and F. D. M. Haldane. Entanglement spectrum as a generalization of entanglement entropy: Identification of topological order in non-abelian fractional quantum hall effect states. *Phys. Rev. Lett.*, 101(1):010504–, July 2008.

[125] Elliott H. Lieb and F. Y. Wu. Absence of mott transition in an exact solution of the short-range, one-band model in one dimension. *Phys. Rev. Lett.*, 20(25):1445–, June 1968.

[126] Hilbert v. Lohneysen, Achim Rosch, Matthias Vojta, and Peter Wolfle. Fermi-liquid instabilities at magnetic quantum phase transitions. *Rev. Mod. Phys.*, 79(3):1015–, August 2007.

[127] Y.-M. Lu and Y. Ran. Symmetry protected fractional chern insulators and fractional topological insulators. *arXiv:1109.0226v1*, 2011.

[128] Yuan-Ming Lu and Ying Ran. z_2 spin liquid and chiral antiferromagnetic phase in the hubbard model on a honeycomb lattice. *Phys. Rev. B*, 84(2):024420–, July 2011.

[129] Yuan-Ming Lu, Ying Ran, and Patrick A. Lee. z_2 spin liquids in the s=1/2 heisenberg model on the kagome lattice: A projective symmetry-group study of schwinger fermion mean-field states. *Phys. Rev. B*, 83(22):224413–, June 2011.

[130] Yuan-Ming Lu, Xiao-Gang Wen, Zhenghan Wang, and Ziqiang Wang. Non-abelian quantum hall states and their quasiparticles: From the pattern of zeros to vertex algebra. *Phys. Rev. B*, 81(11):115124–, March 2010.

[131] Yuan-Ming Lu, Yue Yu, and Ziqiang Wang. Correlation-hole induced paired quantum hall states in the lowest landau level. *Phys. Rev. Lett.*, 105(21):216801–, November 2010.

[132] D. R. Luhman, W. Pan, D. C. Tsui, L. N. Pfeiffer, K. W. Baldwin, and K. W. West. Observation of a fractional quantum hall state at =1/4 in a wide gaas quantum well. *Phys. Rev. Lett.*, 101(26):266804–, December 2008.

[133] A. H. MacDonald, S. M. Girvin, and D. Yoshioka. tu expansion for the hubbard model. *Phys. Rev. B*, 37(16):9753–, June 1988.

[134] J. B. Marston and C. Zeng. Spin-peierls and spin-liquid phases of kagom[e-acute] quantum antiferromagnets. *J. Appl. Phys.*, 69(8):5962–5964, April 1991.

[135] P. Mendels, F. Bert, M. A. de Vries, A. Olariu, A. Harrison, F. Duc, J. C. Trombe, J. S. Lord, A. Amato, and C. Baines. Quantum magnetism in the paratacamite family: Towards an ideal kagomé lattice. *Phys. Rev. Lett.*, 98(7):077204–, February 2007.

[136] Z. Y. Meng, T. C. Lang, S. Wessel, F. F. Assaad, and A. Muramatsu. Quantum spin liquid emerging in two-dimensional correlated dirac fermions. *Nature*, 464(7290):847–851, April 2010.

[137] N. D. Mermin and H. Wagner. Absence of ferromagnetism or antiferromagnetism in one- or two-dimensional isotropic heisenberg models. *Phys. Rev. Lett.*, 17(22):1133–, November 1966.

[138] R. Moessner and S. L. Sondhi. Resonating valence bond phase in the triangular lattice quantum dimer model. *Phys. Rev. Lett.*, 86(9):1881–, February 2001.

[139] G. Moller and S. H. Simon. Paired composite-fermion wave functions. *Phys. Rev. B*, 77(7):075319–, February 2008.

[140] Gregory Moore and Nicholas Read. Nonabelions in the fractional quantum hall effect. *Nuclear Physics B*, 360(2-3):362–396, August 1991.

[141] Joel E. Moore. The birth of topological insulators. *Nature*, 464(7286):194–198, March 2010.

[142] Takao Morinari. Quantum hall effect at half-filled landau level: Pairing of composite fermions. *Phys. Rev. Lett.*, 81(17):3741–, October 1998.

[143] Olexei I. Motrunich. Variational study of triangular lattice spin- 1/2 model with ring exchanges and spin liquid state in kappa - (et)2 cu2 (cn)3. *Phys. Rev. B*, 72(4):045105–, July 2005.

[144] Christopher Mudry and Eduardo Fradkin. Separation of spin and charge quantum numbers in strongly correlated systems. *Phys. Rev. B*, 49(8):5200–, February 1994.

[145] Yoichiro Nambu. Quasi-particles and gauge invariance in the theory of superconductivity. *Phys. Rev.*, 117(3):648–, February 1960.

[146] Chetan Nayak, Steven H. Simon, Ady Stern, Michael Freedman, and Sankar Das Sarma. Non-abelian anyons and topological quantum computation. *Rev. Mod. Phys.*, 80(3):1083–, September 2008.

[147] Chetan Nayak and Frank Wilczek. 2n-quasihole states realize 2n-1-dimensional spinor braiding statistics in paired quantum hall states. *Nuclear Physics B*, 479(3):529–553, November 1996.

[148] T. Neupert, L. Santos, S. Ryu, C. Chamon, and C. Mudry. Fractional topological liquids with time-reversal symmetry and their lattice realization. *arXiv:1106.3989v1*, 2011.

[149] Titus Neupert, Luiz Santos, Claudio Chamon, and Christopher Mudry. Fractional quantum hall states at zero magnetic field. *Phys. Rev. Lett.*, 106(23):236804–, June 2011.

[150] P. Nikolic and T. Senthil. Physics of low-energy singlet states of the kagome lattice quantum heisenberg antiferromagnet. *Phys. Rev. B*, 68(21):214415–, December 2003.

[151] Boris Noyvert. Algebraic approach to parafermionic conformal field theories. *Journal of High Energy Physics*, 2007(02):074–, 2007.

[152] Boris Noyvert. Z(2) x Z(2) graded superconformal algebra of parafermionic type. *Adv. Theor. Math. Phys.*, 13:159–185, 2009.

[153] Masaki Oshikawa and T. Senthil. Fractionalization, topological order, and quasiparticle statistics. *Phys. Rev. Lett.*, 96(6):060601–, February 2006.

[154] Z. Papic, G. Moller, M. V. Milovanovic, N. Regnault, and M. O. Goerbig. Fractional quantum hall state at v=1/4 in a wide quantum well. *Phys. Rev. B*, 79(24):245325–, June 2009.

[155] Z. Papic, N. Regnault, and S. Das Sarma. Interaction-tuned compressible-to-incompressible phase transitions in quantum hall systems. *Phys. Rev. B*, 80(20):201303–, November 2009.

[156] Michael. R. Peterson, Th. Jolicoeur, and S. Das Sarma. Finite-layer thickness stabilizes the pfaffian state for the 5/2 fractional quantum hall effect: Wave function overlap and topological degeneracy. *Phys. Rev. Lett.*, 101(1):016807–, July 2008.

[157] Michael R. Peterson, Th. Jolicoeur, and S. Das Sarma. Orbital landau level dependence of the fractional quantum hall effect in quasi-two-dimensional electron layers: Finite-thickness effects. *Phys. Rev. B*, 78(15):155308–, October 2008.

[158] Christian Pfleiderer. Superconducting phases of f -electron compounds. *Rev. Mod. Phys.*, 81(4):1551–, November 2009.

[159] H. David Politzer. Reliable perturbative results for strong interactions? *Phys. Rev. Lett.*, 30(26):1346–, June 1973.

[160] A. M. Polyakov. Quark confinement and topology of gauge theories. *Nuclear Physics B*, 120(3):429–458, March 1977.

[161] B J Powell and Ross H McKenzie. Quantum frustration in organic mott insulators: from spin liquids to unconventional superconductors, 2011.

[162] R. E. Prange and S. M. Girvin. *The Quantum Hall Effect*. Graduate Texts in Contemporary Physics. Springer, 2nd edition edition, December 1989.

[163] X.-L. Qi. Generic wavefunction description of fractional quantum anomalous hall states and fractional topological insulators. *arXiv:1105.4298v1*, 2011.

[164] X.-L. Qi and S. C. Zhang. Topological insulators and superconductors. *arXiv:1008.2026v1*, 2010.

[165] Xiao-Liang Qi and Shou-Cheng Zhang. The quantum spin hall effect and topological insulators. *Phys. Today*, 63(1):33–38, January 2010.

[166] Iuliana P. Radu, J. B. Miller, C. M. Marcus, M. A. Kastner, L. N. Pfeiffer, and K. W. West. Quasi-particle properties from tunneling in the v = 5/2 fractional quantum hall state. *Science*, 320(5878):899–902, 2008.

[167] R. Rajaraman and S. L. Sondhi. A field theory for the read operator. *Int. J. Mod. Phys. B*, 10:793–, 1996.

[168] Y. Ran, A. Vishwanath, and D.-H. Lee. A direct transition between a neel ordered mott insulator and a $d_{x^2-y^2}$ superconductor on the square lattice. *arXiv:0806.2321v2*, 2008.

[169] Ying Ran, Michael Hermele, Patrick A. Lee, and Xiao-Gang Wen. Projected-wave-function study of the spin-1/2 heisenberg model on the kagomé lattice. *Phys. Rev. Lett.*, 98(11):117205–, March 2007.

[170] E Rastelli, L Reatto, and A Tassi. Quantum fluctuations and phase diagram of heisenberg models with competing interactions. *Journal of Physics C: Solid State Physics*, 19(33):6623, 1986.

[171] N. Read. Order parameter and ginzburg-landau theory for the fractional quantum hall effect. *Phys. Rev. Lett.*, 62(1):86–, January 1989.

[172] N. Read. Excitation structure of the hierarchy scheme in the fractional quantum hall effect. *Phys. Rev. Lett.*, 65(12):1502–, September 1990.

[173] N Read. Theory of the half-filled landau level. *Semiconductor Science and Technology*, 9(11S):1859–, 1994.

[174] N. Read. Lowest-landau-level theory of the quantum hall effect: The fermi-liquid-like state of bosons at filling factor one. *Phys. Rev. B*, 58(24):16262–, December 1998.

[175] N. Read. Wavefunctions and counting formulas for quasiholes of clustered quantum hall states on a sphere. *Phys. Rev. B*, 73(24):245334–, June 2006.

[176] N. Read and Dmitry Green. Paired states of fermions in two dimensions with breaking of parity and time-reversal symmetries and the fractional quantum hall effect. *Phys. Rev. B*, 61(15):10267–, April 2000.

[177] N. Read and E. Rezayi. Quasiholes and fermionic zero modes of paired fractional quantum hall states: The mechanism for non-abelian statistics. *Phys. Rev. B*, 54(23):16864–, December 1996.

[178] N. Read and E. Rezayi. Beyond paired quantum hall states: Parafermions and incompressible states in the first excited landau level. *Phys. Rev. B*, 59(12):8084–, March 1999.

[179] N. Read and Subir Sachdev. Valence-bond and spin-peierls ground states of low-dimensional quantum antiferromagnets. *Phys. Rev. Lett.*, 62(14):1694–, April 1989.

[180] N. Read and Subir Sachdev. Large-n expansion for frustrated quantum antiferromagnets. *Phys. Rev. Lett.*, 66(13):1773–, April 1991.

[181] E. Rezayi and N. Read. Fermi-liquid-like state in a half-filled landau level. *Phys. Rev. Lett.*, 72(6):900–, February 1994.

[182] Subir Sachdev. Kagome and triangular-lattice heisenberg antiferromagnets: Ordering from quantum fluctuations and quantum-disordered ground states with unconfined bosonic spinons. *Phys. Rev. B*, 45(21):12377–, June 1992.

[183] Masatoshi Sato and Satoshi Fujimoto. Existence of majorana fermions and topological order in nodal superconductors with spin-orbit interactions in external magnetic fields. *Phys. Rev. Lett.*, 105(21):217001–, November 2010.

[184] Masatoshi Sato, Yoshiro Takahashi, and Satoshi Fujimoto. Non-abelian topological order in s-wave superfluids of ultracold fermionic atoms. *Phys. Rev. Lett.*, 103(2):020401–, July 2009.

[185] Jay D. Sau, Roman M. Lutchyn, Sumanta Tewari, and S. Das Sarma. Generic new platform for topological quantum computation using semiconductor heterostructures. *Phys. Rev. Lett.*, 104(4):040502–, January 2010.

[186] Andreas P. Schnyder, Shinsei Ryu, Akira Furusaki, and Andreas W. W. Ludwig. Classification of topological insulators and superconductors in three spatial dimensions. *Phys. Rev. B*, 78(19):195125–, November 2008.

[187] L. Seehofer, G. Falkenberg, and R.L. Johnson. Stm study of the structure and phases of pb on ge(111). *Surface Science*, 290(1-2):15–25, June 1993.

[188] Alexander Seidel and Dung-Hai Lee. Abelian and non-abelian hall liquids and charge-density wave: Quantum number fractionalization in one and two dimensions. *Phys. Rev. Lett.*, 97(5):056804–, August 2006.

[189] J. Shabani, T. Gokmen, Y. T. Chiu, and M. Shayegan. Evidence for developing fractional quantum hall states at even denominator 1/2 and 1/4 fillings in asymmetric wide quantum wells. *Phys. Rev. Lett.*, 103(25):256802–, December 2009.

[190] J. Shabani, T. Gokmen, and M. Shayegan. Correlated states of electrons in wide quantum wells at low fillings: The role of charge distribution symmetry. *Phys. Rev. Lett.*, 103(4):046805–, July 2009.

[191] D.N. Sheng, Zheng-Cheng Gu, Kai Sun, and L. Sheng. Fractional quantum hall effect in the absence of landau levels. *Nat Commun*, 2:389–, July 2011.

[192] Y. Shimizu, K. Miyagawa, K. Kanoda, M. Maesato, and G. Saito. Spin liquid state in an organic mott insulator with a triangular lattice. *Phys. Rev. Lett.*, 91(10):107001–, September 2003.

[193] Manfred Sigrist and Kazuo Ueda. Phenomenological theory of unconventional superconductivity. *Rev. Mod. Phys.*, 63(2):239–, April 1991.

[194] Steven H. Simon, E. H. Rezayi, N. R. Cooper, and I. Berdnikov. Construction of a paired wave function for spinless electrons at filling fraction $\nu = 2/5$. *Phys. Rev. B*, 75(7):075317–, February 2007.

[195] Steven H. Simon, Edward H. Rezayi, and Nicolas Regnault. Quantum hall wave functions based on s3 conformal field theories. *Phys. Rev. B*, 81(12):121301–, March 2010.

[196] Philippe Sindzingre, L Seabra, Nic Shannon, and Tsutomu Momoi. Phase diagram of the spin-1/2 j 1 - j 2 - j 3 heisenberg model on the square lattice with ferromagnetic j 1. *Journal of Physics: Conference Series*, 145(1):012048, 2009.

[197] Philippe Sindzingre, Nic Shannon, and Tsutomu Momoi. Phase diagram of the spin-1/2 j 1 - j 2 - j 3 heisenberg model on the square lattice. *Journal of Physics: Conference Series*, 200(2):022058, 2010.

[198] Rajiv R. P. Singh and David A. Huse. Ground state of the spin-1/2 kagome-lattice heisenberg antiferromagnet. *Phys. Rev. B*, 76(18):180407–, November 2007.

[199] Rajiv R. P. Singh and David A. Huse. Triplet and singlet excitations in the valence bond crystal phase of the kagome lattice heisenberg model. *Phys. Rev. B*, 77(14):144415–, April 2008.

[200] Ady Stern, Felix von Oppen, and Eros Mariani. Geometric phases and quantum entanglement as building blocks for non-abelian quasiparticle statistics. *Phys. Rev. B*, 70(20):205338–, November 2004.

[201] Michael Stone and Suk-Bum Chung. Fusion rules and vortices in px +i py superconductors. *Phys. Rev. B*, 73(1):014505–, January 2006.

[202] Kai Sun, Zhengcheng Gu, Hosho Katsura, and S. Das Sarma. Nearly flatbands with nontrivial topology. *Phys. Rev. Lett.*, 106(23):236803–, June 2011.

[203] Kazunori Takada, Hiroya Sakurai, Eiji Takayama-Muromachi, Fujio Izumi, Ruben A. Dilanian, and Takayoshi Sasaki. Superconductivity in two-dimensional coo2 layers. *Nature*, 422(6927):53–55, March 2003.

[204] Evelyn Tang, Jia-Wei Mei, and Xiao-Gang Wen. High-temperature fractional quantum hall states. *Phys. Rev. Lett.*, 106(23):236802–, June 2011.

[205] D. J. Thouless, M. Kohmoto, M. P. Nightingale, and M. den Nijs. Quantized hall conductance in a two-dimensional periodic potential. *Phys. Rev. Lett.*, 49(6):405–, August 1982.

[206] C. C. Tsuei and J. R. Kirtley. Pairing symmetry in cuprate superconductors. *Rev. Mod. Phys.*, 72(4):969–, October 2000.

[207] D. C. Tsui, H. L. Stormer, and A. C. Gossard. Two-dimensional magneto-transport in the extreme quantum limit. *Phys. Rev. Lett.*, 48(22):1559–, May 1982.

[208] Villain, J., Bidaux, R., Carton, J.-P., and Conte, R. Order as an effect of disorder. *J. Phys. France*, 41(11):1263–1272, 1980.

[209] G. E. Volovik. *Exotic Properties of Superfluid Helium 3*. Series in Modern Condensed Matter Physics. World Scientific Pub Co Inc, December 1991.

[210] Fa Wang. Schwinger boson mean field theories of spin liquid states on a honeycomb lattice: Projective symmetry group analysis and critical field theory. *Phys. Rev. B*, 82(2):024419–, July 2010.

[211] Fa Wang and Ashvin Vishwanath. Spin-liquid states on the triangular and kagomé lattices: A projective-symmetry-group analysis of schwinger boson states. *Phys. Rev. B*, 74(17):174423–, November 2006.

[212] Qiang-Hua Wang, Dung-Hai Lee, and Patrick A. Lee. Doped t-j model on a triangular lattice: Possible application to naxcoo2yh2o and na1-xtio2. *Phys. Rev. B*, 69(9):092504–, March 2004.

[213] Franz J. Wegner. Duality in generalized ising models and phase transitions without local order parameters. *J. Math. Phys.*, 12(10):2259–2272, October 1971.

[214] X. G. Wen. Chiral luttinger liquid and the edge excitations in the fractional quantum hall states. *Phys. Rev. B*, 41(18):12838–, June 1990.

[215] X. G. Wen. Topological orders in rigid states. *Int. J. Mod. Phys. B*, 4(2):239, 1990.

[216] X. G. Wen. Non-abelian statistics in the fractional quantum hall states. *Phys. Rev. Lett.*, 66(6):802–, February 1991.

[217] X. G. Wen. Theory of fractional quantum hall edge state. *Int. J. Mod. Phys. B*, 6:1711–1762, 1992.

[218] X. G. Wen and Q. Niu. Ground-state degeneracy of the fractional quantum hall states in the presence of a random potential and on high-genus riemann surfaces. *Phys. Rev. B*, 41(13):9377–, May 1990.

[219] X. G. Wen and A. Zee. Classification of abelian quantum hall states and matrix formulation of topological fluids. *Phys. Rev. B*, 46(4):2290–, July 1992.

[220] X.-G. Wen and A. Zee. Topological degeneracy of quantum hall fluids. *Phys. Rev. B*, 58(23):15717–, December 1998.

[221] Xia-Gang Wen and Yong-Shi Wu. Chiral operator product algebra hidden in certain fractional quantum hall wave functions. *Nuclear Physics B*, 419(3):455–479, May 1994.

[222] Xiao-Gang Wen. Edge transport properties of the fractional quantum hall states and weak-impurity scattering of a one-dimensional charge-density wave. *Phys. Rev. B*, 44(11):5708–, September 1991.

[223] Xiao-Gang Wen. Topological orders and edge excitations in fractional quantum hall states. *Advances in Physics*, 44(5):405–473, 1995.

[224] Xiao-Gang Wen. Projective construction of non-abelian quantum hall liquids. *Phys. Rev. B*, 60(12):8827–, September 1999.

[225] Xiao-Gang Wen. Quantum orders and symmetric spin liquids. *Phys. Rev. B*, 65(16):165113, Apr 2002.

[226] Xiao-Gang Wen. Quantum orders in an exact soluble model. *Phys. Rev. Lett.*, 90(1):016803–, January 2003.

[227] Xiao-Gang Wen and Patrick A. Lee. Theory of underdoped cuprates. *Phys. Rev. Lett.*, 76(3):503–506, Jan 1996.

[228] Xiao-Gang Wen and Zhenghan Wang. Classification of symmetric polynomials of infinite variables: Construction of abelian and non-abelian quantum hall states. *Phys. Rev. B*, 77(23):235108–, June 2008.

[229] Xiao-Gang Wen and Zhenghan Wang. Topological properties of abelian and non-abelian quantum hall states classified using patterns of zeros. *Phys. Rev. B*, 78(15):155109–, October 2008.

[230] Xiao-Gang Wen, Yong-Shi Wu, and Yasuhiro Hatsugai. Chiral operator product algebra and edge excitations of a fractional quantum hall droplet. *Nuclear Physics B*, 422(3):476–494, July 1994.

[231] F. Wilczek. *Fractional Statistics and Anyon Superconductivity*. World Scientific Pub Co Inc, December 1990.

[232] Frank Wilczek. Quantum mechanics of fractional-spin particles. *Phys. Rev. Lett.*, 49(14):957–, October 1982.

[233] Frank Wilczek. Majorana returns. *Nat Phys*, 5(9):614–618, September 2009.

[234] R. Willett, J. P. Eisenstein, H. L. Stormer, D. C. Tsui, A. C. Gossard, and J. H. English. Observation of an even-denominator quantum number in the fractional quantum hall effect. *Phys. Rev. Lett.*, 59(15):1776–, October 1987.

[235] Y.-S. Wu and Y. Yu. Mean-field and perturbation theory of vortex-like composite fermions. *arXiv:cond-mat/9608061v1*, 1996.

[236] Di Xiao, Wenguang Zhu, Y. Ran, N. Nagaosa, and Satoshi Okamoto. Interface engineering of quantum hall effects in digital heterostructures of transition-metal oxides. *arXiv:1106.4296v1*, 2011.

[237] Cenke Xu and Subir Sachdev. Majorana liquids: The complete fractionalization of the electron. *Phys. Rev. Lett.*, 105(5):057201–, July 2010.

[238] K Izawa Y Matsuda and I Vekhter. Nodal structure of unconventional superconductors probed by angle resolved thermal transport measurements, 2006.

[239] Minoru Yamashita, Norihito Nakata, Yoshinori Senshu, Masaki Nagata, Hiroshi M. Yamamoto, Reizo Kato, Takasada Shibauchi, and Yuji Matsuda. Highly mobile gapless excitations in a two-dimensional candidate quantum spin liquid. *Science*, 328(5983):1246–1248, 2010.

[240] Simeng Yan, David A. Huse, and Steven R. White. Spin-liquid ground state of the s = 1/2 kagome heisenberg antiferromagnet. *Science*, 332(6034):1173–1176, 2011.

[241] A. B. Zamolodchikov and V. A. Fateev. Disorder fields in two-dimensional conformal quantum-field theory and n=2 extended supersymmetry. *Sov. Phys. JETP*, 63(5):913, 1985.

[242] A. B. Zamolodchikov and V. A. Fateev. Nonlocal (parafermion) currents in two-dimensional conformal quantum field theory and self-dual critical points in z/sub n/-symmetric statistical systems. *Sov. Phys. JETP*, 62(2):215–, Aug 1985.

[243] S. C. Zhang, T. H. Hansson, and S. Kivelson. Effective-field-theory model for the fractional quantum hall effect. *Phys. Rev. Lett.*, 62(1):82–, January 1989.

[244] Guo-qing Zheng, Kazuaki Matano, D. P. Chen, and C. T. Lin. Spin singlet pairing in the superconducting state of $na_xcoo_2 \cdot 1.3h_2o$: Evidence from a co59 knight shift in a single crystal. *Phys. Rev. B*, 73(18):180503–, May 2006.

[245] Guo-qing Zheng, Kazuaki Matano, R L Meng, J Cmaidalka, and C W Chu. Na content dependence of superconductivity and the spin correlations in $na_xcoo_2 \cdot 1.3h_2o$. *Journal of Physics: Condensed Matter*, 18(5):L63, 2006.

[246] Sen Zhou and Ziqiang Wang. Nodal $d + id$ pairing and topological phases on the triangular lattice of $naxcoo2 \cdot yh2o$: Evidence for an unconventional superconducting state. *Phys. Rev. Lett.*, 100(21):217002, May 2008.